Effect of Fly Ash, External Moisture, and Air Content on D-Cracking of Concrete

by

Trevor Triffo

A thesis
presented to the University of Manitoba
in partial fulfillment of the
requirements for the degree of
Master of Science in Civil Engineering
in
Department of Civil Engineering

Winnipeg, Manitoba

ISBN 0-315-37178-1

EFFECT OF FLY ASH, EXTERNAL MOISTURE, AND AIR CONTENT ON D-CRACKING OF CONCRETE

BY

TREVOR TRIFFO

A thesis submitted to the Faculty of Graduate Studies of the University of Manitoba in partial fulfillment of the requirements of the degree of

MASTER OF SCIENCE

I hereby declare that I am the sole author of this thesis.

I authorize the University of Manitoba to lend this thesis to other institutions or individuals for the purpose of scholarly research.

Trevor Triffo

I further authorize the University of Manitoba to reproduce this thesis by photocopying or by other means, in total or in part, at the request of other institutions or individuals for the purpose of scholarly research.

Trevor Triffo

ABSTRACT

This paper deals with the Deterioration Crack (D-Crack) susceptibility and general freeze-thaw durability of Portland Cement Concrete (PCC). In particular, a study was conducted which dealt with the effect of a fly ash admixture, air content of cement paste, and availability of external moisture on the magnitude and occurrence of distress caused by the repeated exposure of PCC specimens to laboratory freeze-thaw cycles.

Test results showed that specimens in which 20 percent (by weight) of the cement was replaced with fly ash experienced a sharp drop in freeze-thaw resistance, compared to ordinary PCC specimens containing the same coarse aggregate. This was the case even though the 28 day compressive strengths of the fly ash mixes were higher than the ordinary PCC control mixes. Distress in the ordinary PCC specimens was caused primarily by aggregate fracture, while an aggregate/paste interfacial failure was responsible for distress in the specimens containing fly ash.

The freeze-thaw resistance of specimens for which external moisture was available increased with increasing air content. Generally, identical specimens for which external moisture was not available did not elongate to the same degree, although two exceptions were observed which showed that protection from external moisture does not guarantee an increase in frost resistance. An increase in the air content of the cement paste appeared to increase the freeze-thaw resistance of the coarse aggregates.

ACKNOWLEDGMENTS

This work would not have been possible without the assistance and guidance, and support of a number of sources. The author wishes to express his gratitude to the following people and agencies:

1. Dr. Len Domaschuk, for his invaluable guidance and suggestions throughout the course of the project.

2. Transport Canada, and in particular Mr. Gani Ganipathy, who provided financial assistance for the research.

3. My fellow graduate students, including Mr. Glen Hermanson and especially Mr. Gregg Garychuk whose advice and assistance in the early stages of the project was essential to its successful completion.

4. My family and friends, who provided support and encouragement.

CONTENTS

Chapter page

LIST OF TABLES

LIST OF FIGURES

Figure page

Figure page

Chapter I

INTRODUCTION

1.1 BACKGROUND

In North America, billions of dollars are spent annually maintaining the transportation infrastructure. The use of rigid (Portland Cement Concrete) pavements in temperate zones in some areas has led to environment related distress which can decrease the service life of rigid pavements and significantly increase maintenance and user costs. Often, the mechanism of deterioration is related to the frequency and severity of freeze-thaw cycles that occur annually in the area.

It is well documented that cement paste can be adequately protected from the harmful effects of frost action through the introduction of air entrainment to the paste. However, the mechanism responsible for frost damage in concrete aggregates, and the aggregate properties affecting the magnitude of distress remain topics for research. As highway agency budgets decrease and maintenance/reconstruction costs increase, a more complete understanding of freeze-thaw durability of rigid pavements is becoming increasingly important. This need has necessitated the development of testing procedures that can provide information on the suitability of aggregates for use in a freeze-thaw environment.

1.2 SCOPE OF THE INVESTIGATION

This thesis is concerned with a certain type of rigid pavement deterioration known as Deterioration Cracking, hereafter referred to as D-Cracking. Although it could theoretically occur in any type of concrete structure, D-Cracking occurs primarily in pavements subjected to a freeze-thaw environment.

A review of the technical literature pertaining to freeze-thaw durability of PCC pavements was carried out. The importance of the structure of both cement paste and concrete aggregates was considered along with an overview of the existing theories concerning the mechanisms of deterioration due to freezing. The effects of air entraining agents and fly ash admixtures on the properties of fresh and hardened concrete were also studied.

Laboratory freeze-thaw tests were performed to determine the effect of a fly ash admixture, availability of external moisture, and air content of cement paste on D-Cracking and general freeze-thaw durability of Portland Cement Concrete. The tests were performed using an automated freeze-thaw cabinet to provide information on the relative durability of mix designs and/or aggregates. Concrete specimens prepared in accordance with design criteria were placed in the freeze-thaw cabinet and subjected to cycles of freeze-thaw. The specimens were frozen in air and thawed in water.

Details concerning testing equipment, the preparation of test specimens and test details are given in Chapter III. The limitations of the testing equipment are discussed and modifications which were required to increase the reliability of the testing equipment are also detailed.

The results of the study of the effect of fly ash on freeze-thaw durability are given in Chapter IV.

The results and analysis of the freeze-thaw test concerned with the effect of external moisture and air content of cement paste, are presented in Chapter V.

Chapter VI presents conclusions derived from the testing program as well as recommendations for improvements and ideas for further research.

Chapter II

LITERATURE REVIEW

2.1 INTRODUCTION

D-Cracking is defined as a crack pattern that first occurs parallel to internal longitudinal, transverse, and structural cracks in a concrete pavement slab (1). These finely spaced cracks can continue around corners and progress toward the center of the slab. Once the distress is initiated it cannot be stopped (2,3). D-Cracking may be preceded by slight staining or darkening of the concrete (4). At the time of formation, these cracks are thought to represent contours of equal saturation.

Because the occurrence of D-Cracking is a function of the intensity of the freeze-thaw environment, it is not surprising that in North America D-Cracking occurs primarily in the mid-western United States and in southern Canada. There is also some evidence of D-Cracking in Churchill, Manitoba. A relatively small number of freeze-thaw cycles may be required to initiate distress in concrete pavements in northern areas due to extremely low temperatures and to the duration of freezing periods.

A review of the technical literature pertaining to D-Cracking and freeze-thaw durability of concrete in general is presented. The word durability is used extensively in this thesis. There are many types of durability problems associated with concrete. However, for purposes of this thesis, durability was taken as freeze-thaw durability of concrete as

a whole, including the cement paste, whereas D-Cracking is associated with the freeze-thaw durability of concrete with respect to coarse aggregate only.

2.2 FACTORS AFFECTING THE INCIDENCE OF D-CRACKING

As stated above, the occurrence of D-Cracking is a function of the intensity of the freeze-thaw environment. However, the presence of this adverse environmental condition is not the only important factor. Researchers have noted that concrete pavements may begin to deteriorate in as little as three to five years after placement while others do not show signs of distress after twenty or more years (5,6). Stark (7) has shown cases where two adjacent pavement slabs, which were placed at the same time but using different sources of coarse aggregate, have shown different rates of D-Crack progression. This indicates that the source of coarse aggregate has a pronounced effect on the incidence of D-Cracking. This observation has also been documented by a number of other researchers (1,2,4,5,6,8,9). Whether or not a particular aggregate is D-Crack susceptible is also dependent on the pore properties of the aggregate and and the cement in which it is encased.

Moisture and drainage also seem to have an effect on the incidence of D-Cracking. However, literature in this area is inconclusive. Usually, D-Cracking is initiated in the lower third of a pavement slab where moisture is accessible from the subbase (5). Stark (10), and in his review of the paper by Axon et. al. (11), stated that most coarse aggregates that are D-Crack susceptible in pavements do not cause distress in bridge decks. Apparently this is due to free water not being available from a subbase and the beneficial effect of periodic drying on both sides of the

slab. Both of these mechanisms serve to moderate the water content of bridge decks.

Stark (10) documented field observations which correlated type of subbase and drainage provided to D-Cracking performance. Many highway agencies use a standard design in which the concrete slab is cast on a coarse subbase which rests on a less permeable subgrade. In these designs, water can accumulate in the granular subbase which would then be available to the lower portion of the concrete slab. The installation of carefully constructed longitudinal drains has been shown to delay and in some cases eliminate D-Cracking (10).

In their reveiw of early studies, Girard et. al. (1) also found that drainage had an effect on the incidence of D-Cracking. However, Traylor (2) stated that drainage and type of subbase did not significantly affect the magnitude of D-Cracking. Both Girard et. al. (1) and Stark (10) found that the insertion of a polyethylene vapor barrier between the concrete and subbase enhanced deterioration.

It therefore seems that three general conditions have to be met in order for D-Cracking to occur. Firstly, the concrete pavement must be placed in a freeze-thaw environment. Secondly, the coarse aggregate used in the pavement must be susceptible to D-Cracking. Thirdly, moisture must be available to increase the level of saturation of the concrete. The importance of these conditions with respect to the mechanisms of freeze-thaw deterioration in concrete will be explored in a later section.

2.3 STRUCTURE OF CONCRETE

As mentioned previously, the freeze-thaw durability of concrete is a complex function involving environmental conditions, availability of water or degree of saturation, and the pore structure of the coarse aggregate and the surrounding cement paste. Any attempt to categorize the freeze-thaw durability of concrete should take all of these factors into consideration. A number of theories have been proposed (8,12,13,14,15,16). However, in order to fully appreciate these theories, a knowledge of the structure of cement paste and coarse aggregate is essential. The structure of hardened cement paste will be examined first.

2.3.1 Structure of Hardened Cement Paste

The behavior of concrete when subjected to freeze-thaw conditions is, in part, a function of the structure of the cement paste surrounding the coarse aggregate particles. Characteristics such as the distribution and melting points of water held in cement pores, which are dependent on the structure of the cement paste, is in turn related to frost susceptibility of concrete.

Cement is comprised of exceedingly small particles which combine to form a porous gel. Interstitial cavities, or gel pores, exist between the individual gel particles. These gel pores, which constitute about 28 percent of the paste volume after hydration, form an interconnected network of voids (17). The gel pores are believed to be approximately 15 to 20 Angstroms (1A = 10^{-10} m) in diameter (18,19). Thus the gel itself has a reasonably high porosity but an extremely low permeability because of the small size of the interstitial spaces.

Larger pores are formed between agglomerates of gel particles. These

pores, known as capillary cavities or capillaries, average about 5000 Angstroms in diameter and are formed by free water in excess of that required for hydration (18,19). The capillary cavities constitute from 0 to 40 percent of the paste volume, depending on the degree of hydration and the water/cement ratio (17). Although the products of hydration occupy over twice the volume of cement in its original form, at water/cement ratios over 0.38 the volume of the gel is not sufficient to fill all of the space available to it, even after complete hydration (17,20). This remaining space forms the capillary cavities which are randomly interconnected throughout the paste (20). These pores are the primary component which determine the permeability of the paste. Paste permeability is an important variable concerning the frost resistance of concrete as will be shown later. According to Neville (17), reducing the w/c ratio of the cement paste from 0.7 to 0.3 lowers the coefficient of permeability a thousandfold for pastes with the same degree of hydration.

Entrained air bubbles are much larger than the capillary cavities and vary greatly in size. Diameters ranging from 10,000 to 10,000,000 Angstroms are typical (19). Figure 2.1 gives a schematic diagram showing the structure of cement paste (after Cordon).

2.3.1.1 Distribution of Water in Cement Paste

As stated previously, freeze-thaw deterioration cannot occur without sufficient moisture present in the concrete. Water can be drawn into cement paste by surface adsorption and capillary action (19). Neville (17) stated that water is adsorbed onto gel particles even at low ambient humidities (vapor pressures). Because of the extremely small size of the gel pores, only three or four layers of adsorbed water are required for

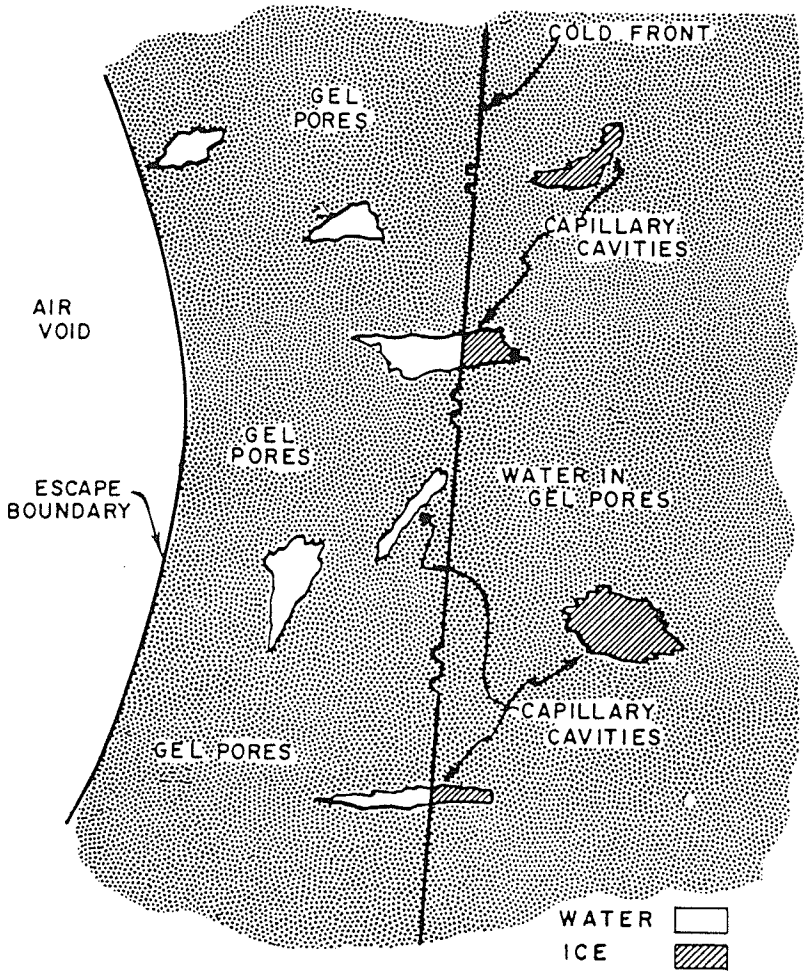

Figure 2.1: Structure of Cement Paste
(Air Bubble not Drawn to Scale)

complete saturation of the gel. Water held in the gel pores will have vapor pressures and mobility different from that of bulk water (21). It can easily be shown that the degree of saturation of the capillary cavities and entrained air bubbles will remain largely unaffected by surface adsorption. Capillary water is completely evaporable at humidities below 40 percent (21).

Capillary action also serves to draw water into the porous cement paste. Pores exert a suction force on water which is inversely

proportional to the radius of the pore (19). Hence, when introduced to a water source, the smallest capillary pores of cement paste will become saturated first and the larger capillaries will remain dry. Only a small percentage of the pores will be partially saturated. If water is continually available, pores of greater and greater volume will become water filled until complete saturation is achieved. This implies that even if a sample of cement paste is only partly saturated on a global scale, localized areas will be 100 percent saturated. Also, some pores are too large to effectively draw in moisture by the mechanism of capillary action, even if the rest of the paste is completely saturated. This is the case with entrained air bubbles. It is this characteristic that makes air entrainment effective in controlling frost action in cement paste (19). The effect of air entrainment on D-Cracking of concrete is a topic of interest for this thesis and will be examined subsequently.

2.3.1.2 Melting Points of Water in Cement Paste

A knowledge of the freezing characteristics of water in cement paste is essential to understanding frost action in concrete. A large amount of the evaporable water in cement paste is not freezable at $0^{o}C$. Because the pores (both gel and capillary) are small, surface tension places the water in the pores under pressure which lowers the melting point of the water in the pore (19). Since this pressure is inversely proportional to the radius of the pore, freezing will occur in the largest of the saturated pores first. As the temperature decreases further, the water in progressively smaller pores will freeze. It is estimated that freezing in the large capillaries is initiated in the temperature range of 0 to $-4^{o}C$ (15).

Dissolved alkalis are usually present in the pore water of cement paste. When ice forms in a solution it is relatively pure and therefore its formation further increases the solute concentration in the remaining solution. In this way the melt point of the remaining solution is further reduced. Dimensional and solute concentration effects are considered to be additive (18).

There is some evidence that deicing salts can accelerate D-Cracking (4,6). For extended freezing periods, osmotic pressures may be created due to different solute concentrations in the gel and capillary pore fluids (8). The effect of osmotic pressure may be enhanced by the application of deicing salts.

In addition to surface tension, the water in the gel pores is adsorbed onto the gel particles as stated previously. This structural difference makes the gel water much more difficult to freeze (19). Cordon (18) stated that a temperature of -78°C would have to be reached before the surface held water in gel pores would begin to freeze. The difference between the freezing temperature of gel and capillary water is important in understanding the mechanisms of frost action in concrete.

2.3.2 Structure of Course Aggregate

It is generally accepted that coarse aggregate is the single most important physical variable with respect to D-Crack susceptibility of concrete pavements (1,2,4,5,6,7,8,9). As noted previously, the source of the coarse aggregate was found to influence the D-Crack potential of a concrete pavement slab (5,6). Observations have shown that D-Cracking occurs almost exclusively in concrete containing sedimentary rocks

composed of both carbonate and silicate materials (2,5). Both gravel andcrushed rock have been associated with D-Cracking (5).

Verbeck and Landgren (9) stated that freeze-thaw durability of concrete aggregates is dependent on the rate at which the aggregates become critically saturated. This in turn is dependent on the permeability and thickness of the surrounding paste. The durability of the aggregate once it becomes critically saturated is dependent on certain pore properties of the aggregate. The effects of these physical characteristics are interrelated and some may have several and opposing effects (9). The pore properties of primary interest are porosity, permeability, and pore size distribution (9,19).

2.3.2.1 Porosity, Permeability, and Pore Size Distribution

The pore structure of aggregate used in concrete differs considerably from that of the cement paste in which it is encased. In most aggregates an interconnected network of voids is the primary component of the pore structure (21). Notable exceptions are volcanic rocks and slags which may have isolated pores formed by expanding gas. This network, in which the effective porosity may be taken as the total porosity, is similar to the capillary cavities that occur in cement paste formed at a high w/c ratio. However, in most aggregates there are no cavities similar to entrained air bubbles or gel pores (19). Water contained in coarse grained rocks does not experience a significant freezing point depression, but in fine grained rocks nucleation may not begin until a temperature of -5 to -7^{o}C is reached (9,22).

Porosity of aggregates is usually less than that of cement paste. Although porosity can range from nearly 0 up to 20 percent by solid

volume, values from 1 to 5 percent are most common (20). As mentioned above, aggregate pores are always larger than gel pores and frequently are the size of large capillary pores (20). Permeability and pore size distribution can vary widely depending on the nature of the material and its history (19,20). Researchers have tried to correlate pore size distribution of coarse aggregate to D-Cracking. Using scanning electron microscope techniques, Marks and Dubberke (4) found that durable aggregate is either coarse grained or extremely fine grained. D-Cracking was associated with nonargillaceous aggregates with a pore size distribution bounded by 0.04 um and 0.2 um (4).

Winslow, Lindgren and Dolch (3) developed a mathematical expression which relates an expected durability factor to pore volume and pore size distribution parameters obtained by mercury intrusion porosimetry. Although a reasonable correlation between the relative durability factor and occurrence of D-Cracking was obtained, the test cannot distinguish the magnitude of D-Cracking to be expected or when it will first appear.

The rate at which a given aggregate takes in water is primarily dependent on the vapor pressure (relative humidity) in the aggregate pores (9). Verbeck and Landgren (9) have shown that the relationship between degree of saturation and relative humidity is dependent on the pore size distribution of the aggregate. Aggregates with a fine pore structure (such as traprock) have a higher degree of saturation than do aggregates with a coarse pore structure (such as dolomite) subjected to the same relative humidity. Traprock would reach a higher degree of saturation quicker than dolomite, even if they had the same porosity. Figure 2.2 (after Verbeck and Landgren) illustrates this relationship.

The importance of porosity is made evident in the following

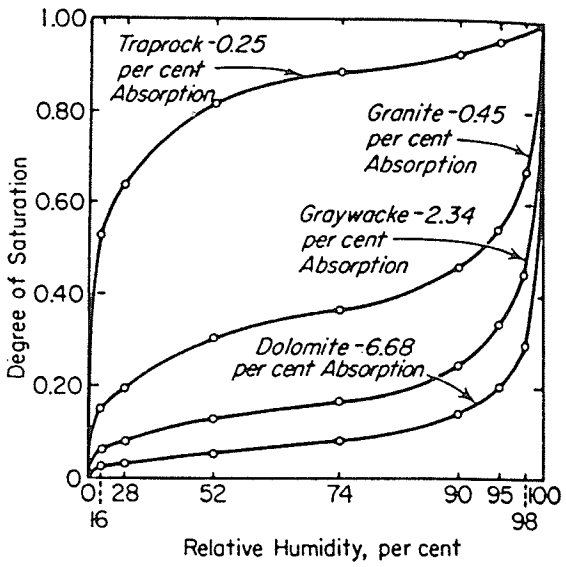

Figure 2.2: Degree of Saturation vs Relative Humidity for Aggregates with Different Pore Size Distributions (Horizontal Scale Drawn Proportional to $\%RH^2$)

illustration put forward by Verbeck and Landgren (9). Consider two aggregates both surrounded by equal thicknesses of saturated paste. In order for the aggregates to increase their degree of saturation, water must be transmitted through the paste and into the pores of the aggregate. If the aggregates have the same pore size distribution but differing porosities, the aggregate with the greater porosity will require a longer period of time to increase its degree of saturation the same amount as the aggregate with the lesser porosity. Therefore, in some cases it may be beneficial for an aggregate to have a high porosity (9). However, if a high porosity aggregate does become critically saturated, relatively large volumes of water may have to be accommodated upon freezing. This is an example of a pore property having multiple and opposing effects depending on conditions.

Verbeck and Landgren (9) stated that a saturated aggregate may cause concrete to deteriorate upon freezing if it cannot meet three criteria. First, an aggregate must be able to elastically accommodate the volumetric

expansion of water upon freezing. An upper limit to the stress that must be withstood can be estimated using elastic parameters and assuming instantaneous freezing. Second, during the freezing process the aggregate must not fail due to critical size effects. Aggregates of high porosity and low permeability are subject to this type of failure. This phenomenon will be examined in an upcoming section. Third, it is possible that the e xplusion of pore water from aggregate may create a failure at the paste/aggregate interface due to the generation of excessive hydraulic pressures in the cement paste. Aggregates of high porosity and high permeability may create this type of failure. In this case the air content of the surrounding paste plays a key role in maintaining the integrity of the concrete.

2.4 PROPOSED MECHANISMS OF FROST ACTION IN CONCRETE

A number of theories have been put forward in an attempt to explain the mechanisms of dilation due to frost action in concrete (8,12,13,14,15,16). It should be noted that none of the proposed theories fully explain all phenomena that have been observed in laboratory and field experiments. In all likelihood a combination of some or all of the proposed mechanisms occurring simultaneously or at different times during a freeze-thaw cycle is the cause of concrete pavement deterioration. Bearing this in mind, the basic theories will be examined in turn.

2.4.1 Hydraulic Pressure Theory

Early theories explaining frost damage in concrete were simply based on the fact that water expands about 9 percent upon freezing (23). Any closed system that is more than 91.7 percent saturated will become stressed if the water is frozen. Concrete and other porous materials, although not closed systems, were assumed to sustain damage if the degree of saturation was above this critical value. However, as mentioned previously, even if the degree of saturation is below this value as a whole there may be localized areas which are fully saturated.

It is now known that damage may be sustained by a porous body by mechanisms other than the inability of the material to elastically accommodate the volumetric expansion of the water/ice phase change. The Hydraulic Pressure Theory proposed by Powers (8) states that if the degree of saturation of an open pore is greater than 91.7 percent, water will be forced to migrate out of the pore during the freezing process. The resistance to this flow is known as hydraulic pressure. In a porous, low permeability material such as concrete, the hydraulic pressure generated during freezing may exceed the tensile strength of the material (8).

The magnitude of the tensile stress created during freezing is proportional to the degree of saturation (above 91.7 percent), viscosity of water, rate of ice production, and the distance to the nearest escape boundary. It is inversely proportional to the coefficient of permeability (8,19). If the distance to an escape boundary is sufficiently small, the tensile strength of the material will not be exceeded and distress will not occur. Also, if the permeability is sufficiently large, excessive hydraulic pressures will not be generated.

Permeability and distance to an escape boundary are both functions of

the pore properties of the material. Rate of ice production is a function of both material pore properties and environmental conditions. The rate of ice production is equivalent to the rate at which water must be expelled through the interconnected pores of the material. This is dependent on the freezing rate and the amount of water available for freezing. The amount of water available for freezing is dependent on degree of saturation, pore size distribution, and porosity. Figure 2.3 shows a schematic diagram of the factors which affect the magnitude of hydraulic pressure created during freezing. It can be readily observed that the magnitude of the tensile force created is related to certain material properties and environmental conditions. In cement paste the critical thickness is usually less than 0.25 mm and can sometimes be as low as 0.0025 mm (24). This of course means that concrete pavements composed of unprotected cement paste are much too thick to undergo freezing in a saturated condition and avoid distress. Although some air is invariably trapped when pouring concrete, the voids are too few and far between to effectively protect the paste (8). Air entrainment must be introduced to the paste to provide additional escape boundaries for the migrating water during freezing and bring the escape distance below the value of critical thickness.

Because of differences in pore structure as already discussed, the critical size of aggregates is much larger than that of cement paste. Verbeck and Landgren (9) have calculated the critical size for a chert and a dolomite to be 0.013 m and 0.84 m respectively.

Hydraulic pressure is dependent on the freezing rate. If the temperature of a concrete sample is held constant at some temperature below the initiation of freezing within the pores, the amount of water

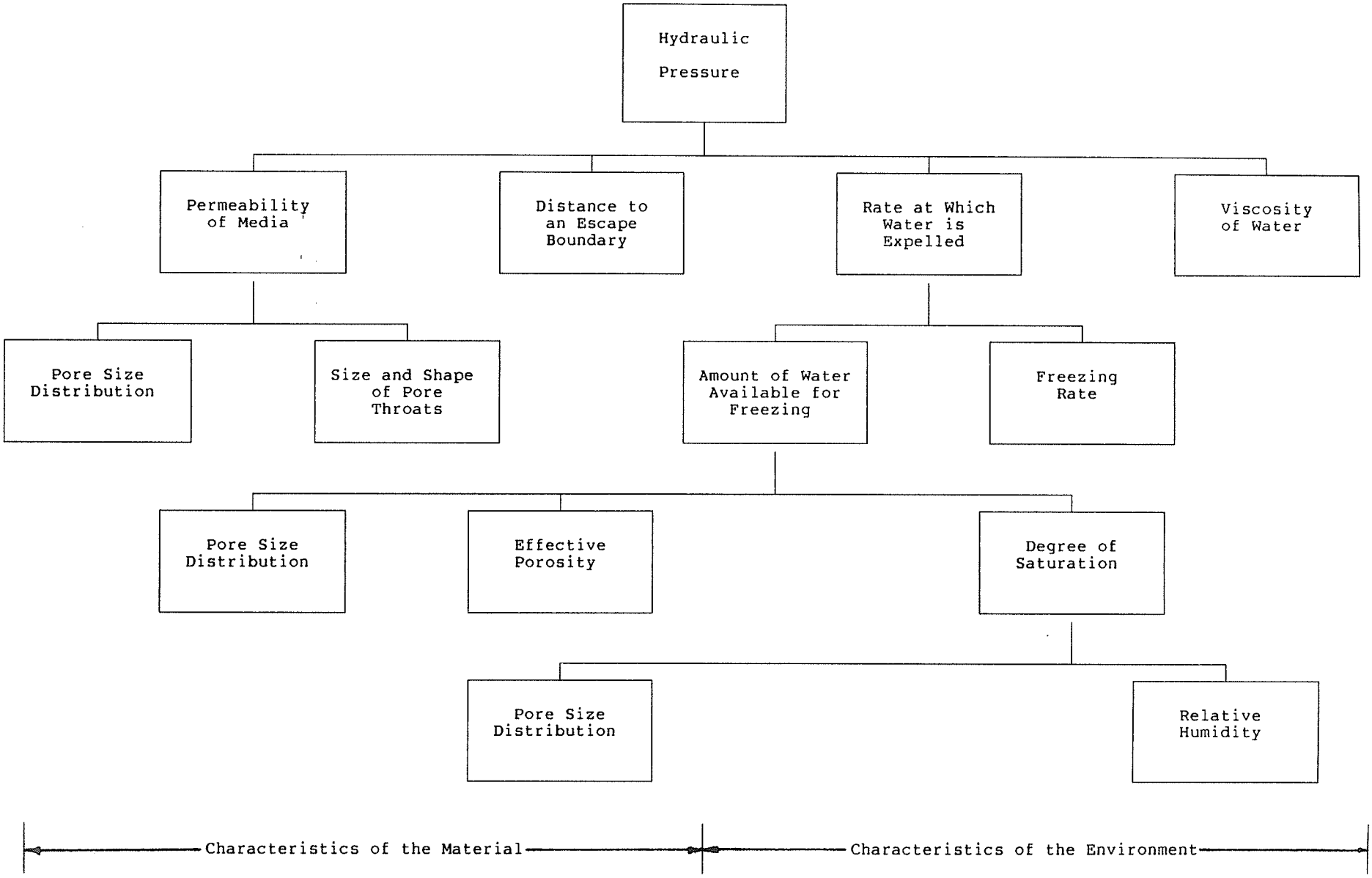

Figure 2.3: Factors Affecting the Magnitude of Hydraulic Pressure

forced to flow through the permeable media will go to zero and no hydraulic pressure should be generated. Therefore, there should be no expansion during this post-freezing period. However, research has shown that in some cases dilation may continue after ice is no longer being formed in the capillary cavities (15). This implies that another mechanism must be at work.

In defense of the hydraulic pressure theory, workers have noted that a decrease in the top size of coarse aggregate is sometimes helpful in controlling the incidence of D-Cracking (1,2,5,7,19). This is a direct consequence of reducing the magnitude of hydraulic pressure generated in the coarse aggregate. Also, as is shown in Figure 2.4 (after Powers and H elmuth), dilation begins at the instant freezing occurs.

2.4.2 Free Energy Difference Theory

The Free Energy Difference Theory was proposed by Powers and Helmuth (15) after it was observed that hydraulic pressure does not account for all phenomena observed when cement paste is subject to freezing and thawing. Data were presented showing the relationship between length change and time at constant temperature for a nonair entrained paste and the effect of air entrainment on length changes with temperature. Figures 2.5 and 2.6 illustrate these relationships (after Powers and Helmuth).

Figure 2.5 shows that dilation can occur at constant temperature when no ice is being produced and hydraulic pressure due to the volumetric expansion of capillary pore water upon freezing cannot exist. Figure 2.6 shows that samples of cement paste can decrease in length if the cement has a sufficiently high air content (low spacing factor). The decrease in length may even be below that expected from thermal contraction. These

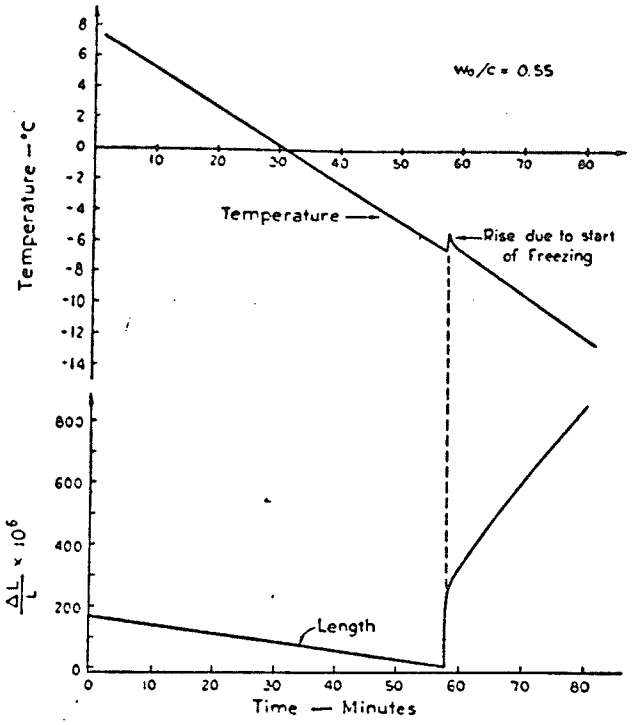

Figure 2.4: Temperature and Dilation Against Time for a Non-Air Entrained Paste

phenomena are believed to be caused by free energy differences between the different phases of the pore water (15).

The free energy of water in hardened cement paste is dependent on its degree of saturation because of adsorption and capillary effects (15). However, for a saturated paste with negligible dissolved alkalies the free energy of gel water is approximately the same as that of bulk water at the same temperature (15). At constant pressure and over a small temperature range, free energy is related to entropy through the equation:

$$\Delta G = -S \ (\Delta T) \qquad (1)$$

where G is free energy, T is temperature, and S is entropy.

If capillary water and gel water are in thermodynamic equilibrium before freezing, then at the moment ice forms in the capillary the equilibrium of the system is disturbed because entropy of ice is less than that of adsorbed water (15). As the temperature decreases, the difference in free energy between the two phases of the pore water increases, creating an energy gradient which causes the gel water to flow into the capillary cavity where it is subject to freezing. The excess ice causes the cavity to enlarge. However, the flow of water out of the gel pores causes a contraction of the gel. Gel water is also diffusing into any air voids containing ice (provided the paste is air entrained).

As mentioned above, free energy is pressure dependent. Figure 2.7 (after Powers and Helmuth) shows the effect of pressure on free energy for an air-entrained paste. At time t_0 all hydraulic pressure due to the volumetric increase of water upon freezing has dissipated. The gel water begins diffusing to the capillary cavities and air voids because it has a higher free energy. The free energy of the capillary ice is higher than the air void ice because of capillary and pressure effects. As water leaves the gel pores its free energy decreases. The free energy of the capillary ice increases because the increasing volume of the ice increases the pressure applied by the pore walls. The energy of the air void ice remains low because the voids are not filled. At time t_2 the free energy of the capillary ice becomes equal to that of the gel water. The direction of flow is reversed and water flows from the capillaries through the gel and eventually to the air voids. At time t_3 the free energies of the three adsorbate phases become equal and the diffusion process terminates. It is now possible to understand the behavior of the cement

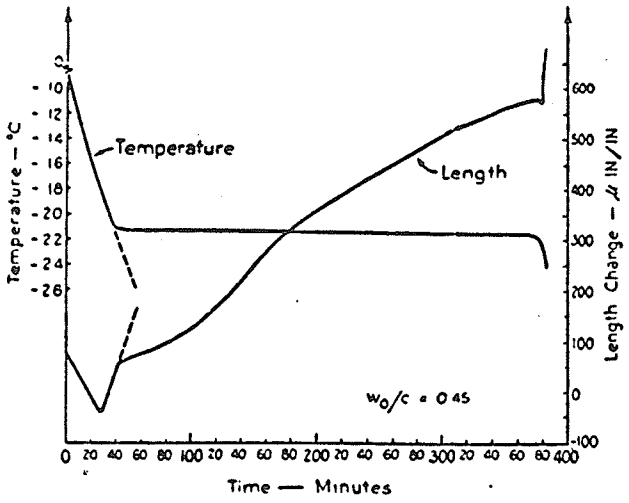

Figure 2.5: Length Changes at Constant Temperature for a Non-Air Entrained Paste

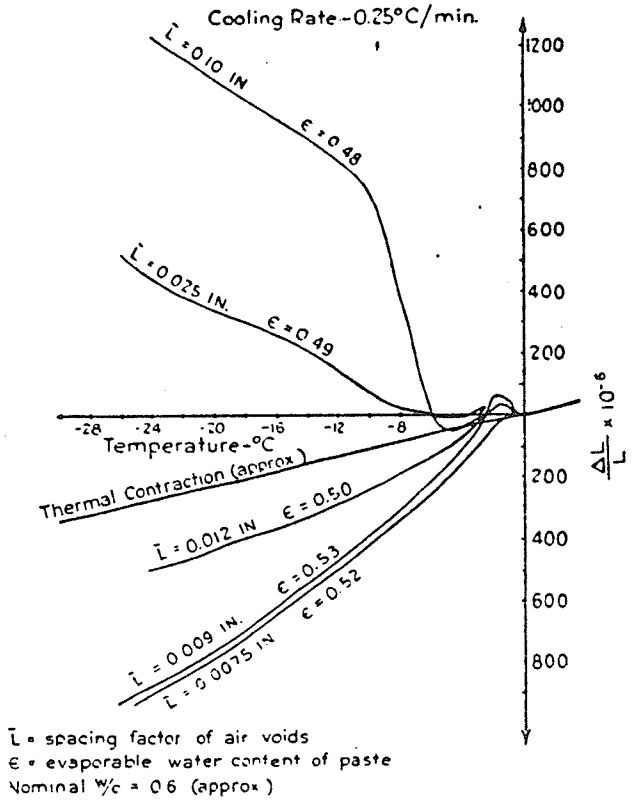

Figure 2.6: Effect of Entrained Air on Length Changes of Cement Paste

pastes shown in Figures 2.5 and 2.6. In the non-air entrained paste shown in Figure 2.5 the diffusion process occurs only between the gel water and the capillary ice. Even though the paste tends to shrink during diffusion, this shrinkage is more than offset by the volume increase of the capillary pores. Hydraulic pressure could also be generated by the movement of water through the pores. If sufficient air entrainment is introduced to the paste, gel water will diffuse mostly to the partly full entrained air voids and thus a net shrinkage will occur. This behavior can be seen in Figure 2.6.

Diffusion processes in concrete are more complicated than in cement paste alone. In coarse grained aggregates all of the pore water is freezable at temperatures close to 0°C (19). Diffusion could theoretically occur across the cement-aggregate interface but the volumes

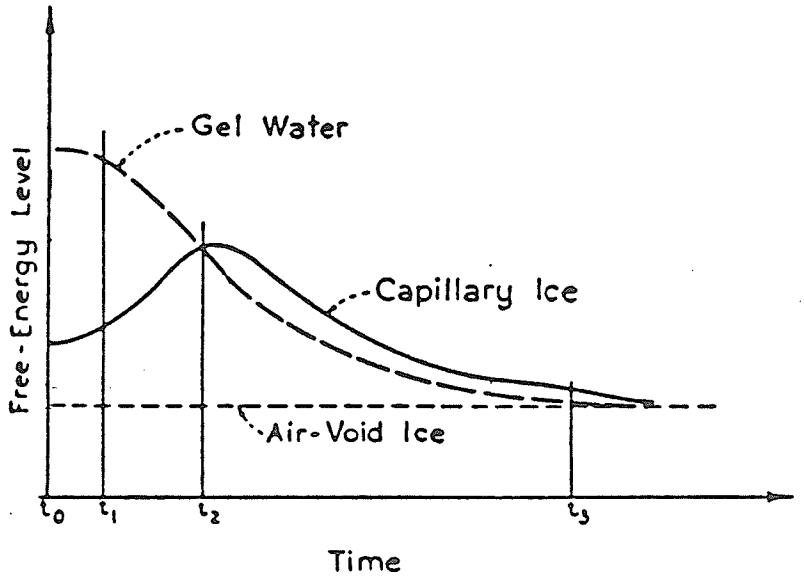

Figure 2.7: Free Energy Differences in Air-Entrained Paste

involved would be extremely small. In fine grained aggregates, however, many of the pores may be small enough to cause a significant freezing point depression. Thus unfrozen water will be in contact with ice within the pores of the aggregate itself. Since most of the unfrozen water will not be in the adsorbed state its free energy will be higher than the free energy of the gel water in the cement paste (19). Therefore, even greater pressure will be built up in the ice filled pores because of the imbalance of free energies within the aggregate itself. In this case expansion is caused by hydraulic pressure and pressure exerted by the growing ice crystals on the pore walls.

2.4.3 Desorption Theory

The desorption or vapour pressure theory proposed by Litvan (13,14) agrees with Power's belief that deterioration of concrete due to frost action is due to hydraulic pressure. However, it is postulated that the mass movement of water is not due to volumetric expansion of water upon freezing but rather to non equilibrium thermodynamic conditions existing between the capillary ice and the surface held water in the gel pores.

As shown previously, in order for a porous body to remain fully saturated, 100 percent humidity must be maintained in the body. There is a significant freezing point depression in the capillary pores in cement paste. Therefore the vapor pressure of the water held in these pores must be equal to the vapor pressure above supercooled water, P_{vs}. This vapor pressure cannot be maintained because part of the vapor will condense on the pore walls and form ice. The vapor pressure is therefore lowered to that of ice, P_{vi}, and the degree of saturation must decrease. Because the difference between these two values increases with decreasing

temperature, the water content of the paste must continually decrease as the temperature drops. The excess water is forced to flow to the surface of the body (or to an entrained air bubble if the paste is air entrained), creating hydraulic pressure as it does so. This implies that a certain amount of water must be expelled from the capillaries, the amount being dependent on the properties of the paste and the conditions prior to freezing rather than the theoretical maximum of 9 percent as in Power's hydraulic pressure theory. Litvan (14) found that in two slowly cooled samples three to four times the expected volumetric increase of water upon freezing was expelled from the samples. Also, expulsion of pore fluid was observed using other absorbates which decrease their volume upon freezing (14).

The desorption process depends on the existence of unfrozen water in the temperature range under study. Water in the pores of coarse grained rocks does not experience a freezing point depression (9,19,22). All of the water freezes in a very narrow temperature range close to 0°C. Fine grained aggregates may contain pores small enough to create a freezing point depression (9,19,22). In this case the desorption process may occur just as it does in cement paste.

If a concrete specimen is only partly saturated, hydraulic pressure should occur only after the difference between the vapor pressures of supercooled water and ice is sufficient to require that water be expelled from the system. At a relative humidity (vapor pressure) of 84 percent, the temperature required for the generation of hydraulic pressure is -18° C (14).

2.4.4 Dual Mechanism Theory

The Dual Mechanism Theory proposed by Larson and Cady (16) combines the Powers hydraulic pressure theory with an ordering process first proposed by Dunn and Hudec (22) to account for post freezing dilations. In this theory the unfrozen water becomes ordered by adsorption processes onto the mineral and ice surfaces. This ordering process entails a volume increase which is responsible for expansion after ice is no longer being formed.

This theory is opposite to that proposed by Litvan who stated that dilations are caused by differences in vapor pressures that require desorption in order for the system to reattain equilibrium (13,14). It is unlikely that adsorption and desorption processes can occur simultaneously (19).

2.5 GENERAL EFFECTS OF ENTRAINED AIR

Entrained air in concrete is defined as the purposeful introduction of small air bubbles into the cement paste, through the use of a suitable agent, at the time of mixing (17,25). Usually, air is entrained through the use of surface active compounds called air entraining agents (eg. Darex). These compounds form a stable foam in the paste (25). Since the foam bubble contains no water, the products of hydration cannot expand into the bubble and it retains its shape as the cement paste hardens. Although entrained air was originally intended solely as an aid in producing frost resistant concrete, it was found that the addition of air entraining agent created a mix of greater workability, especially for lean mixes (17,25). Air entrainment is also useful in controlling bleeding and segregation during casting of concrete. Permeability remains largely

unaffected because the bubbles remain discrete and do not serve to interconnect the existing pore structure to an appreciable extent (17).

The addition of entrained air also results in a loss of strength and lowered density. This is to be expected since the strength of materials is dependent on the relative volumes of voids and solids. The loss of strength occurs through the same stress concentration mechanism that initiates failure in other materials. However, in practise this strength reduction can be compensated for in some cases by a strength increase corresponding to a decreased water/cement ratio made possible by increased workability (17). This can be achieved because of the lubricating effect of the bubbles which act as fine, spherical aggregates of low surface friction (17).

2.5.1 Effect of Air Entrainment on Freeze Thaw Durability

Air entrained concrete contains both entrapped and entrained air. Entrapped air is due to incomplete compaction or improper placement of concrete. Its value with respect to frost protection is limited because of the relatively large size and spacing of entrapped air bubbles (19). The specific surface area of entrapped air bubbles is less than $12mm^2/mm^3$ (17). Conversely, entrained air bubbles are much smaller in diameter and are more uniformly distributed throughout the paste, provided the air entraining agent is added correctly and the concrete is properly mixed. The specific surface of cement paste in adequately air entrained concrete is in the range of 16 to 32 mm^2/mm^3, including entrapped air (17). Air entrained bubbles are larger in size than capillary cavities in cement paste, ranging in size from 0.01 mm to 2 mm (20,25). After hydration, these pores are too large to be filled by capillary effects and

remain essentially dry even after prolonged soaking in water (19). It is this property, together with their large numbers and uniform distribution, that gives entrained air its protective value.

In 1949 Powers (24) put forward a theoretical solution detailing the prediction of the minimum entrained air content required to protect a saturated paste from damage by frost. By assuming that the mechanism of deterioration was hydraulic pressure created by the volume increase associated with the water-ice phase change, Powers calculated that a minimum bubble spacing of 0.25 mm was required for a reasonable freezing rate. In other words, if the bubble spacing is kept below 0.25 mm the shells of influence surrounding the entrained air bubbles will begin to overlap. Thus, hydraulic pressure in excess of the tensile strength of the material is not generated at any point in the paste. The fact that water does migrate to entrained air bubbles during freezing has been shown by Powers and Helmuth (15). As shown previously, test results have shown that cement paste, containing sufficient entrained air, may show a volumetric decrease greater than that expected from thermal contraction alone as shown by Figure 2.5. The extra shrinkage is due to the migration of pore water to the entrained air bubbles. The volume of the paste is partially dependent on the moisture content so shrinkage in addition to thermal contraction is to be expected. Upon thawing, most of the water returns to the paste and the protective capacity of the bubbles is restored for the next freezing cycle (15).

Klieger (26) indicated that the durability of concrete subjected to laboratory freezing and thawing increased significantly with increasing air content until a certain level was reached. After that level, a greater amount of air entrainment did not lead to greater durability. Because of

the strength loss associated with additional air entrainment, the optimum air content was defined as the air content after which additional air entrainment was no longer useful, which corresponded to approximately 9 percent of the mortar volume, regardless of mix design characteristics.

Axon, Willis and Reagel (27) tested the effect of air entrainment on freeze-thaw durability of concrete prisms. Four different coarse aggregates, two cherts and two limestones, were used. The performance of the cherts, which were highly absorptive and had poor service records, were not substantially increased with increasing air content as measured by loss in dynamic modulus. The limestones, which were less absorptive and had good service records, showed considerable improvement in durability.

Bugg (28) tested a number of concretes containing different aggregates at different degrees of saturation. Air entrained concrete showed a slight to marked improvement in performance in every condition. However, variations in air content above three percent did not significantly increase durability.

2.6 EFFECT OF FLY ASH ON PROPERTIES OF CONCRETE

Fly ash is a byproduct formed by the combustion of pulverized coal in thermal power plants. Fly ash particles, which are spherical and range in size from 1 to 150 um, are separated from the flue gas using mechanical collection systems or electrostatic precipitators (29). Carbon particles, often found mixed with the fly ash, are the result of incomplete combustion (29). Fly ash can be useful as an admixture in concrete because it often exhibits pozzolanic properties. A pozzolan is defined as a siliceous or siliceous and aluminous material which in itself possesses little or no cementitious value but will in finely divided form and in the

presence of moisture, chemically react with calcium hydroxide at ordinary temperatures to form compounds possessing cementitious properties (30).

The correct use of fly ash should lead to a mix design which requires less portland cement than a similar mix without fly ash (25). If the unit cost of fly ash is less than that of portland cement, considerable cost savings may be achieved. However, the primary purpose of fly ash is to impart specific engineering properties to both the fresh and hardened concrete (25,29).

Fly ash affects the rheological properties of fresh concrete (29). Because of its spherical shape and small size, fly ash usually acts to give the mix added workability for the same amount of mix water (29,31,32). The probable mechanism is that the fly ash particles act as lubricating spheres in a manner similar to entrained air bubbles (25). Fly ash is also known to decrease bleeding and segregation (25,30,32). Although mineral admixtures can be used to supplement sand that is low in fines, air entrainment is usually used to increase workability for reasons of economy and its effect on freeze-thaw durability (32). Fly ash is also useful for use in mass concrete because it acts to lower the temperature rise associated with hydration (25,29,32).

Fly ash also affects the properties of hardened concrete. For concretes with equal air contents, a straight one to one substitution of fly ash for cement usually results in a reduction of strength at an early age but leads to greater strength as the concrete matures, provided adequate curing is provided (25,29,32,33). While this gradual strength gain may be acceptable in mass concrete, structural and pavement concretes generally require higher early strengths (32). Fortunately, strengths can be manipulated to equal portland cement concrete at any age (29). This is

achieved by replacing the cement removed from the mix with a greater weight of fly ash (29,32).

Fly ash has a similar effect on permeability. Permeability is higher at first because of the reduced effect of hydration. However, with time permeability becomes lower due to the gradual reaction of fly ash to calcium hydroxide which is formed as cement hydrates. A number of researchers (25,29,32,34,35) have reported that fly ash concrete is less susceptible to alkali-aggregate reactions than ordinary concrete.

2.6.1 Effect of Fly Ash on Air Entrainment

Larson (36) has demonstrated that fly ash has a negative effect on the amount of air entrainment in cement paste. This reduction is likely caused by carbon black particles in the fly ash which have the capacity to absorb the surface active compounds used for air entrainment (31,36). A linear relationship was noted between air entraining agent demand to maintain a particular air content and the loss on ignition of fly ash (36).

2.6.2 Effect of Fly Ash on Freeze-Thaw Durability

There are many conflicting reports on the effect of fly ash on concrete freeze-thaw durability. This may be due in part to differences in the test procedures and curing methods used by various researchers (34). Another reason may be that fly ash, being the product of a relatively uncontrolled process, is a highly variable material and as such its influence on engineering properties of concrete will vary with time and location.

In his review of the performance of fly ash in concrete, Abdun-nur (34) states that with proper curing and air entrainment fly ash concrete

should perform adequately in a freeze-thaw environment, even though laboratory tests may show a somewhat lower durability in comparison to ordinary concrete. Larson (37) compared two fly ash concretes with a one to one substitution for 25 percent cement to a control mix without fly ash. In the first mix the air entrainment lost due to carbon adsorption was not compensated for while the air content of the second mix was brought up to the same percentage as the control specimens. Both fly ash mixes showed deterioration greater than the standard as measured by the change in sonic modulus. However the first fly ash mix, which was essentially non-air entrained, failed after only five cycles even though it had the highest strength. Significant deterioration of the air entrained fly ash mix did not occur until after 300 cycles of freeze-thaw had been completed.

Larson (36) noted that interpretation of freeze-thaw results could be misleading if the fly ash and ordinary concrete did not have equal strength and air entrainment. If strength and air entrainment were non factors, fly ash and ordinary concrete were found to be equally durable. Fly ash was thought to affect the air entraining agent demand, not the structure of the air entrained paste.

Pasko and Larson (31) found that the effect of fly ash on freeze-thaw durability could not be statistically separated from the effect of variations in air content. Their results showed that the resistance of fly ash concrete was very sensitive to variations in air content close to four percent just as in ordinary concrete. They concluded that small variations in air content had masked the effect of fly ash on freeze-thaw

durability.Washa and Withey (33) noted that Chicago fly ash seemed to have neither a beneficial nor an adverse effect on freeze-thaw deterioration.

Bollen and Sutton (38) performed laboratory tests which showed reduced axial elongation of concrete prisms containing fly ash. Higginson (32) stated that pozzolans decreased the resistance of concrete slightly unless unusually long moist curing was provided.

Klieger and Landgren (39) reported a 30 percent, one to one substitution of fly ash for cement had little effect on freeze-thaw durability of concrete subjected to outdoor exposure.

Chapter III

SPECIMEN PREPARATION, TESTING EQUIPMENT AND TECHNIQUES

3.1 INTRODUCTION

The purpose of this thesis was to conduct a parametric study on the effect of a fly ash admixture, availability of water, and air content of cement paste on D-Crack susceptibility and general freeze-thaw durability of concrete specimens. To this end, a procedure similar to that outlined for Method B in ASTM C666 (40) was employed. The procedure used was a modified one in that length changes were periodically recorded as opposed to measuring the reduction in sonic modulus of concrete specimens. The apparatus used in the test program will be described in greater detail in a later section. First, however, the criteria used for naming the mixes will be described.

3.1.1 Mix Designations

The coarse aggregate for the freeze-thaw program was supplied by two Winnipeg contractors, Building Products and Concrete Supply Limited, and Supercrete Limited. The testing program for this research consisted of two tests. The first test involved a comparison of the freeze-thaw durability of fly ash concrete and ordinary concrete control specimens. In this test three different coarse aggregates were used in the manufacture of concrete specimens. One aggregate type was supplied by Building Products, and test

specimens made with this aggregate were designated as series BP1. Similarly, concrete specimens made with two aggregates supplied by Supercrete were designated as series S1 and S2.

The second test was concerned with the effect of external water and air content of cement paste on durability of concrete. Only one aggregate type was used in this test run, which was supplied by Building Products. In this case the series were designated by the air content of the mix. The aggregate supplied by Building Products was from their Birdshill CN pit. Aggregates supplied by Supercrete were from their pit near Richter, Manitoba. Fine aggregate for all testing was supplied by Building Products from their CN pit. All aggregates were taken from natural gravel deposits.

3.2 PHYSICAL PROPERTIES OF AGGREGATE

ASTM standard tests were performed on all aggregates to determine dry rodded unit weight, bulk specific gravity (saturated surface dry condition), and 24 hour absorption values (41,42,43). In the case of the first freeze-thaw test, the maximum particle size (top size) was obtained from the contractor. These values are recorded in Table 3.1. For the first test the aggregates were incorporated into the mixes as received, at the request of Transport Canada, in order to duplicate field conditions as closely as possible. For the second test the coarse aggregate was sieved and recombined in the desired gradation. Aggregate gradations used in the second test are given in Section 5.2.

Fly ash for the first test was obtained through Supercrete from the Saskatchewan Power Corporation. Physical and chemical analysis of the fly ash used in the testing program was performed by the Coal By-Products Utilization Institute at the University of North Dakota and is given in Appendix A.

Table 3.1

Characteristics of Coarse Aggregate

Fly Ash Test

Supplier	Mix Designation	Top Size (mm)	Dry Rodded Unit Weight (kg/m^3)	Bulk Specific Gravity	24 Hour Absorption (%)
Building Products	BP1	20	1710	2.67	2.02
Supercrete	S1	28	1600	2.66	1.58
Supercrete	S2	14	1640	2.63	2.40

External Moisture/Air Content Test

Supplier	Mix Designation	Top Size (mm)	Dry Rodded Unit Weight (kg/m^3)	Bulk Specific Gravity	24 Hour Absorption (%)
Building Products	A1.9, A5.0, A8.5	25	1792	2.68	1.66

3.3 MIX SPECIFICATIONS

Specifications employed by Transport Canada (44) were used as a guide when mixing trial batches in order to ensure desirable engineering properties in the fresh and hardened concrete. These specifications are shown in Table 3.2. Once it was determined that a mix design met the criteria for the characteristics of fresh concrete the quantity of the batch was scaled up and the test specimens were poured. In some instances the mix properties changed when the batch size was upscaled and as a result occasionally some of the values were slightly outside the specified range. It is felt that the effect of these variations was minimal. The mix designs for the fly ash test were determined by Glenn Hermannson (44). Mix design development for the mixes in the external moisture/air content test are given in Appendix B.

Table 3.2

Mix Specifications

Water/Cement ratio = w/c = 0.45
Slump = 50 mm + 10 mm
Air Content of Concrete = 5% + 1%
28 Day Compressive Strength = 25 MPa

3.4 MIXING PROCEDURE

Coarse aggregate for the mixes in the testing program was prepared as follows:

1.) Coarse aggregate was sieved into graded fractions (second test only).

2.) Coarse aggregate was oven dried to constant weight.

3.) The required dry weight of each coarse aggregate fraction was weighed out and then recombined in the desired gradation (second test only). In the fly ash test the quantity of coarse aggregate required by the mix was weighed out as one unit.

4.) The coarse aggregate was soaked for 24 hours in water prior to mixing.

5.) Coarse aggregate was drained, left in a slightly wet condition, and weighed to determine the amount of free water on the surface of the aggregate. The difference between the weight of the aggregate and the calculated saturated surface dry (SSD) weight is the weight of water in excess of that required to create a SSD condition. This weight was subtracted from the amount of mix water to be added to the mix.

The fine aggregate was prepared for mixing as follows:

1.) Fine aggregate was oven dried to constant weight.

2.) The required batch quantity was weighed out.

3.) It was assumed that the fine aggregate would absorb 80 per cent of its 24 absorption value while in the mixer (45). This weight was added to the mix water.

When preparing both trial and actual batches the aggregates were placed in the mixer first and mixed thoroughly. The Portland Cement (type

10 normal) was then mixed thoroughly with the aggregate. The mix water, which contained the air entraining agent, was then added to the mixer. When the mix was deemed homogeneous, slump and air content measurements (by the pressure method) were performed on the fresh concrete. Successive trial mixes were prepared in this way until the properties of the fresh concrete were within the above specifications. At this time the trial mix quantities were scaled up to a quantity sufficient to form the required number of specimens for the test series and compression test cylinders. If for some reason the larger batch did not meet the specifications for fresh concrete, the batch was discarded and the mix design altered slightly if it was felt that the mix characteristics would significantly affect the freeze-thaw test results. A new batch would then be made following the procedure outlined above. Freeze-thaw specimens were formed only after the properties of the fresh concrete were deemed acceptable. In the fly ash test air content and slump were measured. In addition to these properties, density of the fresh concrete was also determined in the external water/air content test.

3.5 SPECIMEN MOLDS AND FORMATION

Once it was determined that the engineering properties of the fresh concrete were satisfactory, the concrete was cast into molds with dimensions of 76 * 76 * 350 mm as quickly and carefully as possible. The molds were constructed of clear Plexiglas using a tongue and groove system which could be easily assembled for use or disassembled for cleaning. A photograph of a specimen mold is shown in Figure 3.1. As mentioned previously, the deterioration of the specimens were monitored by periodically measuring residual axial length changes after repeated cycles

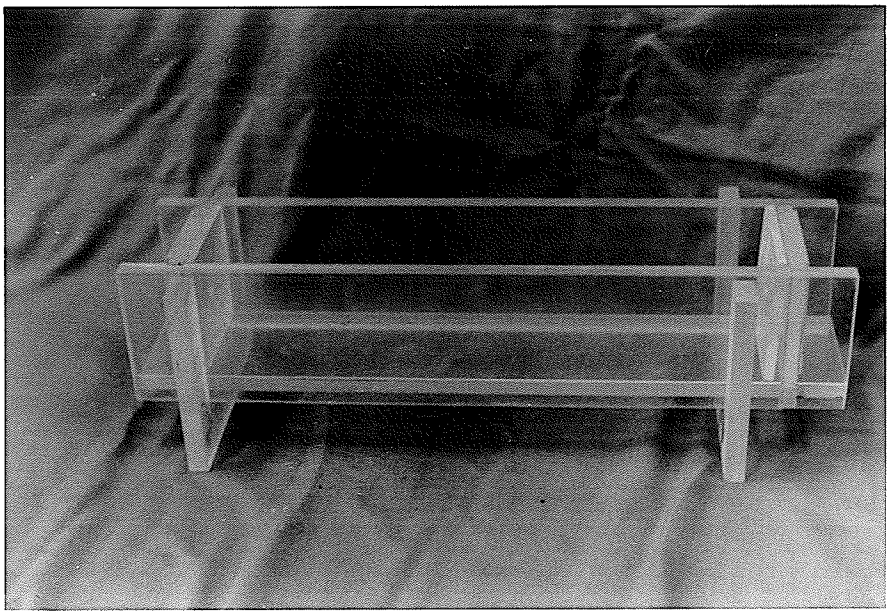

Figure 3.1: Photograph of Plexiglas Specimen Molds

of freeze-thaw. Rigid reference points on the specimens that would not deteriorate with time were required. For this reason 6.3 mm diameter hex bolts 25 mm in length were embedded in the specimen. Only the ends of the bolts, which were machined to a 6.3 mm radius were left protruding.

In the fly ash test concrete was placed in the molds in two lifts. Each lift was compacted using a 9.4 mm diameter bullet-nosed tamping rod. In the external moisture/air content test concrete was compacted in two lifts on a vibrating table. Both procedures were in accordance with ASTM C192 (46). Specimens were then struck off and finished with a trowel. Care was taken not to over work the mix while finishing.

Compression test cylinders were then poured, two for seven day compression tests and three for 28 day tests. Cylinders 150 mm in diameter and 300 mm in height were usually used except for cases when coarse aggregate was in short supply, in which case cylinders 100 mm in diameter and 200 mm in height were employed. After striking off the compression test cylinders the specimens and cylinders were placed in a 100 per cent humidity curing room. After 24 hours the molds of both the freeze-thaw specimens and the compression cylinders were removed and the specimens and cylinders marked for identification. Individual freeze-thaw specimens were identified either by the type of coarse aggregate they contained or by air content, depending on the test, as discussed previously. Each specimen from a particular mix was also marked with a numerical suffix to differentiate it from others formed from the same mix. The date the specimens were poured was also recorded. Compression test cylinders were identified by mix designation and date poured.

As noted above, compression tests were performed on the concrete cylinders after seven and 28 days. Cylinders were first removed from the curing room and towelled dry. The remaining surface water was allowed to evaporate. The cylinders were then capped with a sulfur compound, which was allowed to cure for several hours, and tested in compression using a constant strain rate loading machine. Compressive strengths will be reported in the following chapters.

Since it was not possible to pour all test series on the same day, freeze-thaw specimens were cured until the "youngest" series had cured for 28 days. After this time the specimens were removed from the curing room and the freeze-thaw test commenced.

In the case of the second test, specimens to be coated with an epoxy

sealant were removed from the curing room, towelled dry, and coated immediately with the epoxy sealant and allowed to dry overnight. The following day a second coating was applied and allowed to dry overnight in a similar fashion. After the epoxy was dry the remaining specimens were removed from the curing room and the test was commenced.

3.6 EXPERIMENTAL EQUIPMENT

Testing equipment consisted of an automated M & L freeze-thaw cabinet, a length comparator meeting the requirements of ASTM C490 (47), and a temperature bath. The characteristics of this equipment and modifications made prior to testing are discussed in the following subsections.

3.6.1 Freeze-Thaw Apparatus

The testing program entailed the use of automated freeze-thaw equipment. To this end an M & L freeze-thaw cabinet was employed, a photograph of which is shown in Figure 3.2. A previous study at the University of Manitoba indicated that ASTM C666 Method B test results correlated well with service records (2,44). The test involved freezing in air from 4°C to -18°C and thawing in water from -18°C to 4°C. The above process entails one freeze-thaw cycle.

3.6.1.1 Description of the Apparatus

Basically, the equipment consisted of an insolated cabinet approximately 2 meters in length, 0.75 meters in width, and 0.25 meters in depth. The cabinet itself rested on a metal frame which held it approximately one meter above the floor. A refrigeration unit was mounted on the frame supporting the freeze-thaw apparatus. An insolated tank

constructed of sheet metal which served as a reservoir was also located under the freeze-thaw cabinet.

A cooling panel, which rested on the bottom of the cabinet, was connected to the refrigeration unit. A sheet metal specimen tray was placed on top of the cooling panel. Since a gentle two directional slope was required for the pumping/drainage system, the tray was constructed approximately 125 mm deep in order to ensure that the 75 mm high specimens would be completely covered with water during the thawing portion of freeze-thaw cycles. Warming panels were attached to the outside of the specimen tray to increase the temperature of the thawing water and hence the temperature of the specimens

A switching device was used to supply power alternately to the freezing and thawing equipment. A thermostat was connected to a temperature probe which was inserted into a specially formed temperature control specimen. The mold for this specimen was fitted with end mounts that created cylindrical cavities in the ends of the specimen. During testing the temperature probes were fitted into the cylindrical cavities and sealed with a plastic putty to prevent water from entering the cavity. The cavities were checked for leakage approximately every 30 cycles and drained if necessary. When the temperature inside the control specimens reached 4^{o}C, power was diverted to the freezing unit. Similarly, when the temperature inside the temperature control specimen dropped to -18^{o}C, power was diverted to the thawing unit. A photograph of the freeze-thaw cabinet control panel is shown in Figure 3.3.

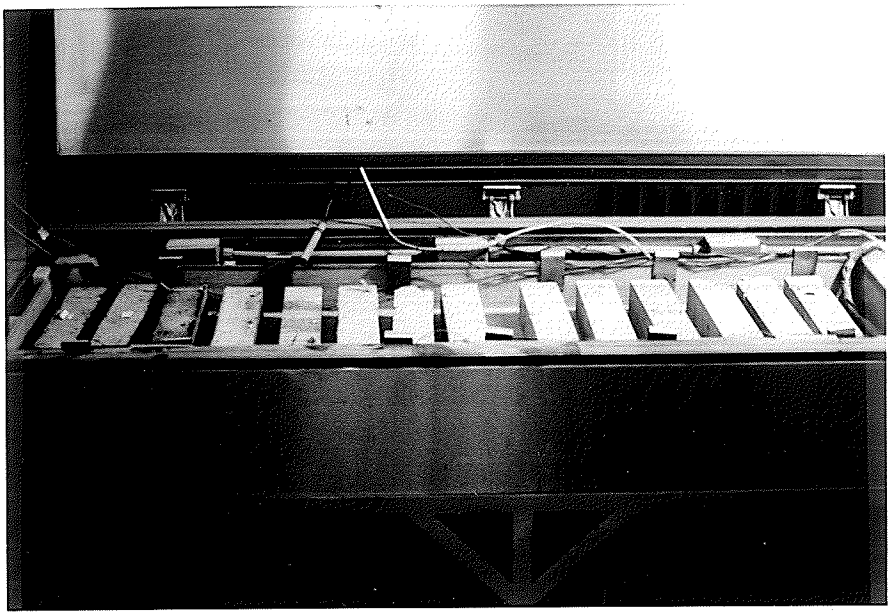

Figure 3.2: Photograph of the Freeze-Thaw Cabinet

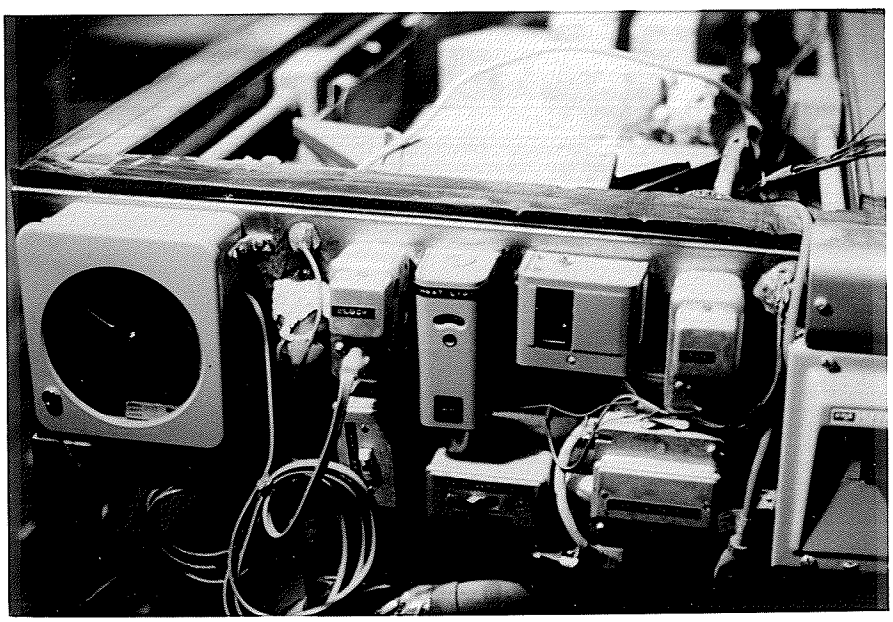

Figure 3.3: Photograph of the Control Panel of the Freeze-Thaw Cabinet

3.6.1.2 Capabilities of the Apparatus

The cabinet employed for the testing program was equipped with adjustable temperature limits. However, the freezing or thawing rate of the specimens could not be adjusted. This is an important point because the freezing rate plays an important role in the generation of hydraulic pressure as discussed in Chapter 2. Early correlations of results from freeze-thaw programs involving large freezing rates (often in excess of 50°C per hour) with field records did not lead to encouraging results (8). While large cooling rates reduced the time required to perform the tests, the tests did not adequately simulate environmental conditions which occurred in the field. Instead, concrete specimens were subjected to an environment many times more severe than could possibly be expected outdoors. The maximum cooling rate of the specimens in the writer's test program was approximately 10°C per hour. Time-temperature curves for the interior of the temperature monitoring specimen were recorded on circular charts automatically and are shown in Appendix C.

3.6.2 Modifications to the Freeze-Thaw Apparatus

The freeze-thaw cabinet at the University of Manitoba originally could only perform Method A of the ASTM C666 test; that is both freezing and thawing in air or freezing and thawing in water. As noted above, a better correlation with service records has been observed with Method B. Intuitively, this method seems to most accurately model field conditions since one would expect drainage conditions to be poor during periods of melting. Also, Method A calls for the specimens to be held in rigid containers which are subsequently filled with water and subjected to freezing. The containers are often damaged by the pressure created by the

volume increase of water as it freezes. Of course, the concrete specimens are also subjected to this pressure and care must be taken when interpreting test results using this procedure. For these reasons the cabinet was modified to perform the Method B test. However, after an initial test run it became apparent that further modifications would be necessary to increase the reliability of the cabinet and increase the quality of the results. To this end the drainage system and water reservoir were redesigned. The pumping system was changed to incorporate a water circulation phase during the thaw period to minimize temperature gradients in the thaw water. Modifications to the pumping/drainage system will be examined first.

3.6.2.1 Pumping/Drainage System

The new drainage system was comprised of four phases, each corresponding to a different interval within a freeze-thaw cycle. This was accomplished by wiring the drainage system into the switching mechanism. The four phases occur in sequence as follows:

1.) Phase one consisted of filling the specimen tray with water in a manner such that all of the specimens were completely submerged. No water would be present in the specimen tray during the freezing portion of a freeze-thaw cycle. However, when the temperature probe detected that the temperature at the center of the specimen had reached -18^{o}C, the thermostat diverted power to the thaw equipment (this consisted of warming panels attached to the sides of the specimen tray). At this time the first phase of the drainage system was activated because it was also wired to the thermostat. Phase one was terminated when the specimen tray was filled and all of the

specimens were completely submerged. This is accomplished through the use of a timer. A trail and error method using dummy specimens prior to testing was used to determine the timer setting and hence the proper volume of water to be pumped from the reservoir to the specimen tray.

2.) The second phase of the drainage sequence involved the circulation of water in the specimen tray to minimize temperature gradients. In phase one the timer was set to fill the specimen tray. At the completion of this task the timer tripped a circuit and power (within the pumping/drainage system itself) was diverted to another pump which circulated the water in the tank. This phase continued until the temperature at the center of the temperature monitoring specimen reached 4°C. At this point the switching mechanism was again tripped and power was diverted back to the freezing equipment.

3.) The third phase consisted of draining the specimen tray at the beginning of the freezing portion of the freeze-thaw cycle. When the switching mechanism activated the refrigeration system used for the freezing portion of the freeze-thaw cycle, power was also supplied to a second circuit in the pumping/drainage system used to drain the specimen tray. Because the freeze-thaw cabinet was gently sloped with the water inlet/outlet positioned at the lowest elevation, it would have been possible to drain the cabinet using gravity alone. However, in order to ensure the inlet/outlet pipe would not become clogged with ice, phase three consisted of draining with the aid of a pump as well as by gravity. Again, a timing mechanism was utilized to turn off the pump before the water level in the specimen tray became too low and air became trapped in the pump which would render it inoperative for

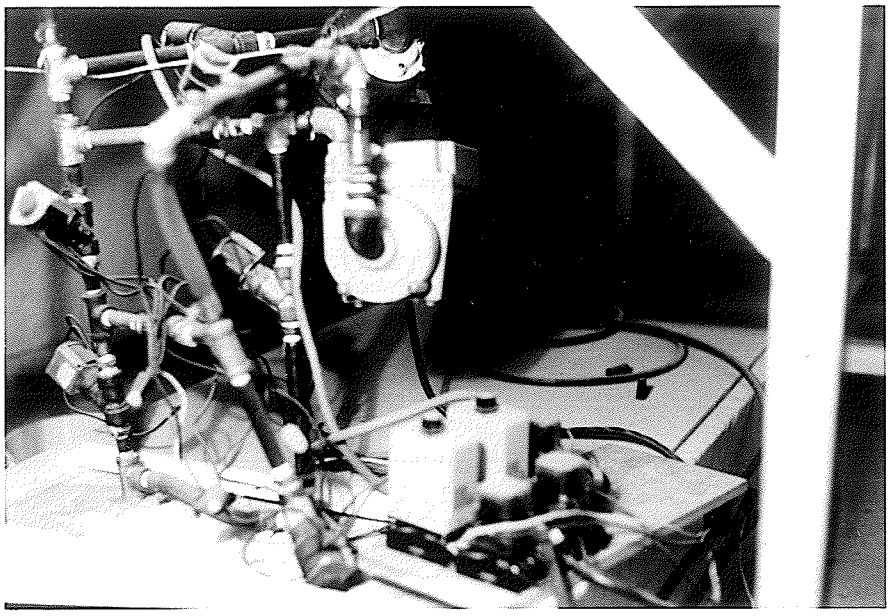

Figure 3.4: Photograph of the Pumping/Drainage System and Supporting Circuitry

the next time its use was required.

4.) The fourth phase consisted of draining the remainder of the water in the specimen tray by gravity. The fourth phase remained in operation until the start of a new thawing cycle.

Figure 3.4 shows a photograph of the pumping/drainage system and the supporting electronic circuitry.

Other modifications were also introduced to the system. The old specimen tray was warped and therefore replaced. As well, slight modifications in design were required to accommodate the new water inlet/outlet system. The air circulation system was equipped with a more

powerful fan and deflector panels were employed in order to maximize turbulent flow of both air and water around the samples and hence minimize temperature gradients within the cabinet.

3.6.3. Temperature Bath

A temperature bath was constructed for the testing program. Previously, prisms were held at 4°C and length measurements taken at room temperature. It was felt that length readings would be more reliable if the temperature of the specimens was brought up to that of the ambient conditions during measurement.

The temperature bath consisted of two 61 mm diameter tanks connected by two pieces of steel tubing. A pump was connected to one of the steel pipes. One tank contained a heating element; the other served as a reservoir for the specimens. The temperature of the holding tank was monitored continuously and the thermostat set at 22°F. Samples were placed in the temperature bath for a minimum of three hours to ensure no temperature gradients existed within the sample at the time of length measurement. A photograph of the temperature bath is shown in Figure 3.5.

3.6.4 Length Comparator and Length Measurement Technique

A length comparator similar to that described in ASTM C490 (47) was used to measure axial length changes in the specimens as the test proceeded. Reading were taken with a precision of 0.005 mm. A photograph of the length comparator used in the testing program is shown in Figure 3.6. The procedure used to obtain length measurements was as follows:

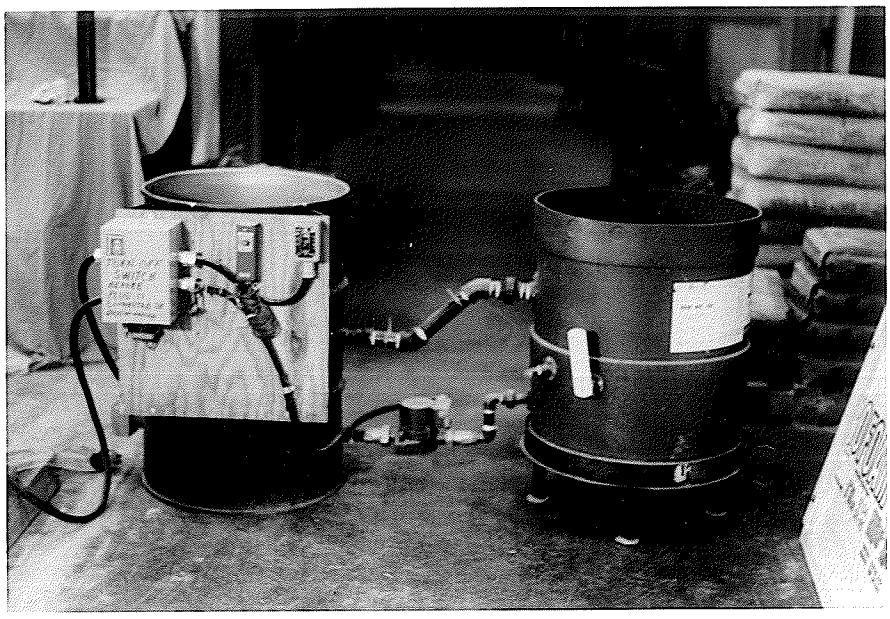

Figure 3.5: Photograph of the Temperature Bath Used in the Testing Program

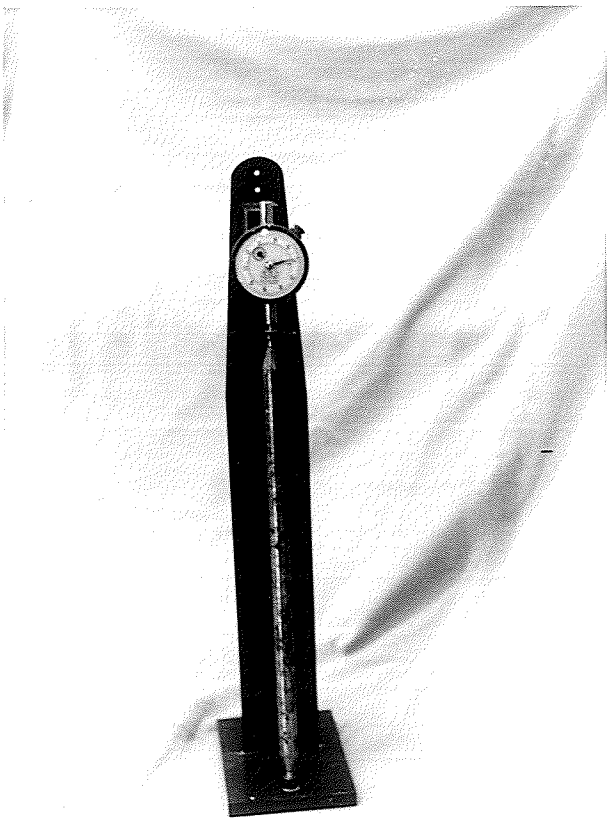

Figure 3.6: Photograph of Length Comparator Used to Determine Axial Length Changes of the Test Specimens

1.) Before the start of the test (in order to determine the initial length), and approximately every thirty cycles thereafter, the specimens were removed from the freeze-thaw cabinet during a thaw cycle and placed in metal racks or baskets which were then placed in the temperature bath. At the beginning of a test the specimens were removed from the curing room and placed directly in the temperature bath. An exception to this rule occurred in the second test when some samples were first coated with an epoxy sealant. At this time the cabinet was turned off to prevent the continuation of freeze-thaw cycles.

2.) All specimens from a particular test series were removed from the temperature bath and placed in the length comparator. Prior to testing, all specimens were arbitrarily marked with an arrow. The end the arrow was pointing toward was designated "north" and the measuring peg located on that end of the specimen was always inserted into the uppermost recepticle on the length comparator. An exception to this rule occurred in the second test run when some specimens were coated with an epoxy sealant. For these specimens metal tags were attached at the "south" end and the measuring peg closest to the metal tag were always inserted into the lower receptacle on the length comparator.

3.) The specimen was rotated slowly clockwise until the dial gauge reading approached a constant value. At this point the length was recorded and the specimen examined for signs of distress. A subjective rating scheme was used to rate the relative severity of the distress that occurred. These comments are recorded in Appendix D.

4.) After axial measurements were taken and distress recorded, the specimen was returned to the freeze-thaw cabinet three positions to

the right of where it was removed and rotated 90 degrees. This was done to minimize the possible effect of temperature gradients, thereby assuring that all specimens were subjected to the same environmental conditions over the course of the test.

5.) After the above procedure was completed for all specimens, the freeze-thaw cabinet was activated and the test continued until 300 freeze-thaw cycles had been completed. At this point the temperature at the center of the temperature control specimen would have increased to over 4°C and a freeze cycle would commence immediately.

The length of the specimens was obtained by comparing the recorded dial reading to the dial reading of a steel rod of known length. The original length of a specimen, or the length at any time in the test, is given by the following equation:

$$L = A - (B - X) \qquad (2)$$

where:

L = Length of the specimen at 22°C in mm.

A = 355.600 mm = Length of steel rod determined with calipers at 22°C.

B = Dial reading in mm which was preset on the measuring gauge when steel bar was measured.

X = Dial reading on gauge when specimen was being measured.

The axial elongation of a specimen at any time in the test is given by:

$$E_{(cycle)} = \left[\frac{L_{(cycle)} - L_o}{L_o}\right] * 100 \qquad (3)$$

where:

$E_{(cycle)}$ = Residual axial elongation after a given number of cycles at 22°C expressed as a percentage.

$L_{(cycle)}$ = Length of a specimen after a given number of cycles at at 22°C in mm.

L_o = Original length of specimen at 22°C in mm.

Chapter IV

EFFECT OF FLY ASH TEST

4.1 INTRODUCTION

Laboratory testing for this study consisted of two freeze-thaw tests. The results and analysis of the first test involving the partial replacement of cement with fly ash in the mix design are presented in this chapter. Before examining the effect of a fly ash admixture on general freeze-thaw durability and D-Cracking of PCC freeze-thaw specimens, some properties of the mixes involved in this test run are examined.

4.2 PROPERTIES OF CONCRETE MIXES

Basically, three similar mixes containing three different coarse aggregates were employed for the first test. Three additional mixes were then prepared simply replacing 20 per cent of the cement (by weight) with fly ash.

Previous research has shown that a reduction in the top size of coarse aggregate used in a mix can reduce or eliminate D-Cracking (1,2,5,7,19). However, associated with a decrease in the top size is an increase in the unit cost of concrete due to an increased cement content. This cost increase could be lowered or eliminated by the partial replacement of cement with fly ash.

Aggregate properties of interest are given in Table 4.1 (44). Mixes

were designated by the supplier of the coarse aggregate they contained. For example, specimens poured from the mix containing coarse aggregate supplied by Building Products were designated as series BP1. Additionally, if the mix contained fly ash the letters FA were appended. Finally, a numerical suffix was added in parenthesis to distinguish between specimens formed from the same mix. Aggregates were incorporated into the mixes as received by the university in an effort to duplicate field conditions as closely as possible. The table shows that the mineralogy of all the coarse aggregates used in the test was predominantly carbonate.

The fine aggregate used was the same for all test series. The fine aggregate gradation for mixes involved in the first test is given in Table 4.2.

The characteristics of the mix designs used in the test are given in Table 4.3. The table shows that the fly ash mixes are identical to the control mixes except that 20 percent of the cement (by weight) was

Table 4.1

Properties of Coarse Aggregates

Supplier	Designation	Top Size (mm)	Absorption (%)	Mineralogy[1] Carb.	Ign.	Other
Building Products	BP1	20	2.02	75	23	2
Supercrete	S1	28	1.58	70	27	3
Supercrete	S2	14	2.40	59	35	6

Table 4.2

Fine Aggregate Gradation Used in the Fly Ash Test

Grain Size	Percent Passing
9.42 mm	100.0
4.76 mm	99.0
2.38 mm	86.4
1.19 mm	67.9
0.60 mm	40.0
0.21 mm	15.8
0.15 mm	4.4

replaced by an equal weight of fly ash. In order to maintain a constant w/c ratio for all test series, the water content of the fly ash mixes was reduced by a factor of 0.45 times the weight of the the cement replaced by fly ash.

Characteristics of fresh and hardened concrete are given in Table 4.4. Note that even though the amount of air entraining agent added to the mixes was the same or greater for the fly ash mixes, the amount of air entrainment actually measured by the pressure method was always less for the mixes that contained fly ash. This is due to the fact that fly ash contains carbon black particles which escaped the combustion process and act to absorb the surface active compounds used to create entrained air bubbles as discussed in Subsection 2.6.1. As well, the 28 day compressive strengths of the fly ash concrete were significantly higher than the control mixes formed with the same coarse aggregate. The values of 28 day

Table 4.3

Characteristics of Concrete Mixes

Mix Characteristics	Mix Designation BP1	BP1(FA)	S1	S1(FA)	S2	S2(FA)
Total[1] Water (kg/m^3)	137	109	114	84	134	107
Type 10 Cement (kg/m^3)	304	243	253	186	298	238
Class F Fly Ash (kg/m^3)	0	61	0	47	0	60
Coarse[2] Aggregate (kg/m^3)	1281 1256	1281 1256	1227 1208	1227 1208	1140 1113	1140 1113
Fine[3] Aggregate (kg/m^3)	680	680	575	575	758	758
Air Entraining Agent (ml/m^3)	255	255	261	277	179	300
Water/Cement Ratio	0.45	0.45	0.45	0.45	0.45	0.45
Coarse/Fine Ratio (Dry)	1.85	1.85	2.10	2.10	1.47	1.47

[1]Total Water = All water added to the mix which contributes to the processes of hydration.

Total Water = calculated mix water - free water on coarse saturated coarse aggregate + water absorbed by fine aggregate (80% of 24 hour value).

[2]First value denotes saturated surface dry (SSD) weight, second value denotes oven dry weight.

[3]Dry weight.

Table 4.4

Characteristics of Fresh and Hardened Concrete

Mix Designation	Slump (mm)	Air Content (%)	Average 28 Day Compressive Strength[1] (MPa)
BP1	60	5.6	27.2
BP1(FA)	40	4.8	35.4
S1	50	7.4	20.4
S1(FA)	35	5.5	39.1
S2	65	6.0	28.1
S2(FA)	35	4.2	47.4

[1]Average of Three Cylinders.

compressive strength of the mixes are reproduced from Table 4.4 and presented graphically in Figure 4.1.

As an aside, a fly ash/ordinary PCC compressive strength comparison test was performed. The results of the test are plotted in Figure 4.2. The objective of the test was to observe the effect of fly ash, using the same replacement technique as in the main body of testing, on the development of compressive strength over time. The mix design used was similar to the second mix design used in the second test (see chapter 5) and similar to all three mixes used in the first test. The results are presented in Figure 4.2. Because the water content of the fly ash mixes was reduced to maintain a w/c ratio of 0.45 (not including fly ash), an increase in compressive strength was observed immediately. The increasing difference in compressive strength between the two mixes is an indication of the

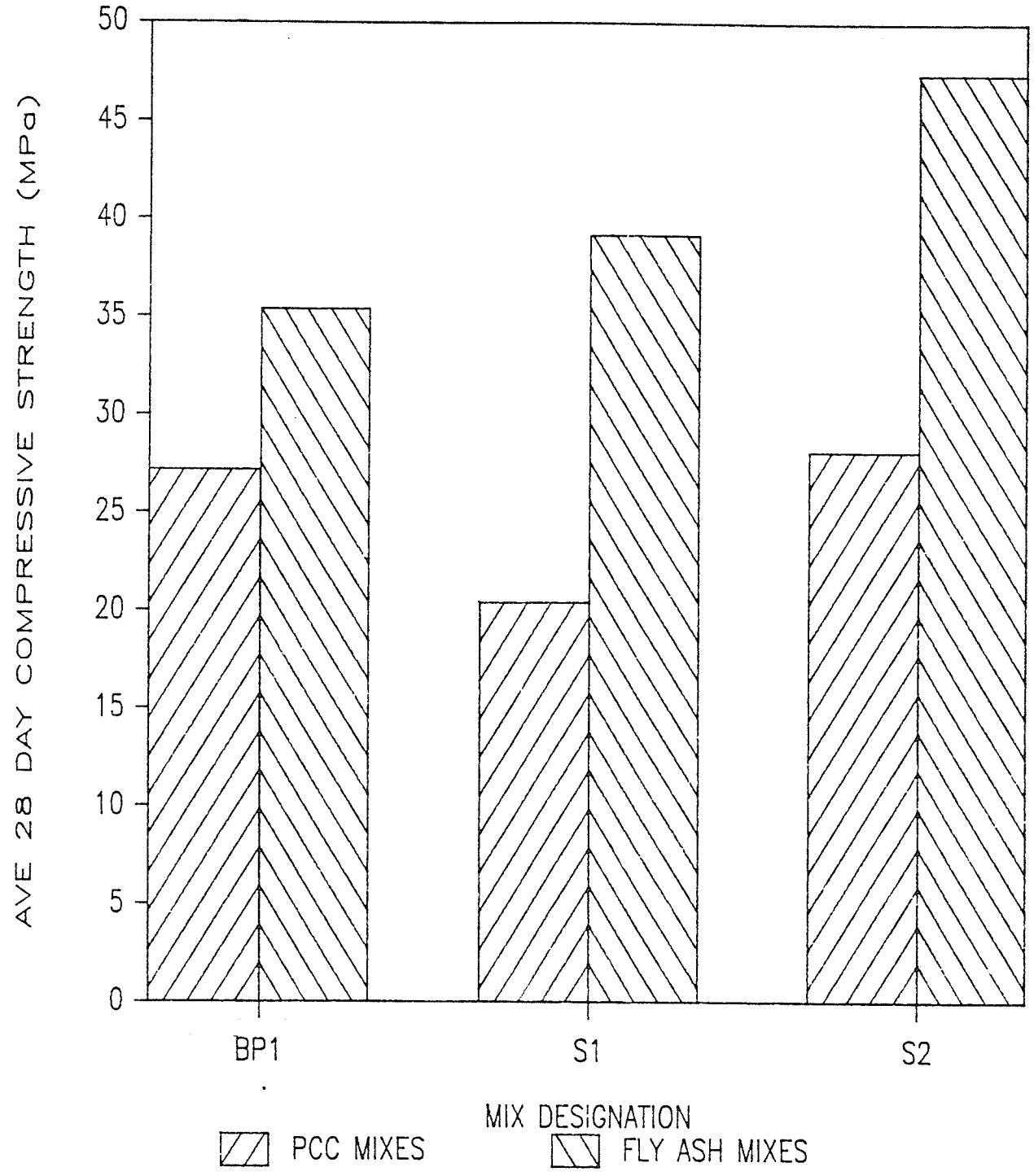

Figure 4.1: Comparison of 28 Day Compressive Strengths of of Ordinary PCC and Fly Ash Mixes Used in the Fly Ash Test

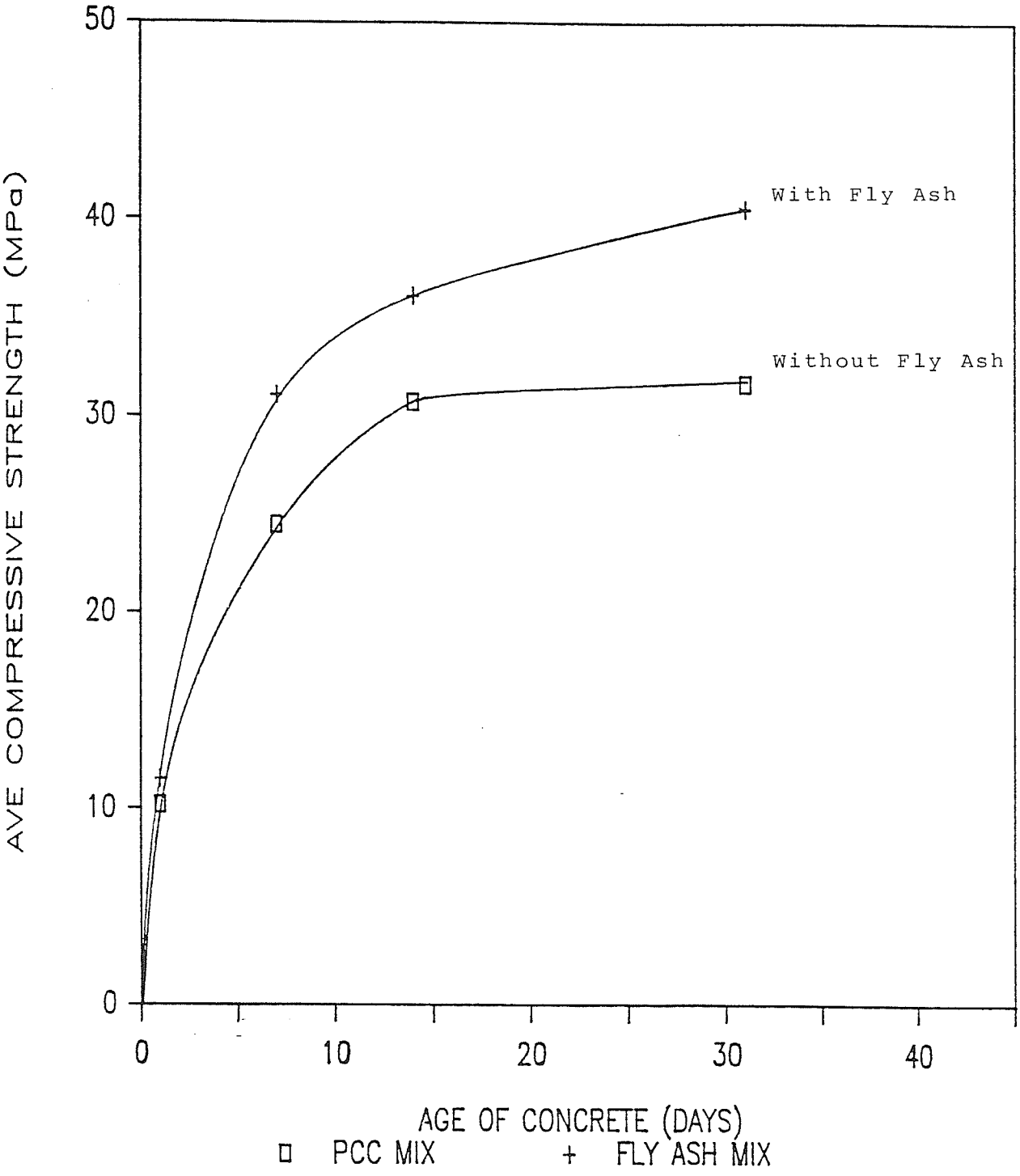

Figure 4.2: Strength Development of PCC With and Without Fly Ash

delayed contribution of fly ash to strength development which was discussed in detail in Section 2.6. The increased strength of the fly ash mix is also due to a decrease in the entrained air content caused by the carbon particles in the fly ash as mentioned above. The results of this test support the strength values obtained for the mixes used in the freeze-thaw test.

4.3 ACCEPTABILITY CRITERIA

The results obtained from the ASTM C666 test must be correlated to field performance. Thompson et. al (9) found that an axial expansion of 0.0032 percent after 350 cycles of laboratory freeze-thaw was the maximum permissible. A figure greater than this value could mean that the use of a similar mix in the field would lead to poor performance. However, a comparison of axial elongation values to observed distress (see Appendix D) on the surface of the specimens showed that all specimens were virtually free of distress whem the axial elongation value was 0.0032 percent. Therefore, this value may be overly conservative for use as an acceptability criteria in this area.

Traylor (2) found that specimens with less than 0.005 percent axial expansion after 350 cycles were associated with excellent field performance; 0.06 to 0.15 percent expansion indicated marginal performance; and axial expansions in excess of 0.20 percent were always associated with poor field performance. Therefore, an expansion acceptability criteria was set at 0.06 percent axial expansion after 350 cycles.

It is not possible to state that one of these values, or any other value, is applicable for use as an acceptability criteria in Manitoba

since an adequate data base has not yet been compiled. However, since Traylor's value seems to be reasonable based on the results of this testing program, it will be referenced occasionally to allow the reader to assign meaning to the axial elongation values in a qualitative fashion at least.

4.4 PERFORMANCE OF SPECIMENS FORMED WITH BUILDING PRODUCTS COARSE AGGREGATE

Six specimens or prisms used in the test were made with coarse aggregate supplied by Building Products. Three specimens, BP1(1,2,3), were made from an ordinary PCC mix. The remaining three specimens, BP1F A(1,2,3), were made from an otherwise identical mix in which 20 percent of cement by weight was replaced with an equal amount of fly ash.

A plot of axial elongation caused during freeze-thaw against number of freeze-thaw cycles for the three ordinary PCC specimens formed with Building Products coarse aggregate is shown in Figure 4.3. The uniformity of the three curves shows that the specimens performed in a similar fashion. This is significant in that it allows the use of the average performance to be used in comparisons to other mixes without misleading results. The plot shows that all three curves meet Traylor's acceptability criteria if magnitude of elongation is used alone. However, after a sharp initial increase in residual axial expansion the slope of the curves first decreased until about 250 freeze-thaw cycles had passed, after which time the curves began to accelerate upward. This acceleration suggests that there was an increase in frost susceptibility and failure may ultimately have occurred. Photographs of specimens BP1(2) and BP1(3) after 300 cycles of freeze-thaw are shown in Figures 4.4 and 4.5 respectively. Figure 4.4

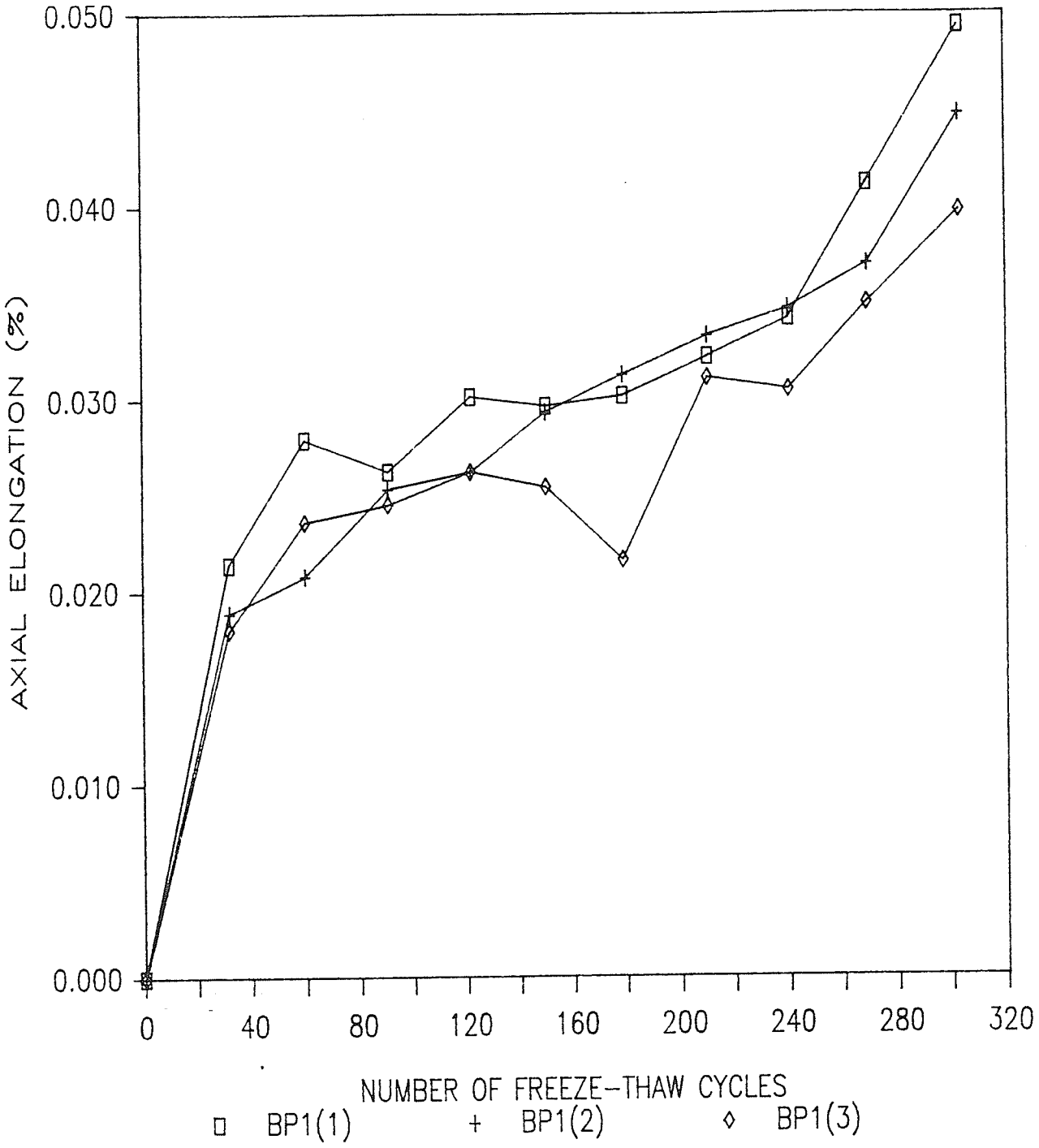

Figure 4.3: Freeze-Thaw Performance of Ordinary PCC Specimens Formed from Mix BP1.

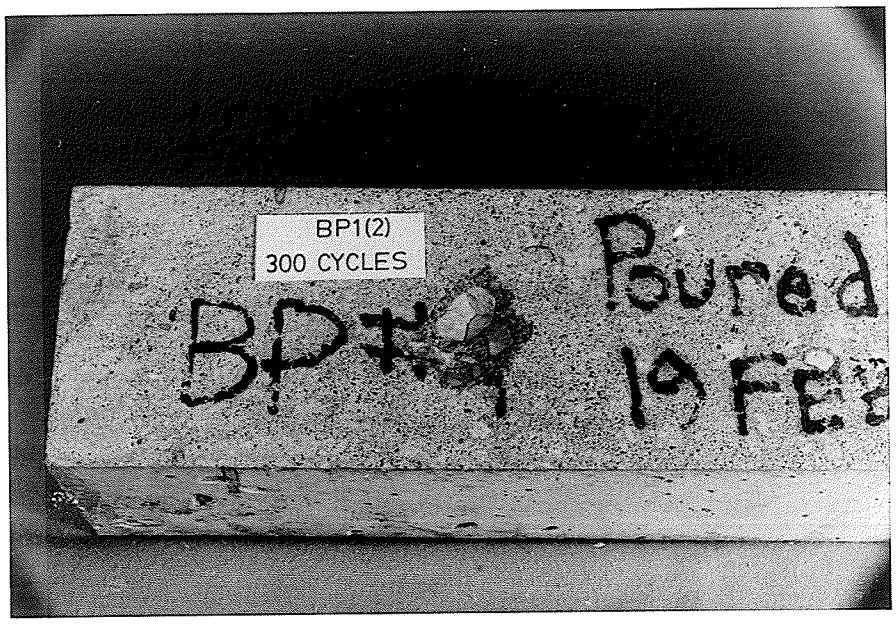

Figure 4.4: Photograph of Specimen BP1(2) After 300 Cycles of Freeze-Thaw Showing a Popout Caused by Frost Susceptible Aggregate.

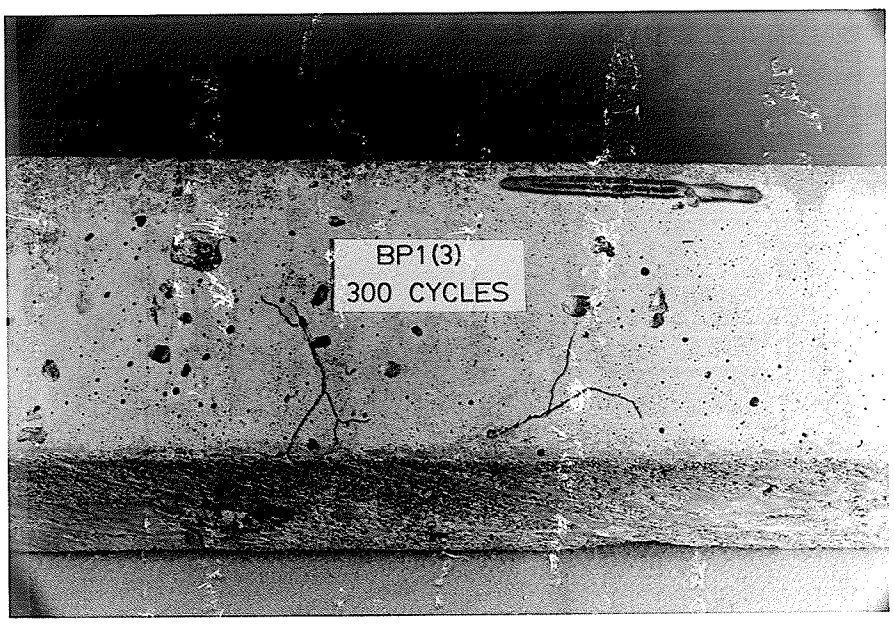

Figure 4.5: Photograph of Specimen BP1(3) After 300 Cycles of Freeze-Thaw Showing Minor Aggregate Related Distress.

shows a popout created by the failure of a piece of coarse aggregate located near the surface of the specimen. The photograph shows evidence of fracturing in the coarse aggregate. Minor cracking caused by freeze-thaw forces in specimen BP1(3) is shown in Figure 4.5. The cracks were outlined with a pencil to make them easier to see on the photograph. In both of the above cases the damage to the specimens was relatively minor which corresponds to the low values of axial expansion which were recorded.

The performance of specimens formed from a mix containing Building Products coarse aggregate and fly ash, designated as series BP1FA, is shown in Figure 4.6. The performance of all of the BP1FA specimens were similar up to approximately 120 cycles. Although the axial elongation values for specimen BP1FA(1) did not increase as dramatically as the other two specimens after this point in the test, it is still reasonable to employ the average behavior of the specimens to model the performance of this mix in view of the fact that there was no significant deviation in performance until the axial elongation values were well beyond the acceptability criteria. The plot shows that the axial elongation values for the BP fly ash specimens were substantially higher than those of the ordinary concrete BP specimens. In fact, all of the BP1FA specimens exceeded the axial expansion criteria for acceptability after approximately 90 cycles of freeze-thaw. A photograph of specimen BP1FA(1) after 300 cycles of freeze-thaw is given in Figure 4.7 The photograph shows both coarse aggregate distress and some scaling of the cement paste, which may indicate inadequate air entrainment or slight overworking of the mix after pouring. The significance of this possibility is discussed in a later section. The failure of specimen BP1FA(3) after 290 cycles is shown in Figure 4.8. Although some coarse aggregate distress is evident, a large

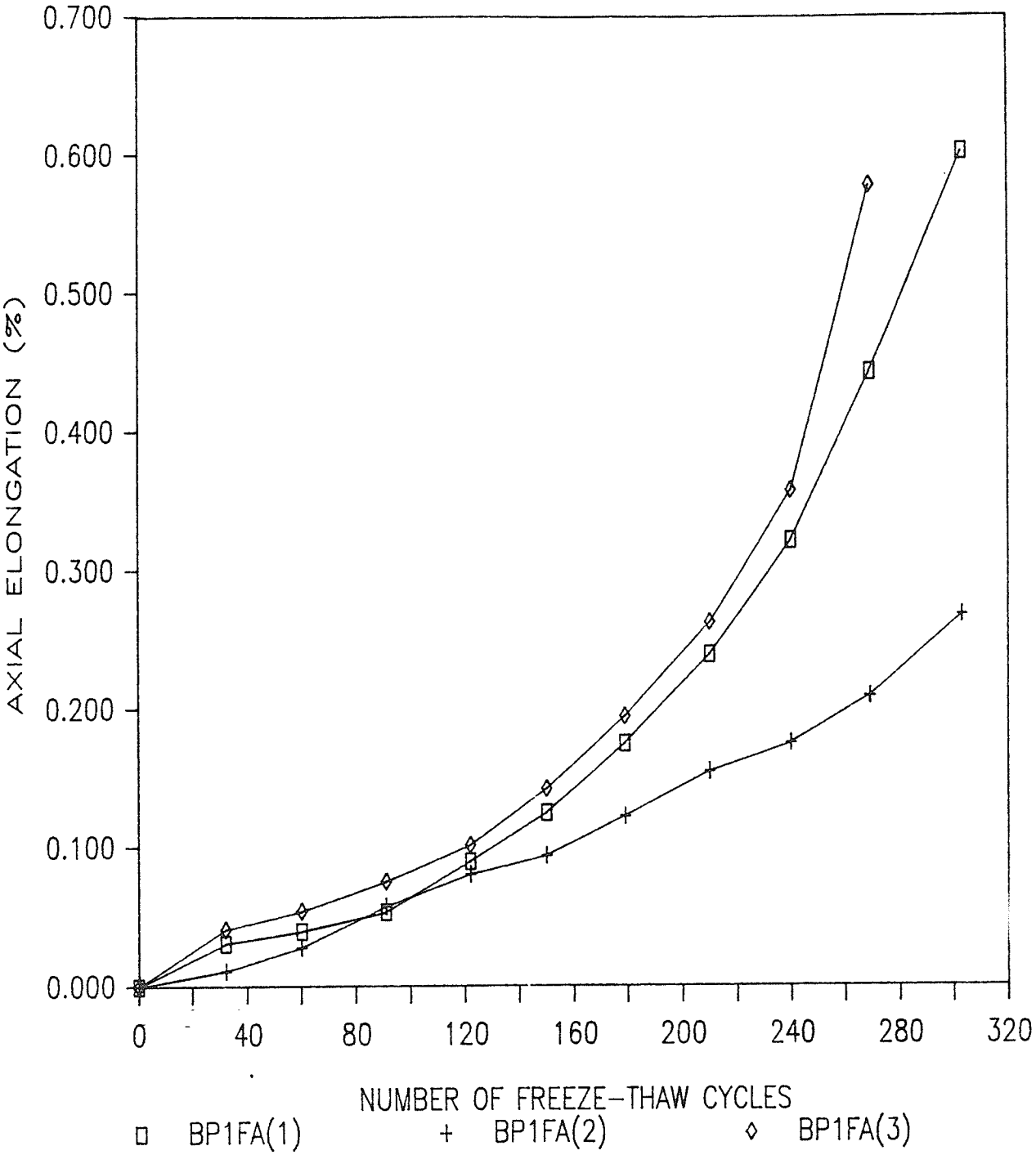

Figure 4.6 Freeze-Thaw Performance of Fly Ash Concrete Specimens Formed from Mix BP1.

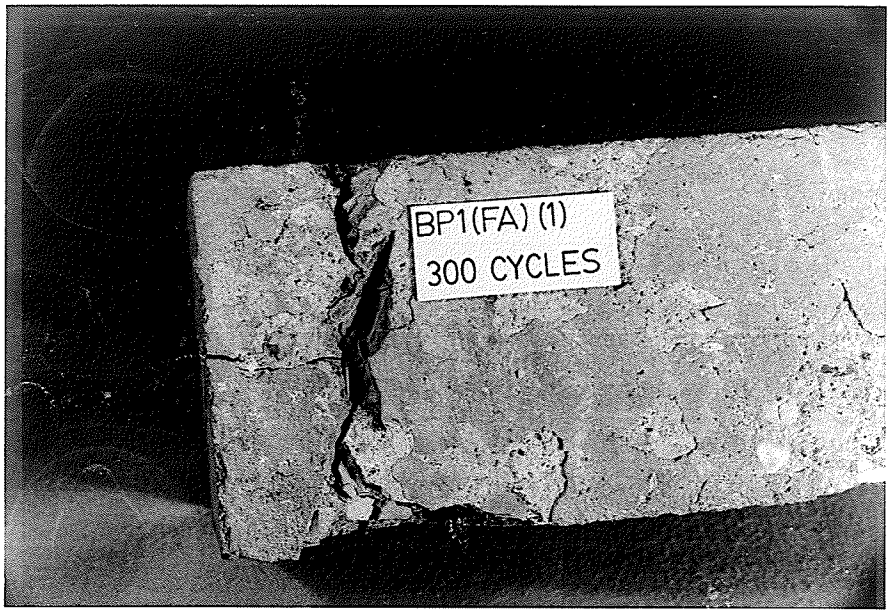

Figure 4.7: Photograph of Specimen BP1FA(1) After 300 Cycles Showing Aggregate and Paste Related Distress.

Figure 4.8: Photograph of Specimen BP1FA(3) After 290 Cycles of Freeze-Thaw Showing Aggregate Distress and and Aggregate/Paste Interfacial Failure.

portion of the failure appears to have occurred along coarse aggregate/cement paste interfaces.

4.5 PERFORMANCE OF SPECIMENS FORMED WITH SUPERCRETE TYPE 1 COARSE AGGREGATE

Three ordinary PCC specimens, designated as S1(1,2,3), were made from a mix incorporating coarse aggregate Type 1 supplied by Supercrete. The difference between the Type 1 and Type 2 aggregate was primarily gradation. Three additional specimens, S1FA(1,2,3), were also made from a similar mix containing fly ash substituted for 20 percent by weight of cement.

The performance of the specimens formed from an ordinary PCC mix when subjected to ordinary freeze-thaw conditions is shown in Figure 4.9. The specimens showed similar performance over the entire range of the test and can be represented by the average axial elongation of the specimens. The shape of the curves are similar to those of the ordinary PCC specimens formed with BP1 type aggregate in that an initially sharp rate of increase in axial elongation measurements at the start of the test was followed by a period when the performance of the specimens improved considerably. This "phase" of the performance curve was again followed by a period of exponential increase in axial expansion values beginning at about 250 cycles. As was the case with the BP series, all three specimens met the axial expansion expandability criterion of 0.06 percent proposed by Traylor (2), but the increase in the rate of expansion renders the criterion inconclusive. Photographs of damage caused by freeze-thaw forces in specimens S1(2) and S1(3) are shown in Figures 4.10 and 4.11 respectively. The cracks were outlined with a pencil for ease of

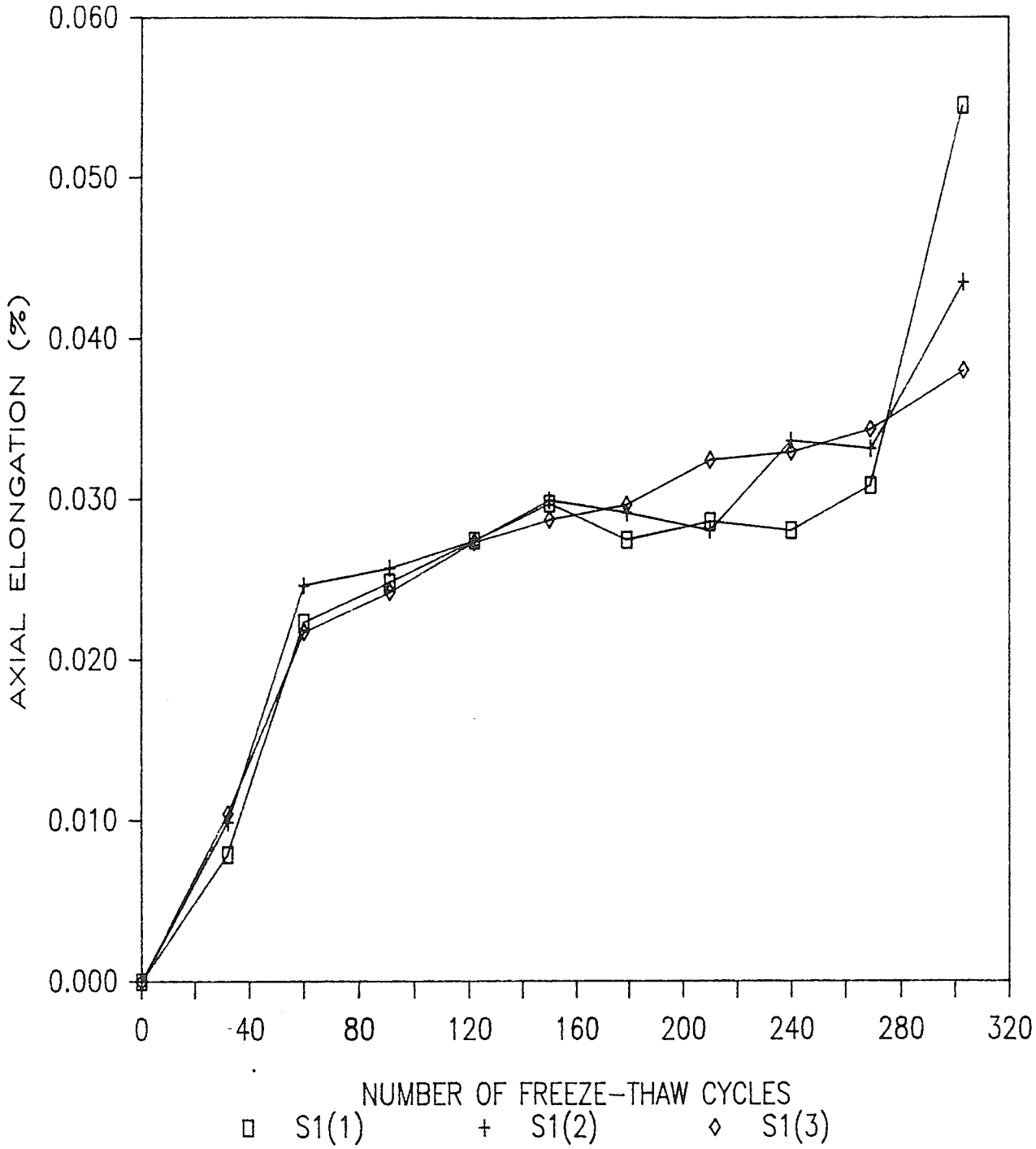

Figure 4.9: Freeze-Thaw Performance of Ordinary PCC Specimens Formed from Mix S1.

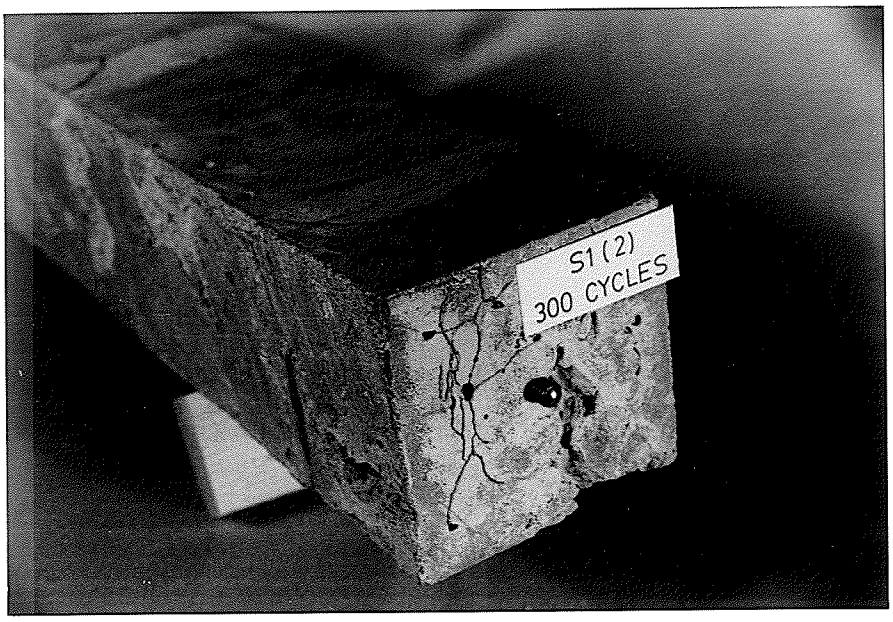

Figure 4.10: Photograph of Specimen S1(2) After 300 Cycles of Freeze-Thaw Showing Aggregate Related Distress.

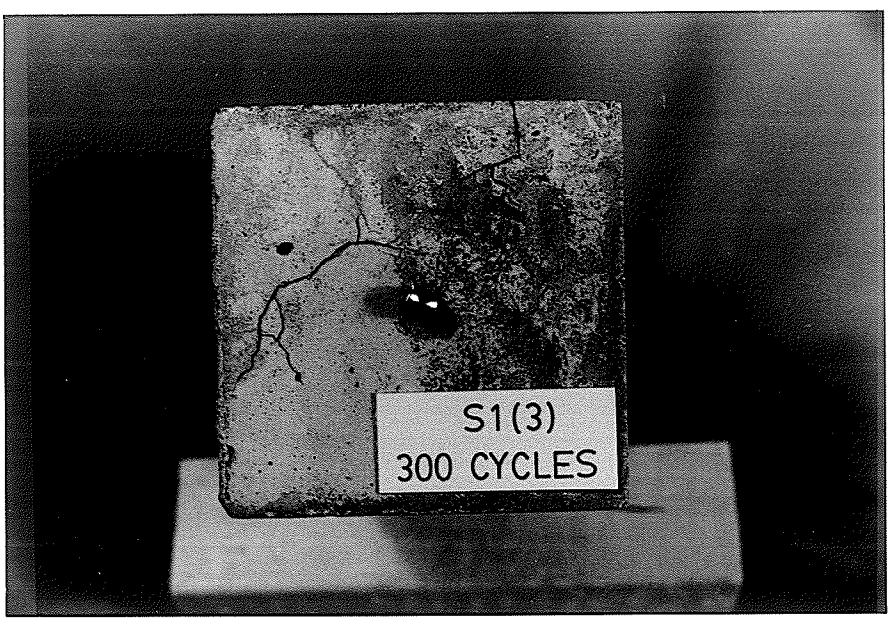

Figure 4.11: Photograph of Specimen S1(3) After 300 Cycles of Freeze-Thaw Showing Aggregate Related Distress.

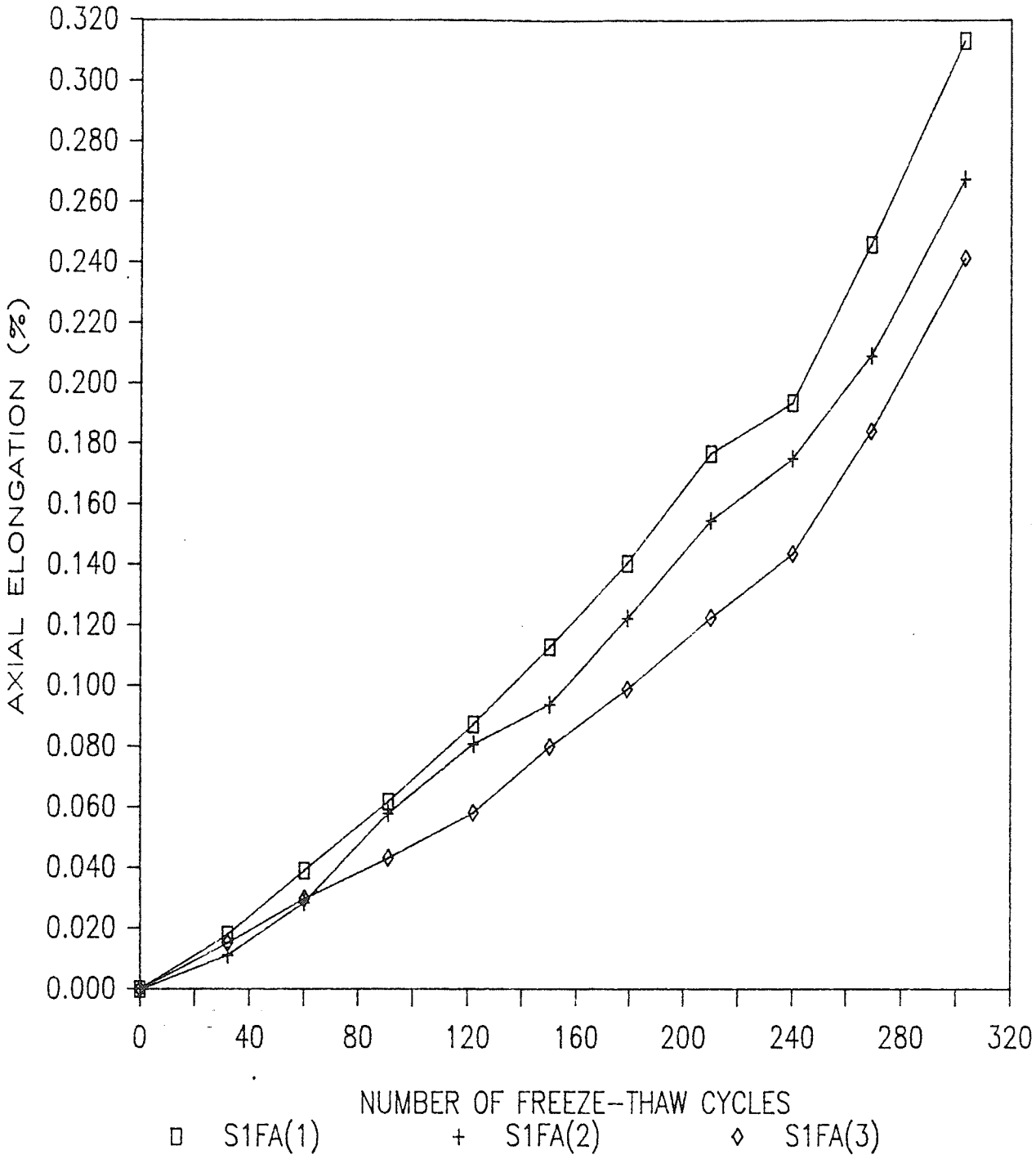

Figure 4.12: Freeze-Thaw Performance of Fly Ash Concrete Specimens Formed from Mix S1.

identification. The photographs show relatively little distress which correlates well with the low values of axial expansion for the number of freeze-thaw cycles used.

The performance of specimens S1FA(1,2,3) with respect to freeze-thaw durability is given in Figure 4.12. Once again, all three fly ash specimens behaved similarly. However, the performance of the fly ash specimens was markedly worse than the ordinary PCC control specimens just presented. The specimens exceeded the failure criterion for axial expansion after approximately 250 freeze-thaw cycles. Possible explanations for this poor performance in comparison to the control mix are examined in an upcoming section.

Photographs of specimens S1FA(1,3) containing S1 coarse aggregate and fly ash are presented in Figures 4.13 and 4.14 respectively. Both specimens show significant distress after experiencing 300 cycles of freeze-thaw.

4.6 PERFORMANCE OF SPECIMENS FORMED WITH SUPERCRETE TYPE 2 COARSE AGGREGATE

Two ordinary PCC specimens, S2(1,2), containing type S2 aggregate were subjected to 300 freeze-thaw cycles. As well, three specimens containing type S2 coarse aggregate and fly ash, designated as S2FA(1,2,3), were also formed.

The performance of these specimens over time is shown in Figure 4.15. The maximum elongation of these specimens was less than 0.02 percent which is considerably less than the criteria of 0.06 percent after 300 cycles. Also, axial elongation did not increase after 160 cycles. Figure 4.16 shows a small popout on the surface of specimen S2(2) after 300 cycles.

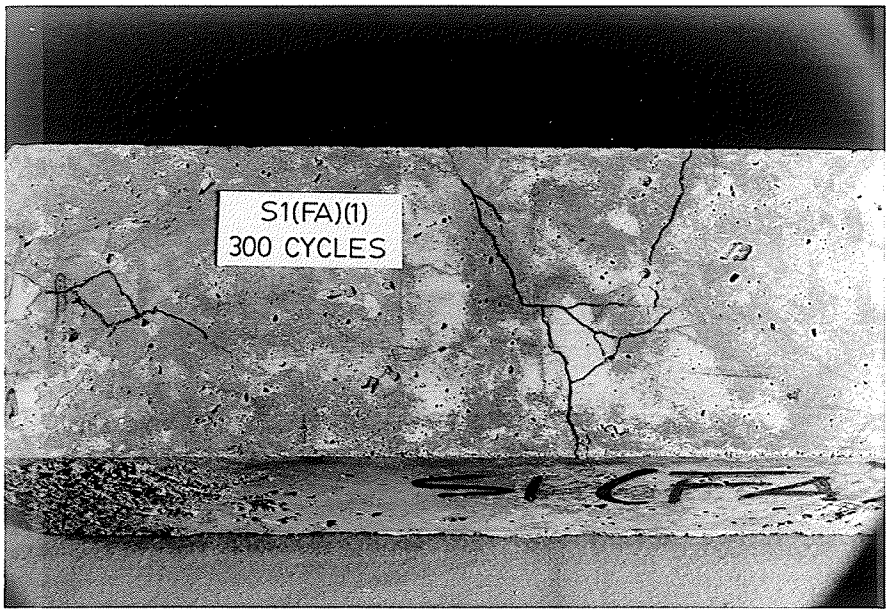

Figure 4.13: Photograph of Specimen S1FA(1) After 300 Cycles of Freeze-Thaw Showing Moderate Aggregate Related Distress.

Figure 4.14: Photograph of Specimen S1FA(3) After 300 Cycles of Freeze-Thaw Showing Moderate Aggregate Related Distress.

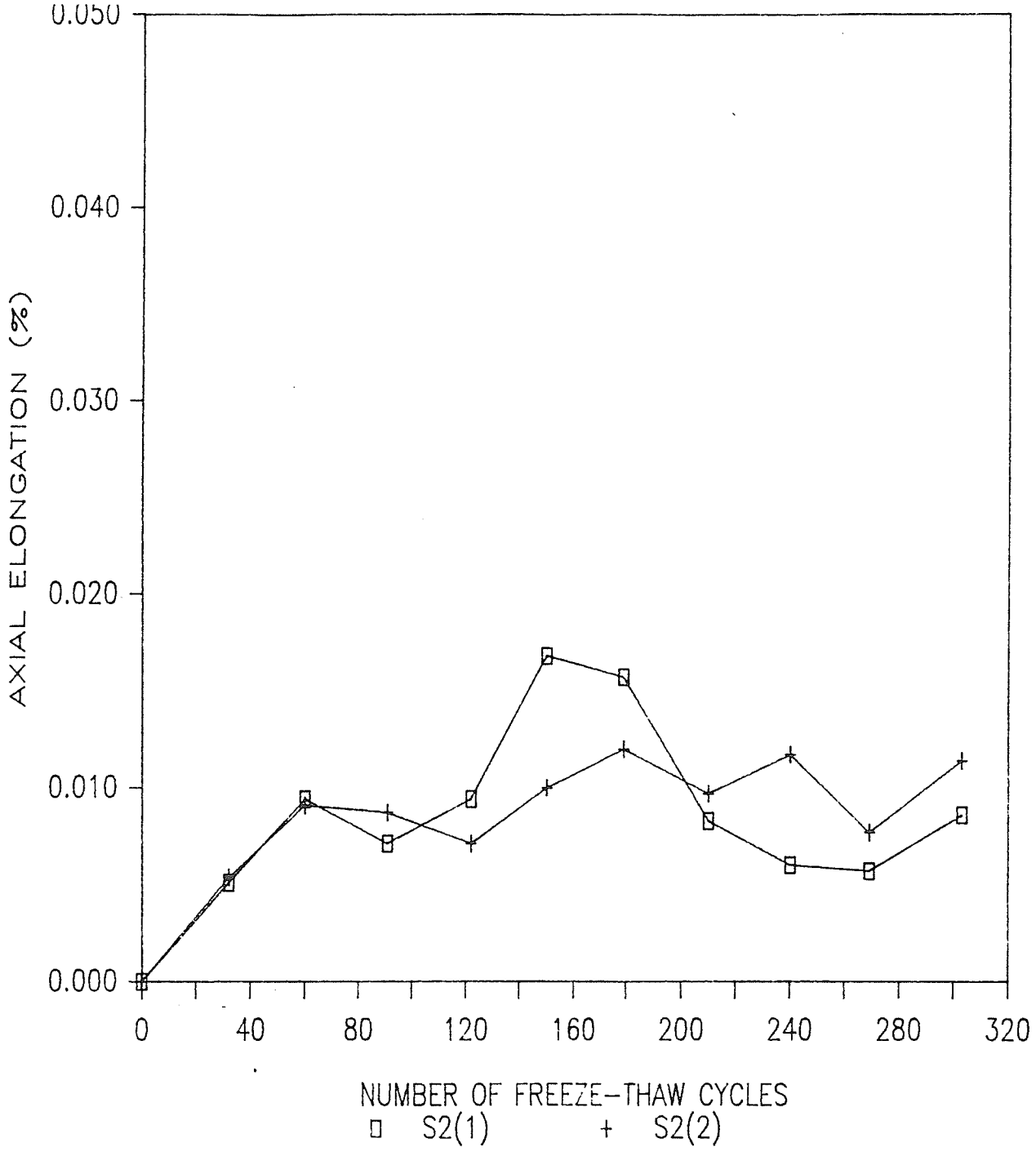

Figure 4.15: Freeze-Thaw Performance of Ordinary PCC Specimens Formed from Mix S2.

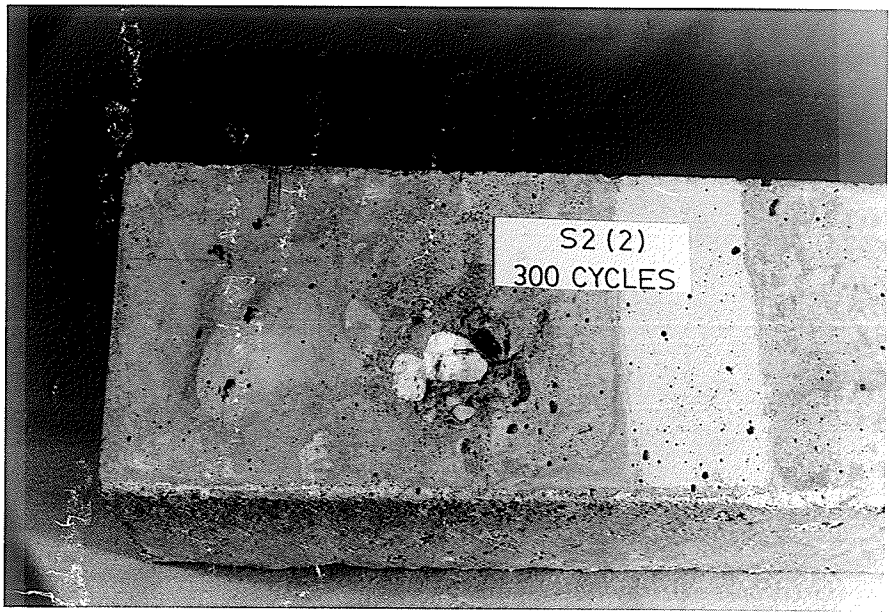

Figure 4.16: Photograph of Specimen S2(2) After 300 Cycles of Freeze-Thaw Showing Popout Caused by Frost Susceptible Aggregate.

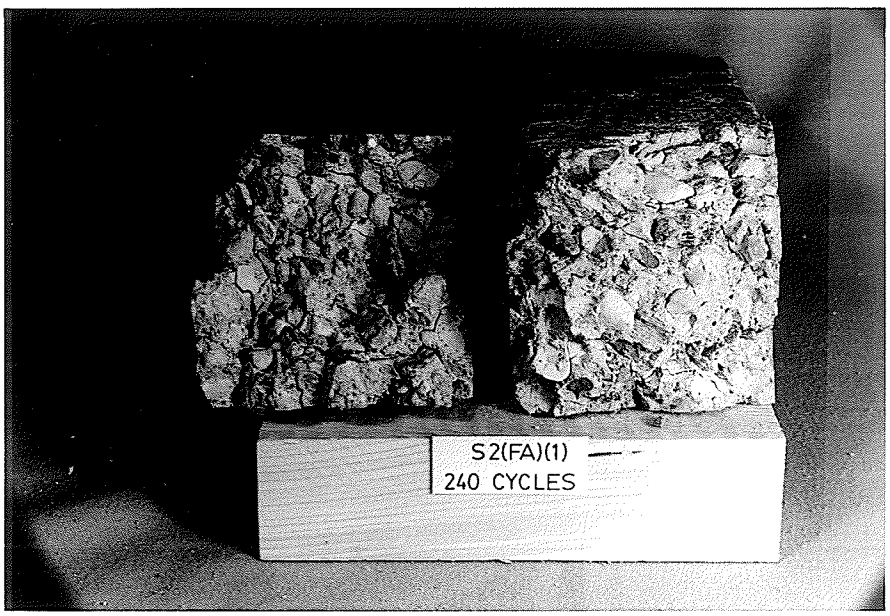

Figure 4.17: Photograph of Specimen S2FA(1) After 240 Cycles of Freeze-Thaw Showing Little Aggregate Distress and an Aggregate/Paste Interfacial Failure.

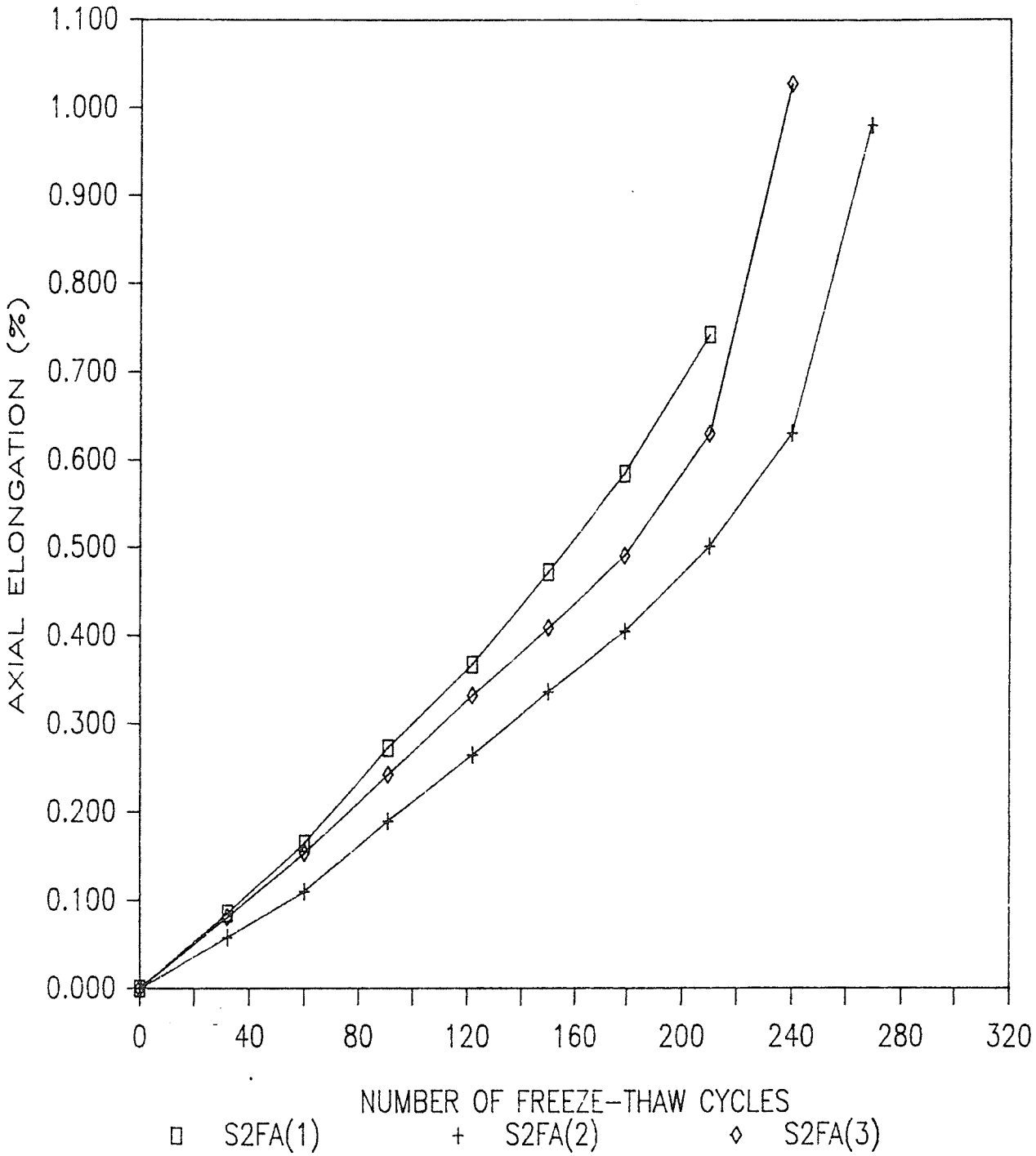

Figure 4.18: Freeze-Thaw Performance of Fly Ash Concrete Specimens Formed from Mix S2.

This was the only area of distress visible on either specimen.

The performance of the fly ash specimens S2FA(1,2,3) is shown in Figure 4.18. The plot shows a dramatic increase in the elongation values in all three specimens compared to the control specimens without fly ash. In fact, all three specimens failed before 300 freeze-thaw cycles were completed and the rate of expansion continually increased. The photograph of specimen S2FA(1) after 240 freeze-thaw cycles is presented in Figure 4.17. The photograph shows very little coarse aggregate distress although the specimen had failed completely. As was the case with the fly ash specimens formed with BP type coarse aggregate, the failure seems to have taken place predominantly at the coarse aggregate/cement interfaces.

4.7 GENERAL DISCUSSION OF RESULTS

In all cases specimens made from the same mix performed similarly and therefore the average elongations of the specimens were used to represent the performance of the mix design from which they were made. The highest degree of similarity between the elongation-time curves for a particular mix design occurred in ordinary concrete specimens, whereas the behavior of the fly ash specimens made from the same mix design showed considerably more variability. Since the test results show that the performance of the ordinary concrete specimens was superior to that of the fly ash concrete specimens, the larger variance in the fly ash results may simply be due to the fact that macrocracks in the fly ash specimens opened earlier in the test. Moisture would then saturate the cracks during the thawing portion of the the freeze-thaw cycles. This moisture would apply pressure to the walls of the cracks during freezing, leading to exponential increases in axial elongation.

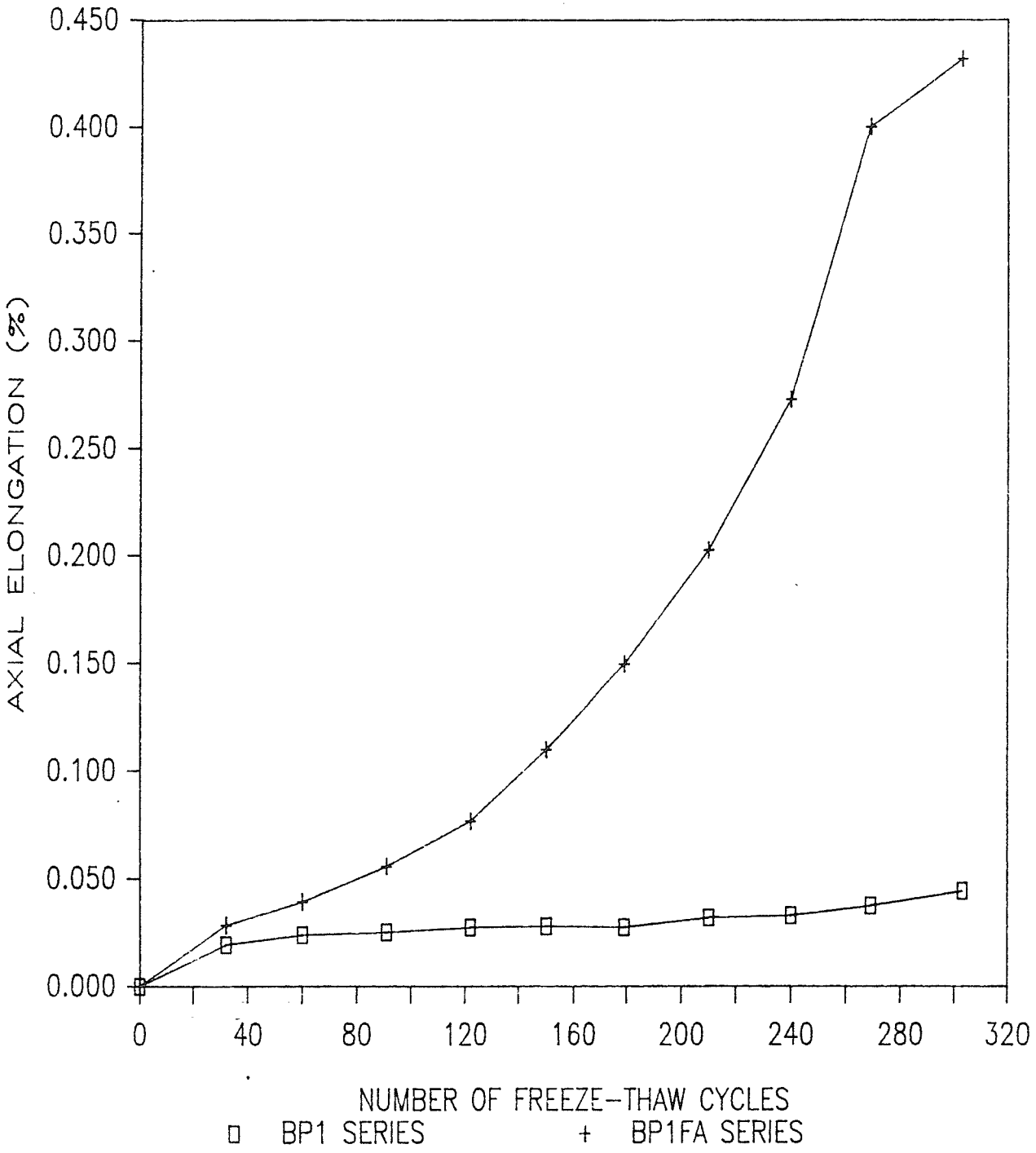

Figure 4.19: Comparison of the Average Freeze-Thaw Performance of Specimens Made From BP1 Coarse Aggregate, With and Without Fly Ash.

As mentioned previously, the fact that specimens made from the same mix design performed similarly throughout the test is significant since it allows the average performance of specimens made from the same mix to be compared to the average performance of the specimens from another mix. In this way the relative durability of the mixes and coarse aggregate wasmade.

A comparison of the average elongation values for specimens made from BP1 coarse aggregate with and without fly ash is shown in Figure 4.19. The figure shows that the residual axial elongation values of the fly ash specimens increased exponentially with increasing number of freeze-thaw cycles. The decrease in the slope of the curve over the last measurement interval was due to the failure of specimen BP1FA(3). Since the axial elongation of specimen BP1FA(3) was the largest of the three in the series, the rate of increase of axial elongation fell off for this interval. Similar curves for the mixes formed with S1 and S2 coarse aggregates are shown in Figures 4.20 and 4.21 respectively. Both curves show that the average performance of the fly ash specimens was very poor in relation to the control specimens without fly ash.

4.7.1 Possible Failure Mechanisms of Specimens

There are a number of possible mechanisms which could be responsible for the poor performance of the fly ash concrete in the freeze-thaw test. At first it was thought that the mechanism of expansion for the fly ash concrete specimens may have been the result of an alkali-carbonate reaction. The results of physical and chemical analysis of the fly ash used in the test program are presented in Appendix A. The chemical analysis showed that the fly ash contained more than the recommended

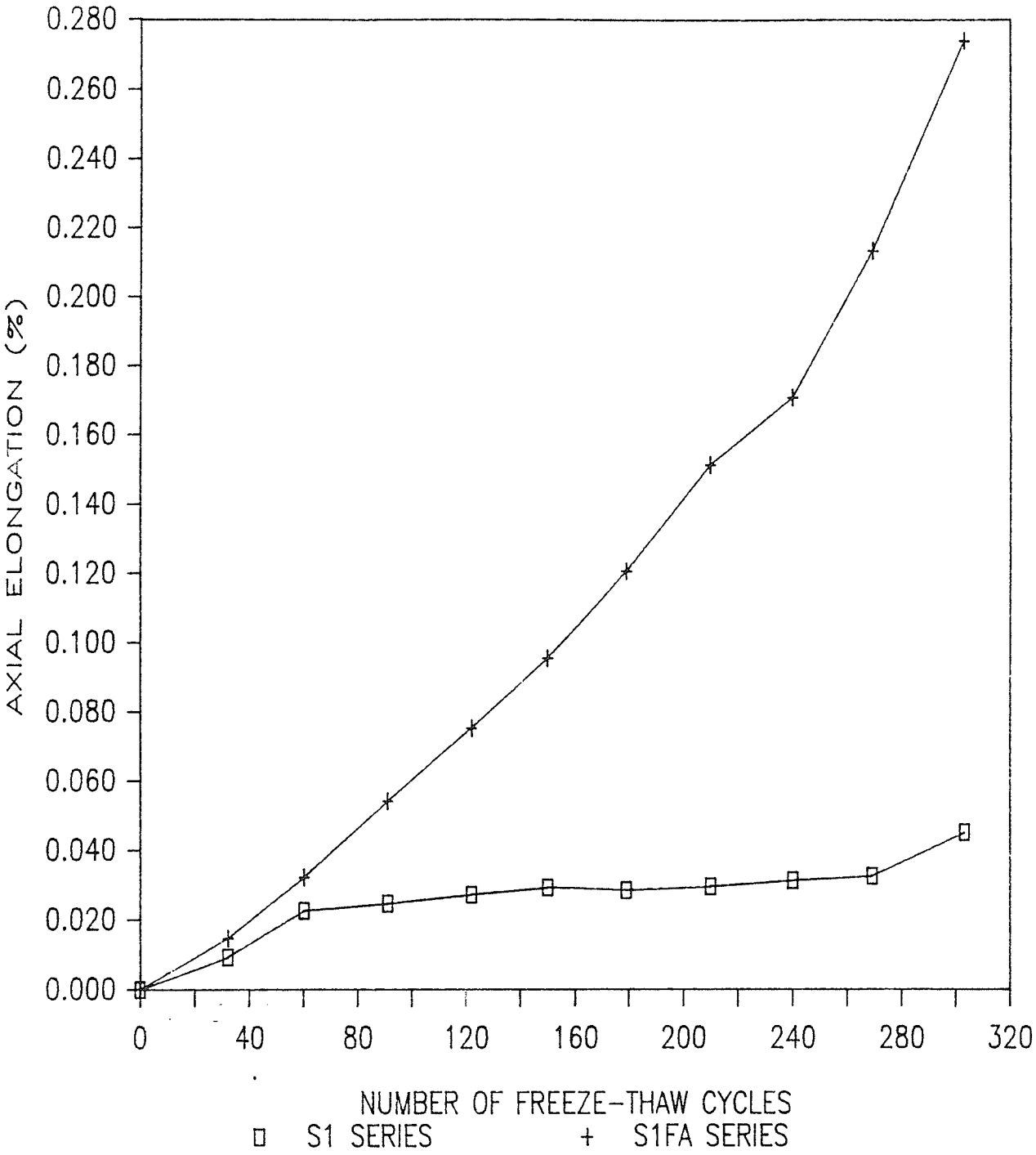

Figure 4.20: Comparison of the Average Freeze-Thaw Performance of Specimens Made From S1 Coarse Aggregate With and Without Fly Ash.

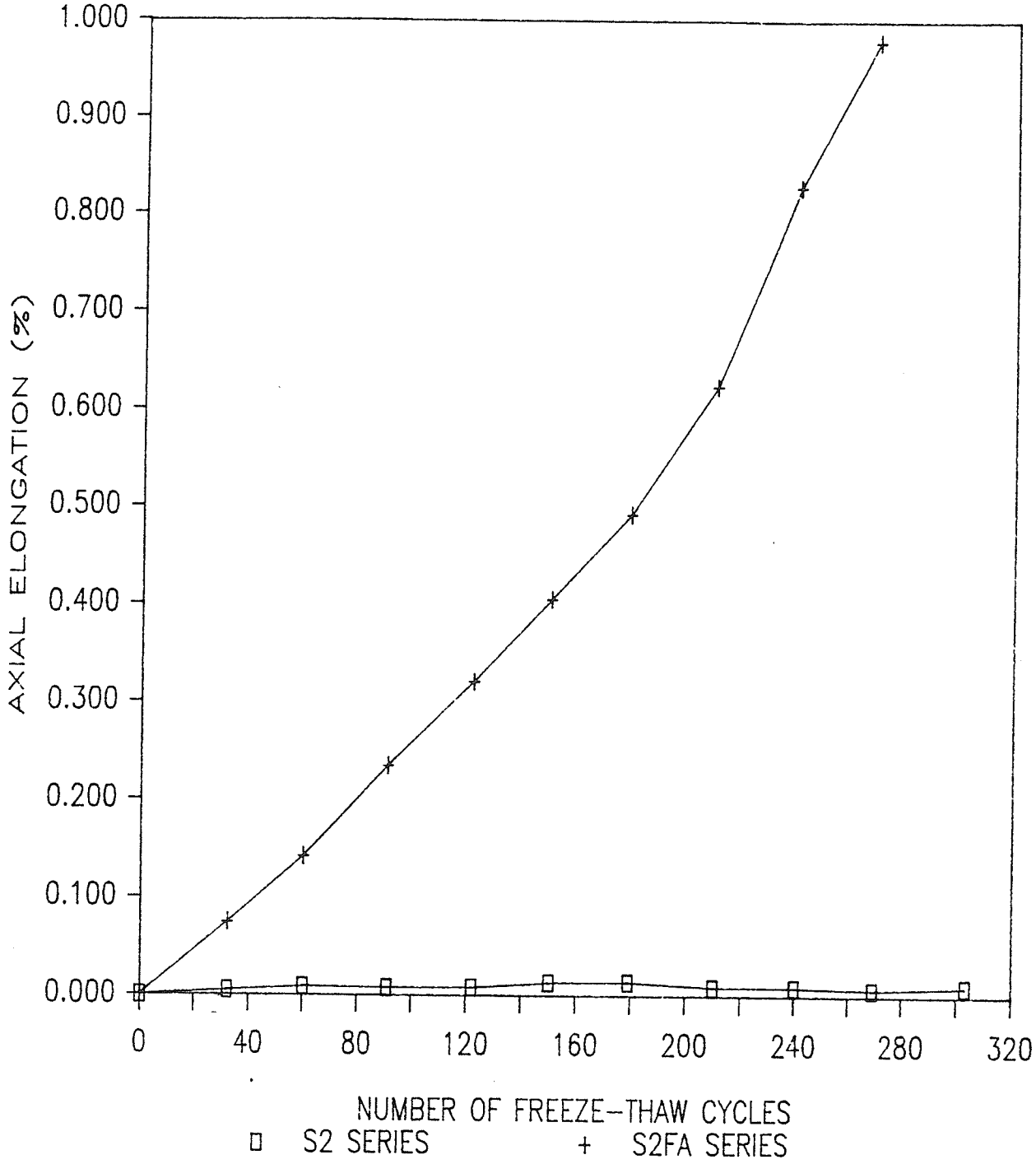

Figure 4.21: Comparison of the Average Freeze-Thaw Performance of Specimens Made From S2 Coarse Aggregate With and Without Fly Ash.

amount of alkali minerals. To further complicate matters, cracking due to an alkali-carbonate reaction would be indistinguishable from D-Cracking in laboratory specimens, especially in the first stages of a test. Since most failures appeared to occur predominantly at aggregate/paste interfaces, it was felt that the mode of failure may have been chemical in nature rather than a physical mechanism related to the pore properties of the aggregate and cement paste. However, locally alkali-carbonate reactions are relatively rare and their existence has not been documented (48). Mysyk and Edwards (49) conducted a mineralogical analysis of D-Crack susceptible aggregates obtained from the taxi apron at Winnipeg International Airport. The aggregate used in the construction of the apron was obtained from the Birdshill esker (50) as was the aggregate used in the present testing program.

Of the four documented types of alkali-carbonate reactions, only one is known to adversely affect the bond between aggregates and cement paste (49). The process, known as dedolomitization, involves the attack of cement alkalis on dolomite grains. The reaction opens microcracks, allowing the intrusion of pore water into the interior of the aggregate. If the aggregate contains sufficient clay minerals, excessive expansive forces may be generated due to adsorption of water onto the surface of the clays (49). A petrographic examination of the aggregates used by Mysyk and Edwards (49) showed that they contained little or no clay minerals. The fact that the aggregate used in the current testing program were obtained from the same source as those used by Mysyk and Edwards (49) does not support an alkali-carbonate reaction deterioration mechanism.

As noted in Section 2.6.2 concerning the durability of fly ash concrete, some researchers have documented little difference in

freeze-thaw durability between fly ash and ordinary PCC concrete of otherwise similar mix design. In fact, Larson (36) noted that the interpretation of freeze-thaw results could be misleading if the fly ash and ordinary concrete did not have equal strength and air entrainment. Larson (37) also found the performance of fly ash concrete could drop off dramatically if compensation was not made for air entrainment lost due to carbon absorption. This was found to be the case even if the compressive strength of the fly ash concrete was higher than the ordinary PCC control mix. The relationship between air content of cement paste and axial elongation after 210 freeze-thaw cycles is shown in Figure 4.22. The data corresponds to 210 cycles because this was the largest number of cycles for which no specimens had failed. Generally an increase in air content resulted in a decrease in elongation for the range of air contents used. The plot shows the sensitivity of axial elongation values of fly ash specimens to paste air contents in the four to five percent range. Care must be taken in drawing conclusions from this plot, however, since the data points were obtained from mixes made from three different coarse aggregates.

Fly ash affects permeability of cement paste in a manner similar to strength development (29). At first the permeability of the paste is higher because the fly ash does not contribute to the development of the structure of the paste initially. As the pozzolan (fly ash) slowly begins to react chemically with the other components of the paste, the strength of the concrete increases and the permeability of the concrete decreases. This seems reasonable considering there is an inverse relationship between strength and void ratio of any engineering material. A decrease in permeability implies an altered paste structure, which may in turn point

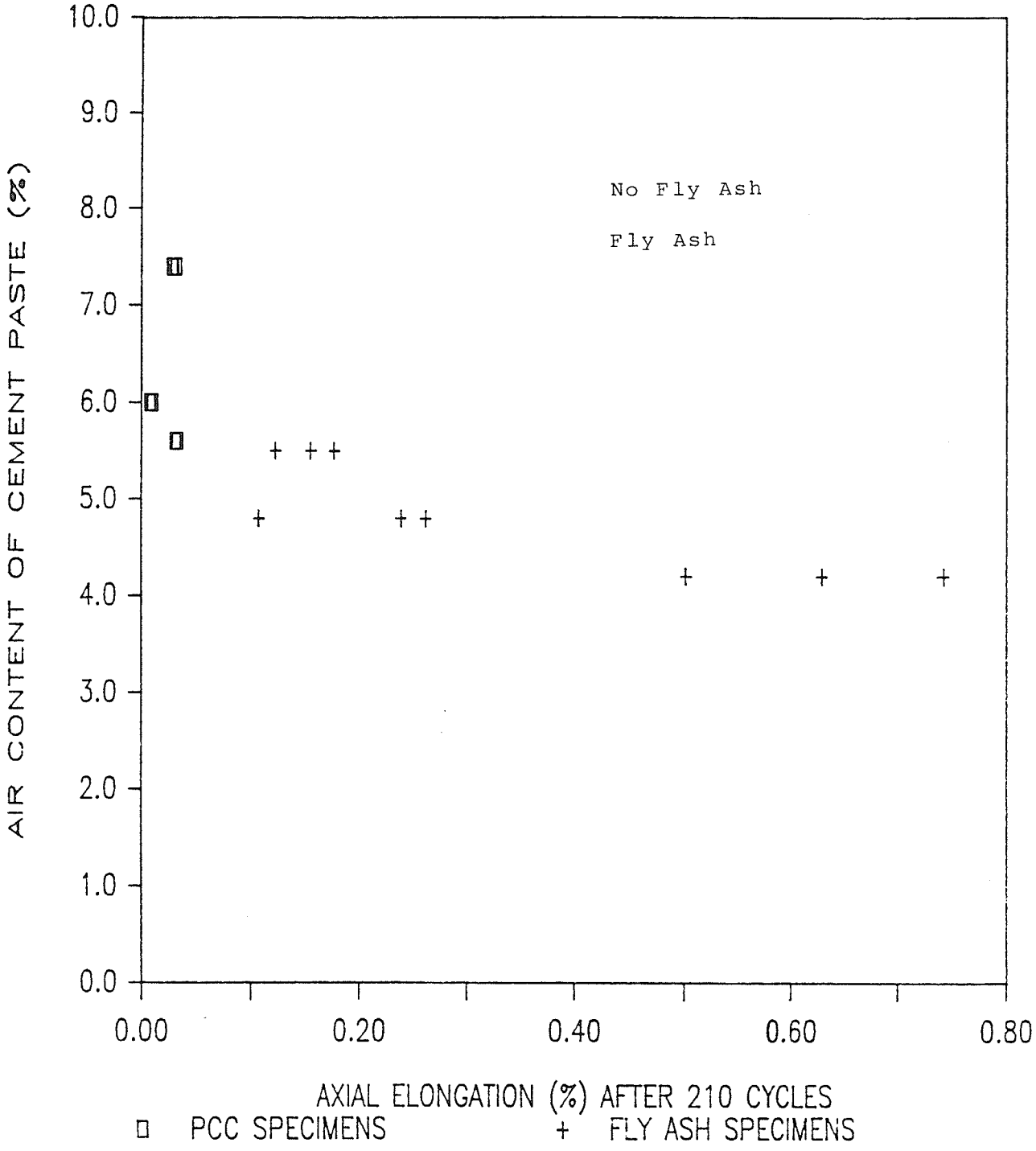

Figure 4.22: Effect of Air Content of Mixes on Axial Elongation After 210 Cycles of Freeze-Thaw.

to a decrease in critical size of the cement paste as discussed in Section 2.4.1. In this case a higher air content would be required to adequately protect a saturated paste from the effects of frost action. This slight structural difference could combine with the lower air content of the fly ash mixes to lower the frost resistance of the fly ash mixes.

A physical mechanism which could account for aggregate/paste interfacial failures has been proposed by Verbeck and Langdren (9). They stated that an aggregate that would not fail due to critical size effects itself could cause a hydraulic pressure type of failure in the surrounding cement paste if the air content of the paste was inadequate to accommodate the moisture which would be forced to flow out of the aggregate during freezing. The fly ash specimens contained air entrainment above the four percent minimum recomended by Transport Canada to ensure adequate air entrainment. However, the fly ash specimens did not perform satisfactorily and the fact that the excessive distress appeared to be related to a coarse aggregate/cement paste interfacial failure tends to lend credence to the above theory. More research is required in this area.

Finally, it may be that the poor performance of the fly ash specimens is related to specific properties of the fly ash used in the testing program. The fly ash used met the specification for chemical composition of Class F fly ash by a narrow margin. Also, the alkali content of the fly ash exceeded the recommended maximum value. The effect of these deviations on freeze-thaw performance of fly ash concrete specimens is unknown at this time. It is recommended that further testing be carried out with different types of fly ash in order to ascertain the effect of fly ash composition on freeze-thaw performance of fly ash concrete specimens.

Chapter V

EFFECT OF AIR CONTENT AND AVAILABILITY OF MOISTURE TEST

5.1 INTRODUCTION

The results and analysis of the test involving air content of the cement paste and availability of moisture are presented in this chapter. Before examining the effect of these two variables on D-Cracking and general freeze-thaw durability, some properties of the mixes involved in this test are examined.

5.2 PROPERTIES OF CONCRETE MIXES

Three different mixes were employed for this test. The same coarse aggregate and gradation were used in all three mixes. The gradation for the coarse and fine aggregate for the test are given in Table 5.1. Coarse aggregate used in the test was obtained from the same source as the aggregate from the first test. The aggregate was known to be D-Crack susceptible. The variable of interest with respect to mix design for this test run was air content. Ideally, it would have been desirable to alter the air content of the mixes over the desired range with all other variables held constant. However, because air content affects both the rheological and hardened properties of a mix, minor differences in cement content and agrregate quantities were required in an effort to keep engineering properties of the mixes within Transport Canada guidelines,

Table 5.1

Aggregate Gradations Used in the Air Content and External Moisture Test

Coarse Aggregate		Fine Aggregate	
Grain Size	Percent Passing	Grain Size	Percent Passing
37.5 mm	100.0	9.42 mm	100.0
25.0 mm	95.0	4.76 mm	98.4
12.5 mm	5.0	2.38 mm	83.2
4.8 mm	0.0	1.19 mm	64.2
		0.60 mm	36.7
		0.21 mm	14.8
		0.15 mm	5.3

It was felt that these slight adjustments to mix design would have no significant effect on the outcome of the test.

Since the coarse aggregate used was the same in all mixes, it was not necessary to include aggregate type in the mix designation. Instead, mixes were designated by their air content as measured by the pressure method. For example, specimens poured from the mix containing 1.9 per cent air entrainment were designated as series A1.9. A numerical suffix was added in parenthesis to distinguish between specimens formed from the same mix. The characteristics of the mix designs used for the test are given in Table 5.2. Although the material quantities vary slightly from mix to mix, depending on the amount of air entraining agent (AEA) added, the w/c ratio was held constant for all mix designs. The w/c ratio was held constant not only in an attempt to keep the compressive strengths of the mixes as similar as possible but also to ensure consistency with respect to

Table 5.2

Mix Design Characteristics

Mix Characteristics	Mix Designation A1.9	A5.0	A8.5
Total[1] Water (kg/m^3)	162.4	158.2	141.3
Type 10 Cement (kg/m^3)	361.0	351.5	314.1
Coarse Aggregate (kg/m^3)	1140.0 SSD 1121.0 Dry	1147.5 SSD 1129.0 Dry	1075.3 SSD 1057.8 Dry
Fine Aggregate (kg/m^3)	768.0 Dry	697.5 Dry	740.2 Dry
Air Entraining Agent (ml/m^3)	0.0	200.0	445.0
Water/Cement Ratio	0.45	0.45	0.45
Coarse/Fine Ratio (Dry)	1.46	1.62	1.43

[1]Total water = All water added to the mix which contributes to the processes of hydration.
Total water = calculated mix water - free water on saturated coarse aggregate + water absorbed by fine aggregate (80% of 24 hour value).

Table 5.3

Characteristics of Fresh Concrete

Concrete Characteristics	Mix Designation A1.9	A5.0	A8.5
Slump (mm)	45	50	80
Air Content (%)	1.9	5.0	8.5
Density (kg/m^3)	2441	2389	2279
Relative Yield	1.00	0.98	1.12
Cement Factor (kg/m^3)	361	358	314

permeability and structure as discussed in Chapter 2. The series A1.9 mix design contained no air entraining agent. The air content of 1.9 per cent in this mix was entrapped air only, which does little to protect concrete from frost deterioration as discussed in Section 2.5.1.

Characteristics of the fresh concrete for the three mixes are given in Table 5.3. Even with adjustments to the amounts of coarse and fine aggregate added to the mix, the slump increased with increasing air content. This is due to the fact that the air bubbles act as spheres of negligible friction as discussed previously in Section 2.5. In fact, the 80 mm slump of mix A8.5 was larger than the 50 mm $\pm$ 10 mm range specified by Transport Canada. It became evident that major changes to mix design A8.5 would have been necessary to bring the slump within the recommended limits. This was deemed undesirable, since major changes to the mix design

would have rendered a comparison of the behavior of the three mixes extremely difficult. Also, as expected, the density of concrete decreased with increasing air content.

The average compressive strength of each mix is shown in Figure 5.1. As one would expect there was an inverse relationship between air content and compressive strength at all ages. The average compressive strength of mix A8.5 was 22.6 Mpa after 28 days of curing. Again, this value is slightly below the Transport Canada minimum standard of 25.0 Mpa for PCC pavements. It will be shown later that, as was the case in the fly ash test, compressive strength plays a secondary role in the freeze-thaw durability of concrete.

5.3 PERFORMANCE OF SPECIMENS WITH AIR CONTENT OF 1.9%

Six specimens (prisms) with air contents of 1.9 per cent were used in the study. As mentioned previously, these specimens were designated as A1.9 followed by a numerical suffix to identify each specimen within the test series. For example, A1.9(1) designated the "first" specimen with an air content of 1.9 per cent. Three of the specimens, A1.9(1,2,3), were sealed with an epoxy coating immediately after curing. The other three specimens A1.9(4,5,6) were left unsealed.

Figure 5.2 shows axial elongation which occurred during freeze-thaw plotted against number of freeze-thaw cycles for the three sealed specimens containing 1.9 per cent entrapped air. The results show minor elongation in specimens A1.9(2) and A1.9(3) throughout the test. Examination of these specimens at intervals throughout the test run showed minimal damage. However, the behavior of specimen A1.9(1) differed markedly from that of the other two sealed specimens. Although axial

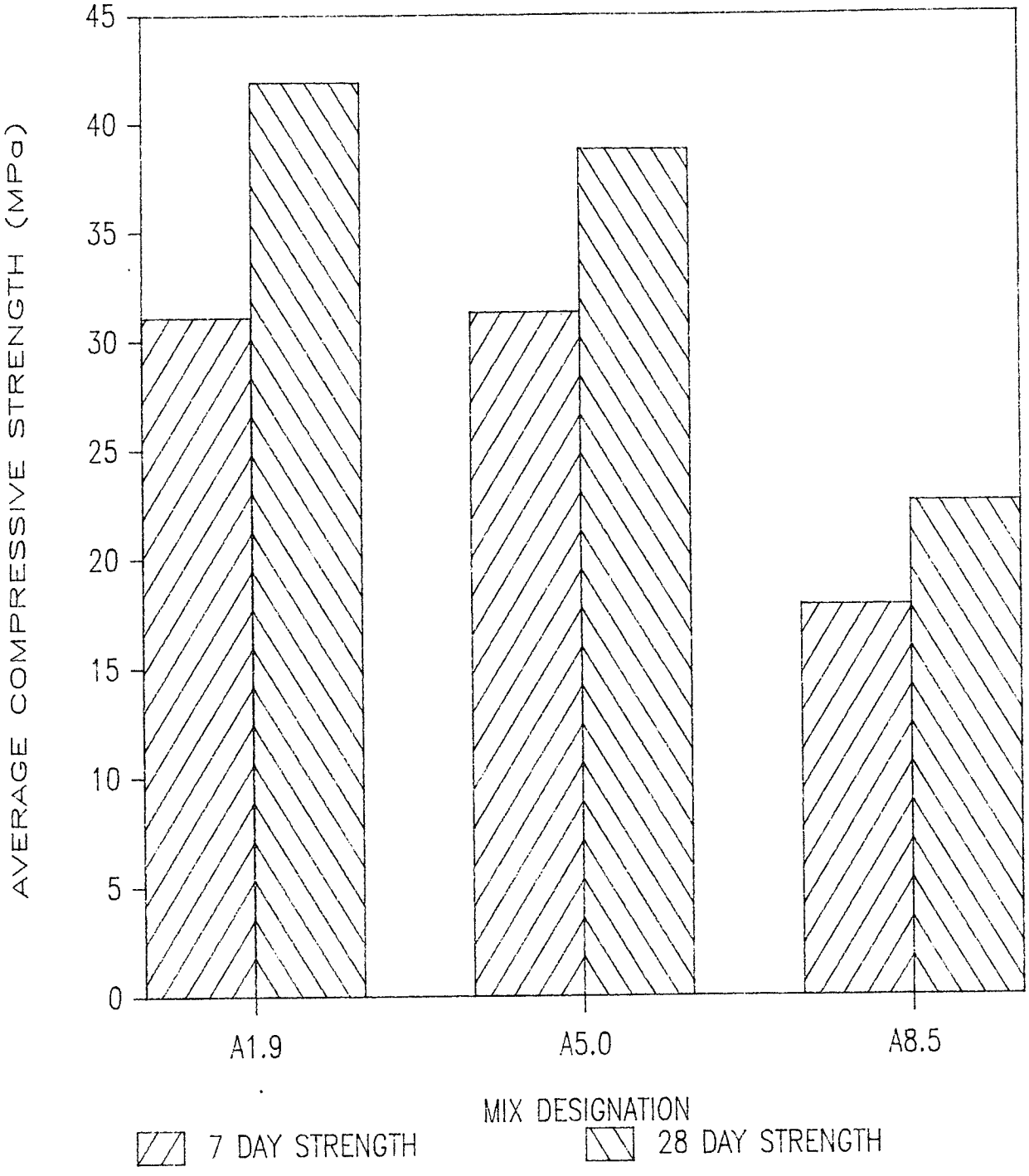

Figure 5.1: Relationship Between Compressive Strength and Air Content For Mixes A1.9, A5.0, and A8.5 After 7 and 28 Days Moist Curing

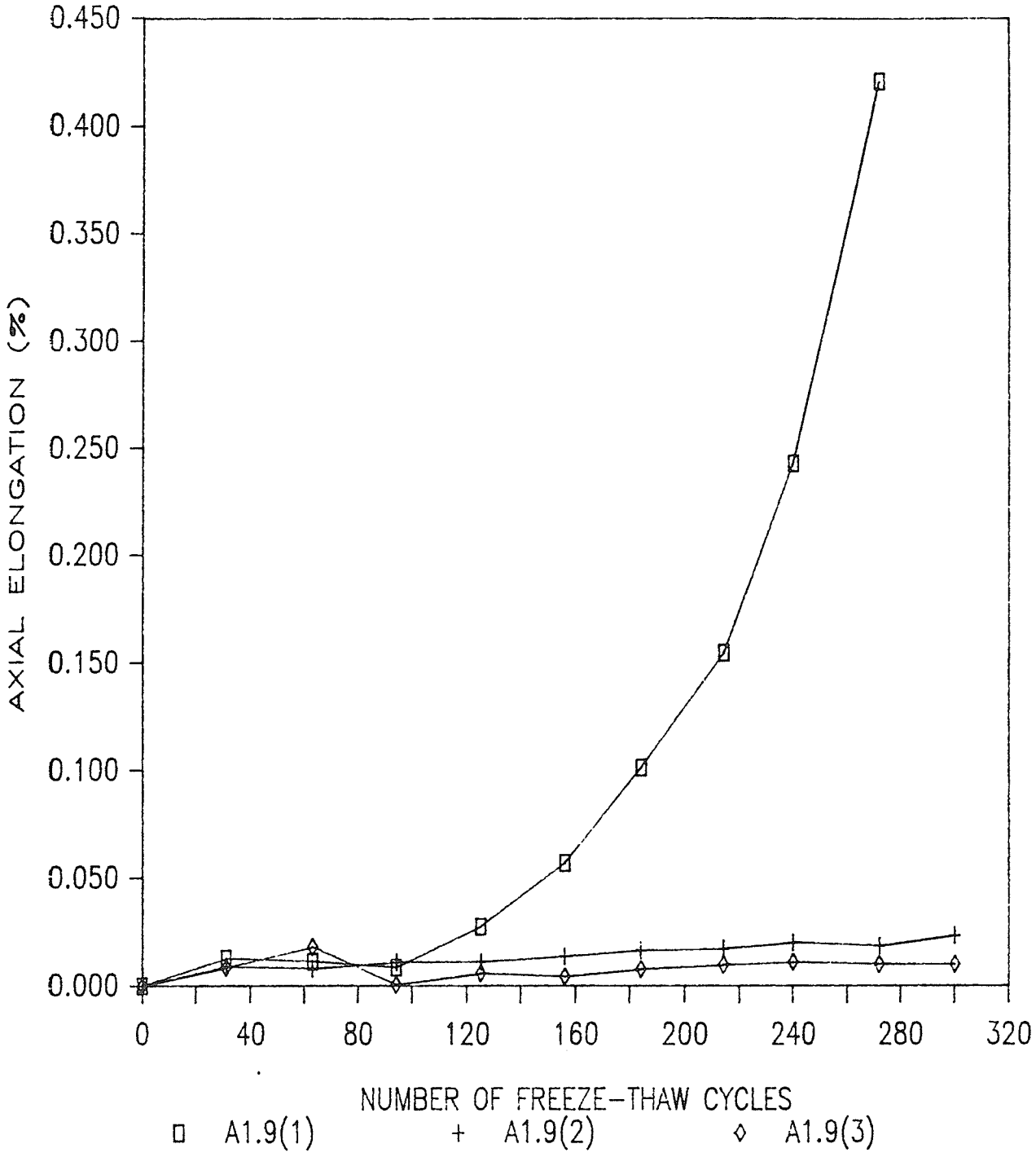

Figure 5.2: Freeze-Thaw Performance of Sealed Specimens Formed from Mix A1.9

elongation was minimal during the first third of the test and compatible with the behavior of specimens A1.9(2,3), axial elongation began to increase exponentially after approximately 90 cycles. It was discovered that the distress may have been caused by a single aggregate particle whose structure rendered it extremely sensitive to frost action during a physical examination of the specimen after failure occurred. Figure 5.3 presents a photograph of specimen A1.9(1) after failure. The photograph shows that the majority of the distress was caused by the large aggregate in the upper right hand corner. The photograph shows severe fracturing of the aggregate along bedding planes which were approximately parallel and spaced about 3 mm apart. The other coarse aggregates showed minimal fracturing. In this case the structure of the aggregate rendered it particularly susceptible to frost action. Prior to mixing, the coarse aggregate was soaked for 24 hours in water. As well, the specimen was sealed with epoxy immediately after removal from the curing room with no drying period in laboratory air allowed. Given these conditions it is probable that the degree of saturation of the aggregate was relatively high at the beginning of the test. In this case a high degree of saturation combined with a pore structure sensitive to frost action combined to cause severe distress in this particular aggregate particle.

A slight tear was noticed in the epoxy sealant on specimen A1.9(1) directly over the area of severe distress during examination of the specimen after 240 cycles. Efforts to repair the tear were unsuccessful. However, since no other tears were noted on any of the other sealed specimens prior to failure, it is assumed that the tear was caused by the excessive expansion of the specimen in that area, rather than the tear being the cause of the excessive expansion.

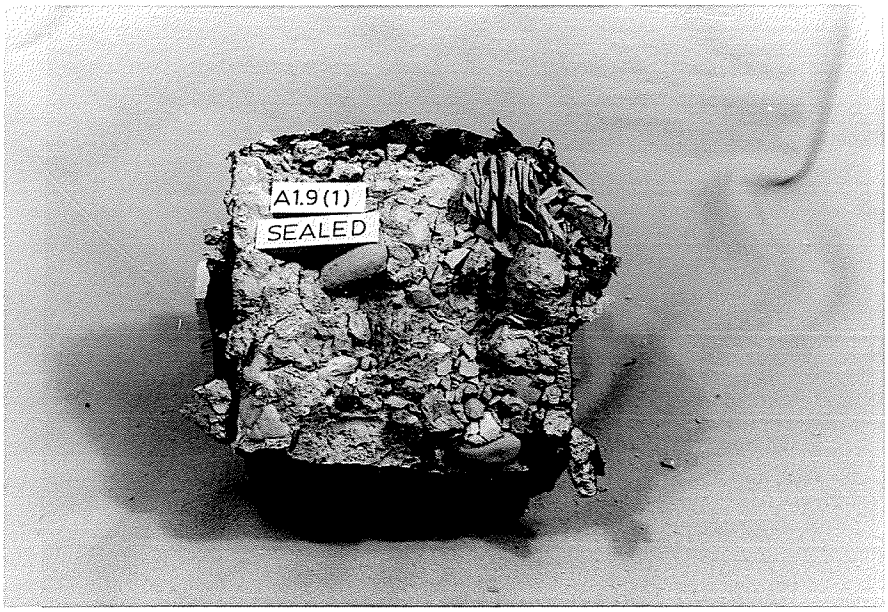

Figure 5.3: Failure of Specimen A1.9(1) After 300 Cycles of Freeze-Thaw

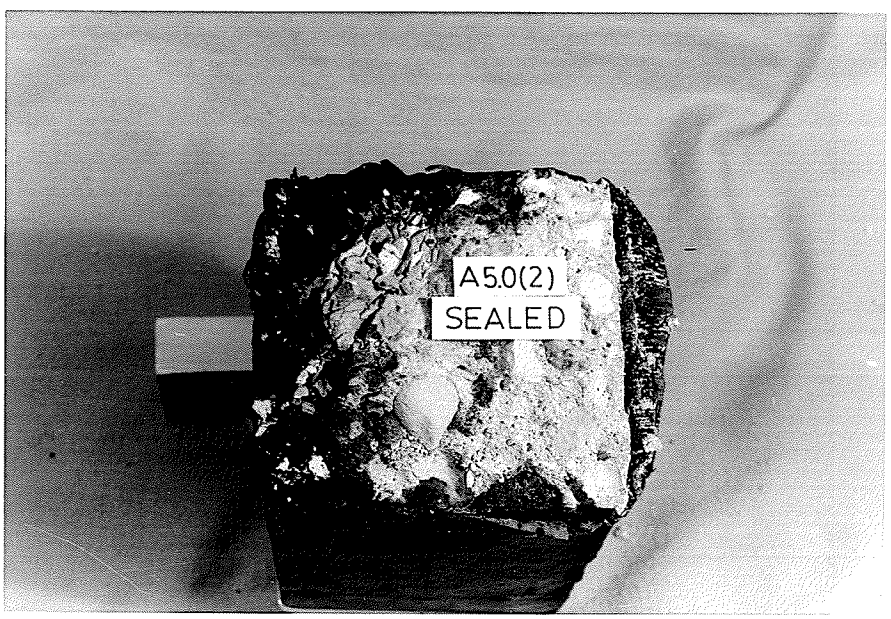

Figure 5.4: Failure of Specimens A5.0(2) After 156 Cycles of Freeze-Thaw

Using Traylor's (2) acceptability criteria of 0.06 percent axial expansion, specimens A1.9(2,3) were well below this value, having axial elongations of 0.024 and 0.010 per cent respectively after 300 freeze-thaw cycles whereas the axial elongation of specimen A1.9(1) was 0.420 per cent after 272 cycles and failure occurred shortly afterward.

The freeze-thaw test results for specimens A1.9(4,5,6), which were unsealed, are presented in Figure 5.5. The plot shows that all of the specimens surpassed Traylor's acceptability criteria after approximately 50 cycles of freeze-thaw. All three specimens exhibited exponential increases in axial elongation with increasing freeze-thaw cycles. Associated with the large elongations were signs of severe physical distress. Figure 5.6 shows a photograph of specimen A1.9(4) at the end of the test. A large aggregate failure is shown. Because this aggregate was close to the surface, a popout was created. The staining which often precedes D-Cracking can also be seen. Figure 5.7 shows specimen A1.9(5) at 272 cycles. Close examination of the massive end failure showed extensive hydraulic fracturing of the coarse aggregate. Surface cracking, and the staining which often precedes it, were also evident. The test was discontinued at this point because the steel stud used to obtain length measurements was loosened destroying the reliability of future measurements.

A comparison of the freeze-thaw performance of sealed and unsealed specimens with a 1.9 percent air content is given in Figure 5.8. Although the unsealed specimens underwent greater elongation than the sealed specimens did, no unequivocal conclusion can be drawn regarding the role of external moisture vs internal moisture because of the performance of specimen A1.9(1). In fact, the results suggest that if the concrete

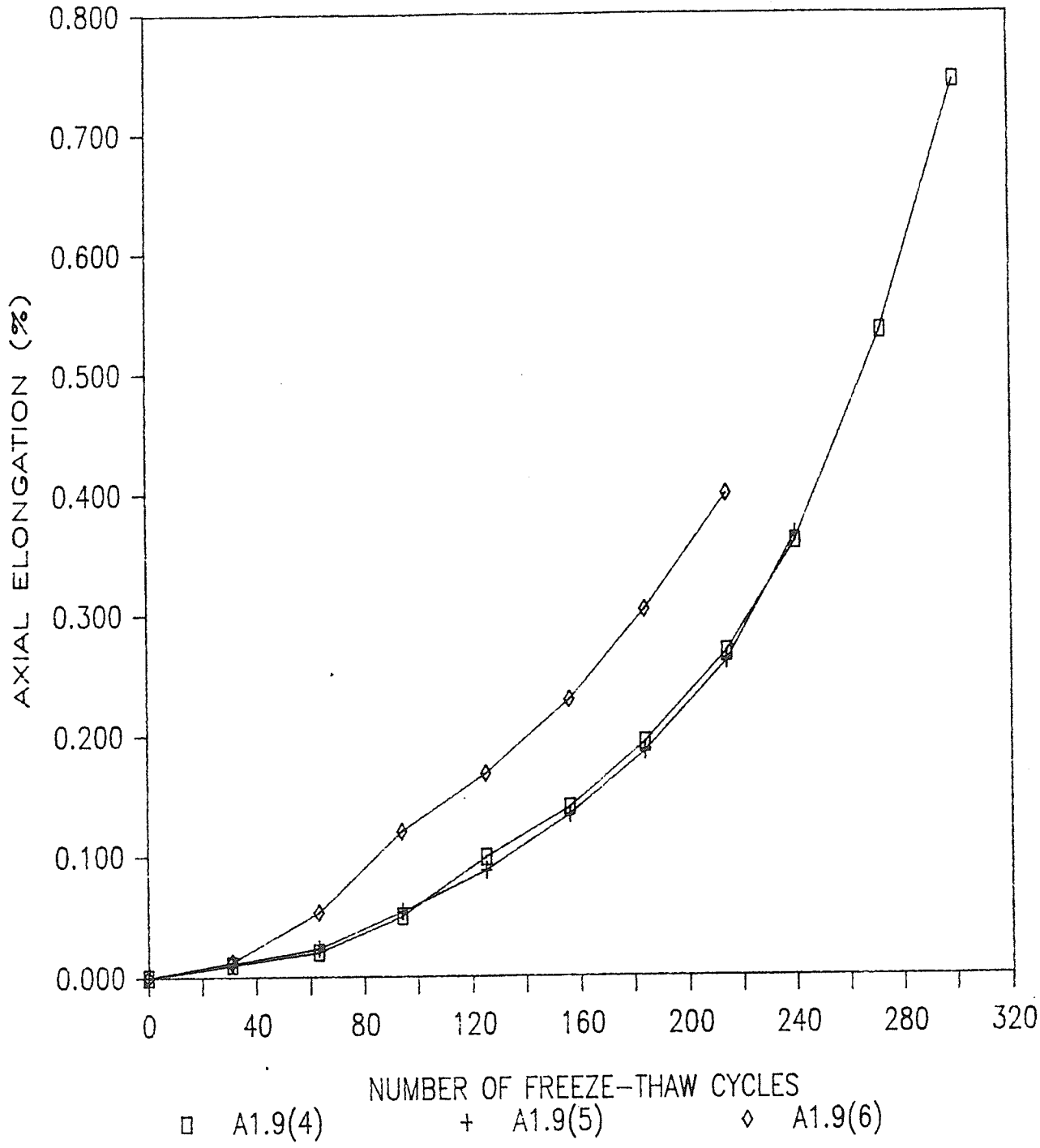

Figure 5.5: Freeze-Thaw Performance of Unsealed Specimens Formed from Mix A1.9

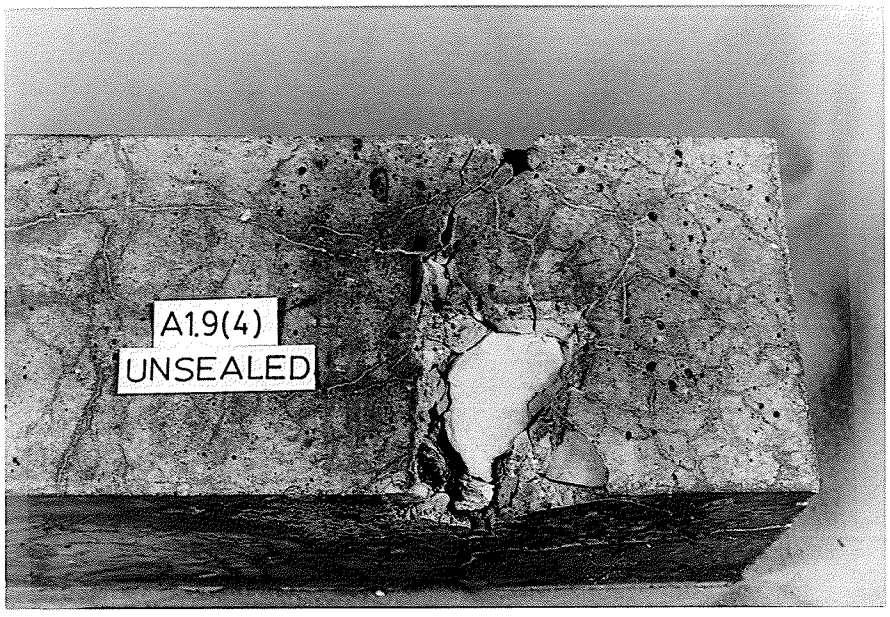

Figure 5.6: Photograph of Specimen A1.9(4) After 300 Cycles of Freeze-Thaw Showing Aggregate Related Distress

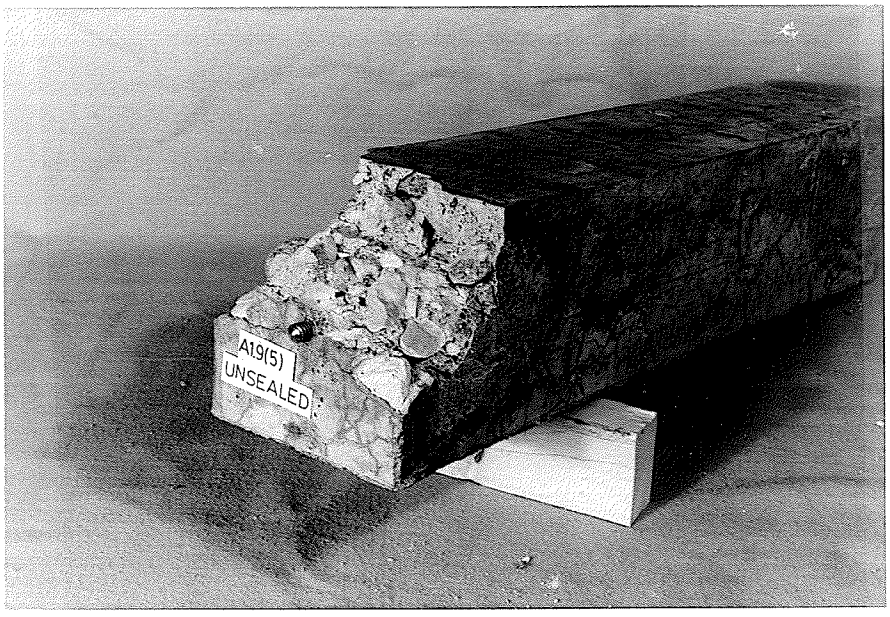

Figure 5.7: Photograph of Specimen A1.9(5) After 272 Cycles of Freeze-Thaw Showing Aggregate Related Distress

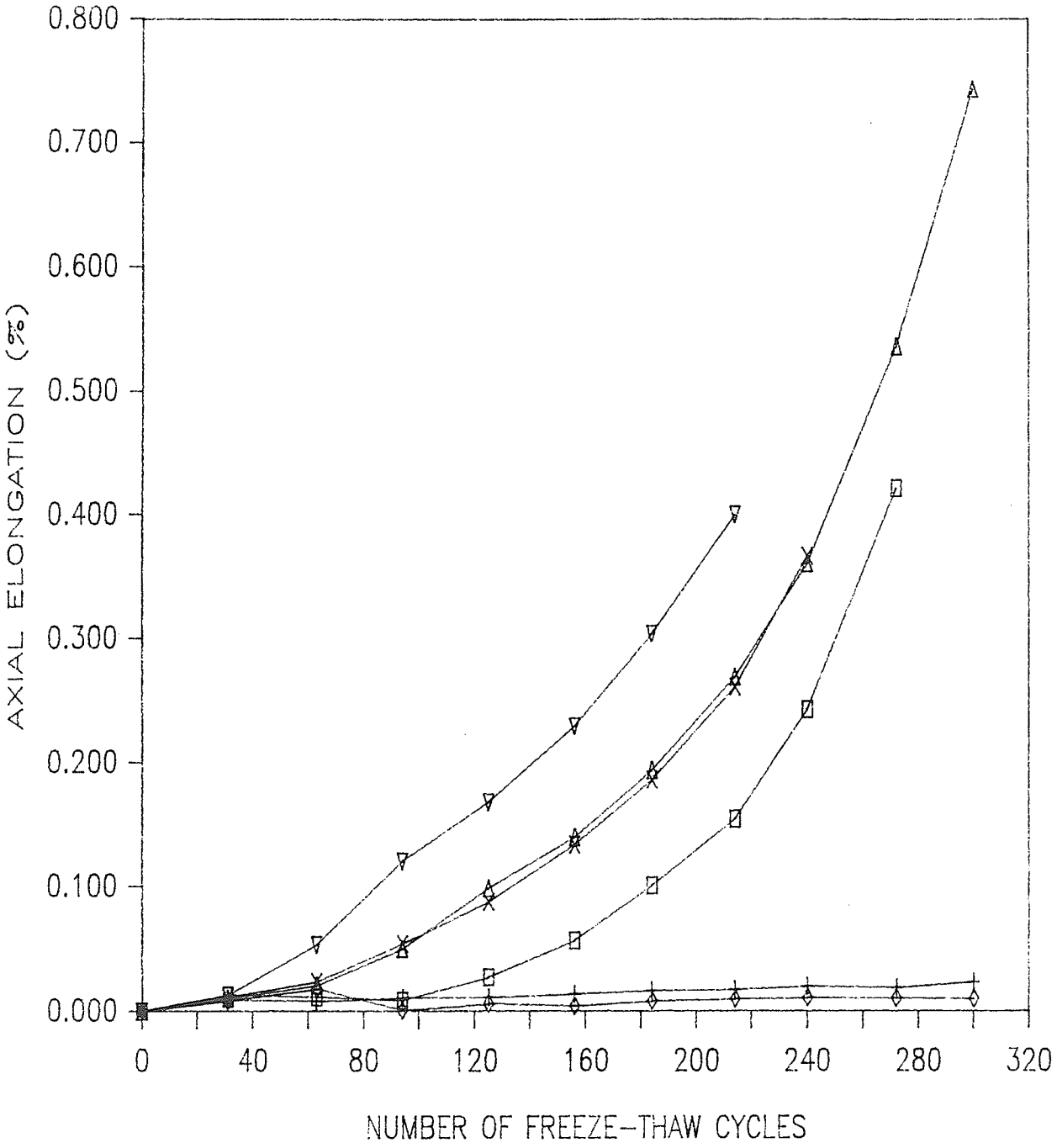

Sealed Specimens		Unsealed Specimens	
□	A1.9(1)	Δ	A1.9(4)
+	A1.9(2)	X	A1.9(5)
◇	A1.9(3)	▽	A1.9(6)

Figure 5.8: Comparison of the Freeze-Thaw Performance of of Specimens With an Air Content of 1.9 Percent

contains aggregate highly susceptible to frost action then deterioration may occur without access to external moisture.

5.4 PERFORMANCE OF SPECIMENS WITH AIR CONTENT OF 5.0%

Five specimens with air contents of 5.0 per cent were included in the freeze-thaw test. Three specimens, A5.0(1,2,3), were sealed with an epoxy coating immediately after curing, while specimens A5.0(4,5) were left unsealed. Although the freeze-thaw cabinet held 18 specimens, it was necessary that one specimen contain temperature monitoring equipment as discussed in Section 3.6.1.1. It was felt that the deterioration of concrete containing five per cent entrained air would lie between the extreme behavior of concrete with air contents of 1.9 and 8.5 per cent. Also, the behavior of a similar mix was documented during the first test involving the freeze-thaw performance of fly ash concrete. Thus only two specimens were used to assess the effects of 5.0 percent air entrainment with free access to moisture.

The variation of axial elongation with number of freeze-thaw cycles for the three sealed specimens is given in Figure 5.9. The results are similar to those of the A1.9 sealed specimens in that one specimen, A5.0(2), experienced significant axial expansion while the remaining two sealed specimens experienced minimal expansion throughout the course of the test. The major difference between specimens A1.9(1) and A5.0(2) was that the shape of the expansion curve for specimen A5.0(2) was approximately linear whereas for specimen A1.9(1) the shape of the curve was exponential. A photograph of specimen A5.0(2) is shown in Figure 5.4. The upper left hand side of the photograph shows a single aggregate that fractured along bedding planes and it is speculated that this aggregate

was the main cause of excessive expansion. No deterioration was evident in the other coarse aggregates. As in the A1.9 test series, the remaining two sealed specimens exhibited very little expansion throughout the test and easily met the acceptability criterion for expansion of 0.06 percent.

Axial elongation is shown plotted against number of freeze-thaw cycles for the A5.0 unsealed specimens in Figure 5.10. The elongation with time increased exponentially and exceeded the acceptability standard as was the case with the A1.9 unsealed specimens.

Figures 5.11 and 5.12 show the deterioration of an A5.0 sealed and an unsealed specimen respectively. Figure 5.11 shows specimen A5.0(1) stripped of epoxy sealant after completion of the test run. Close examination of the photograph shows the classic D-Cracking pattern of finely spaced cracks progressing around corners. The distress had not progressed to an advanced state as shown by the elongation values for the specimen shown in Figure 5.9.

A comparison of the freeze-thaw performance of sealed and unsealed specimens with a 5.0 percent air content is given in Figure 5.13. As was the case with the specimens formed from the mix containing 1.9 percent air entrainment, the performance of one of the sealed specimens, A5.0(2), was similar to that of the unsealed specimens. Again, the test results do not conclusively indicate that external moisture is required for D-Cracking.

5.5 PERFORMANCE OF SPECIMENS WITH AIR CONTENT OF 8.5%

Six specimens with air contents of 8.5 per cent were tested in the second test. These specimens were designated A8.5 followed by a numerical suffix to identify each sample in a fashion identical to that employed for the other series in the test run. The first three specimens, A8.5(1,2,3),

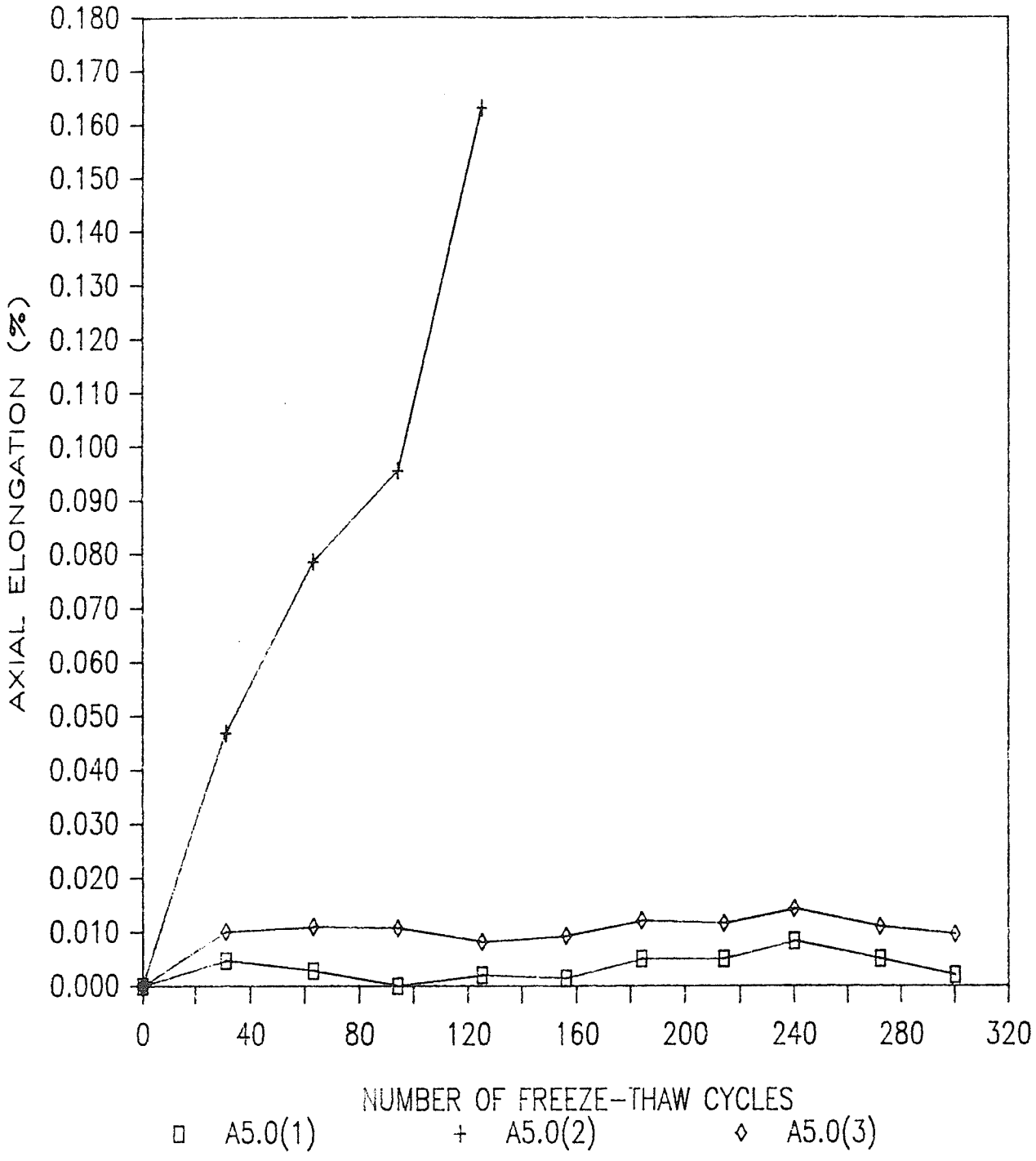

Figure 5.9: Freeze-Thaw Performance of Sealed Specimens Formed From Mix A5.0

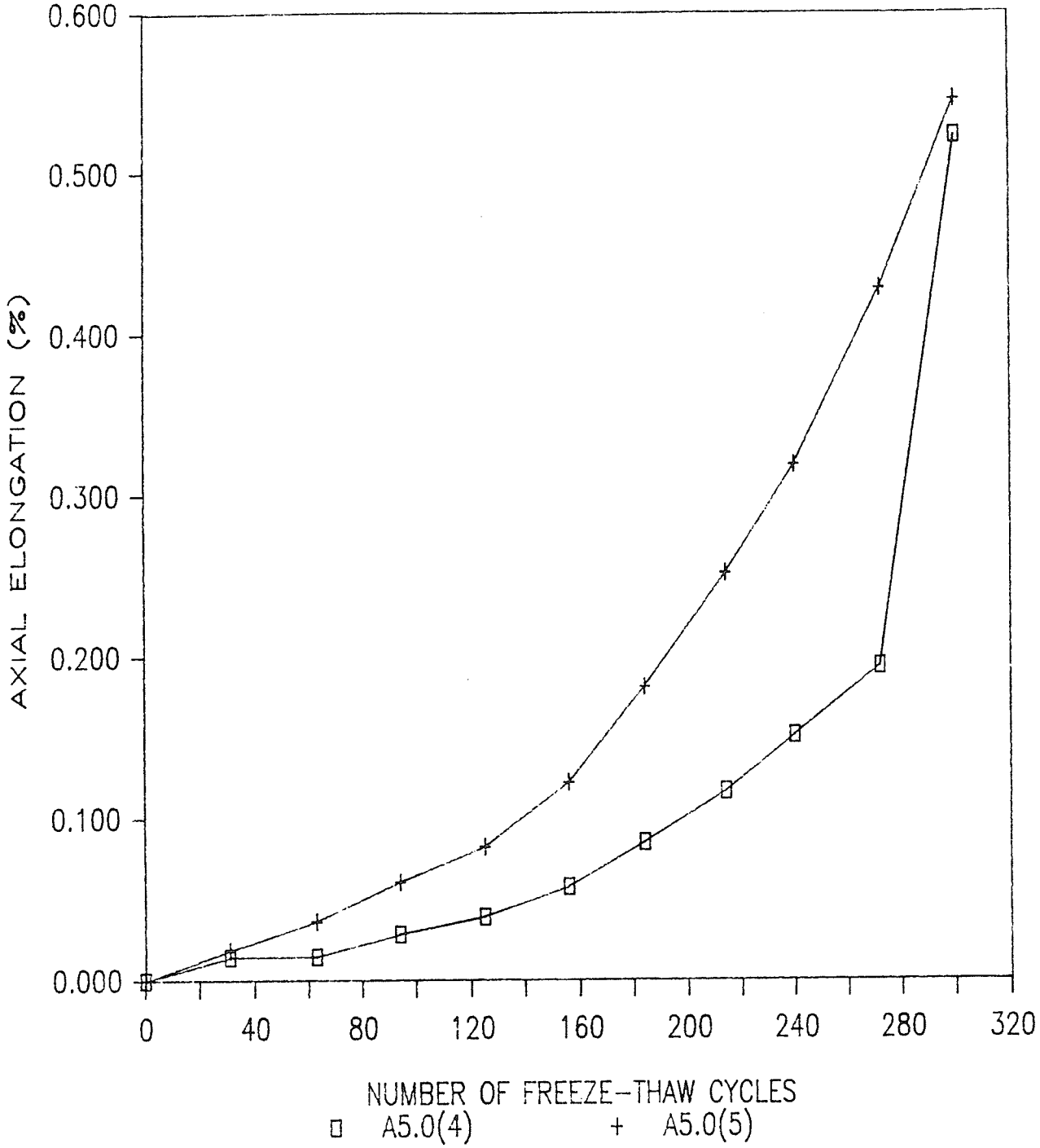

Figure 5.10: Freeze-Thaw Performance of Unsealed Specimens Formed From Mix A5.0

Figure 5.11: Photograph of Specimen A5.0(1) After 300 Cycles of Freeze-Thaw Exhibiting Classic D-Cracking Pattern

Figure 5.12: Photograph of Specimen A5.0(5) After 300 Cycles of Freeze-Thaw Showing Aggregate Related Distress

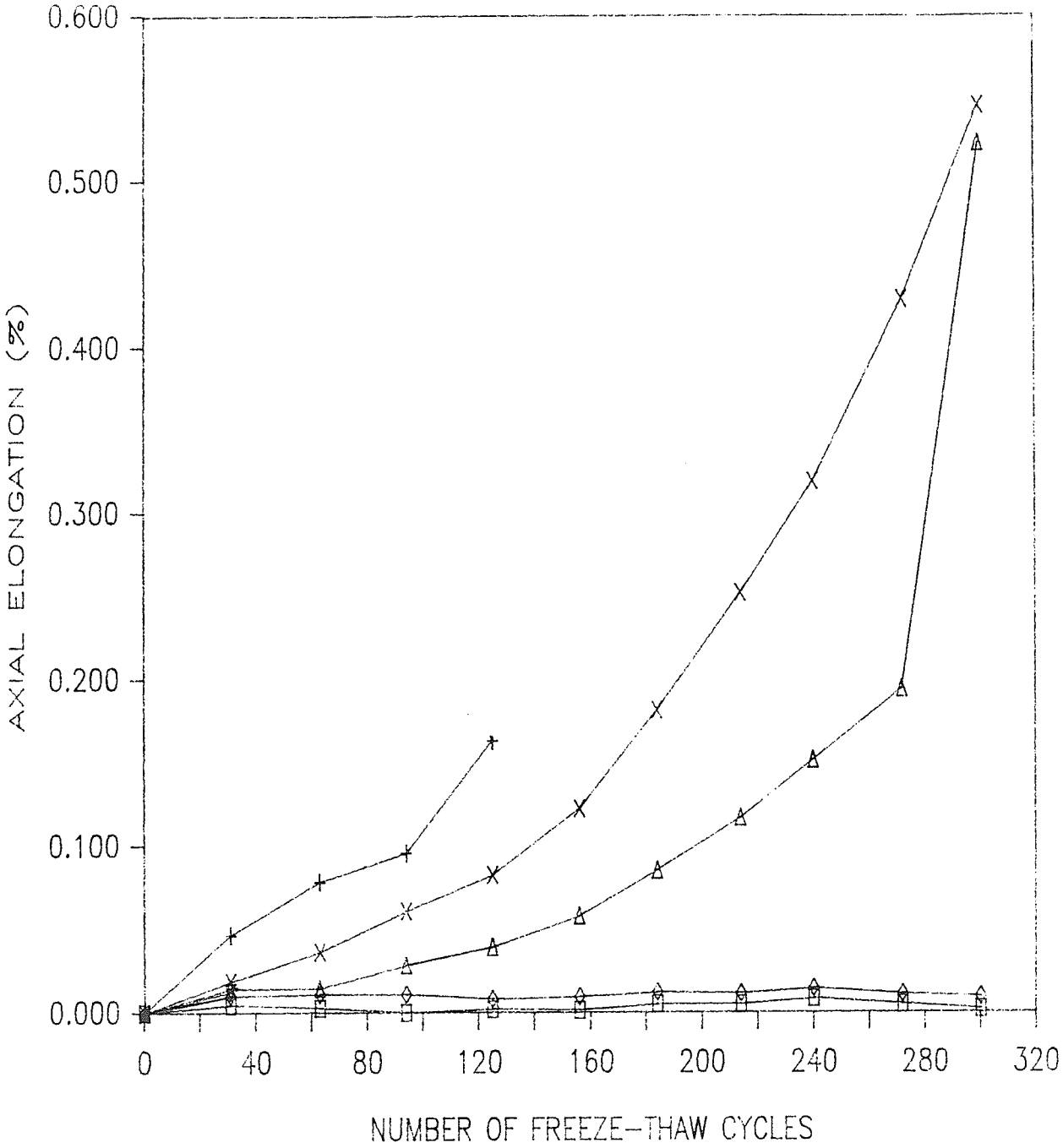

Figure 5.13: Comparison of the Freeze-Thaw Performance of of Specimens With an Air Content of 5.0 Percent

were sealed immediately after curing while specimens A8.5(4,5,6) were left unsealed.

The performance of the sealed specimens is depicted in Figure 5.14. The results show that the A8.5 sealed specimens behaved with remarkable uniformity during the test, and exhibited very little axial expansion. Inspection of these specimens at the end of the test showed minimal damage. The maximum axial elongation was 0.013 which occurred in specimen A8.5(1) after 300 cycles. All three specimens were well below the axial elongation acceptability criteria of 0.06 percent.

The performance of the unsealed specimens is shown in similar fashion in Figure 5.15. Again the behavior of the specimens was uniform. All three specimens experienced a marked decrease in elongation after 180 cycles. The data for specimen A8.5(6) suggests a severe contraction at 210 cycles implying a net negative elongation. This aberration remains unexplained. The maximum elongation for the A8.5 unsealed specimens was 0.016 percent which occurred after 177 freeze-thaw cycles in specimen A8.5(4). Photographs of specimens A8.5(4) and A8.5(6) after 300 cycles are presented in Figure 5.16 and 5.17 respectively. The photographs show that cracking was relatively minor in comparison to the distress experienced by other unsealed specimens containing less entrained air.

In the case of the aggregate failure in specimen A8.5(6) shown in Figure 5.17, it is probable that no amount of entrained air could have prevented the failure given the environmental conditions since it was related to the ability of the aggregate itself to accommodate hydraulic forces.

A comparison of the freeze-thaw performance of the sealed and unsealed specimens with a 8.5 percent air content is given in Figure 5.18. Since there was virtually no difference in the performance of the sealed and

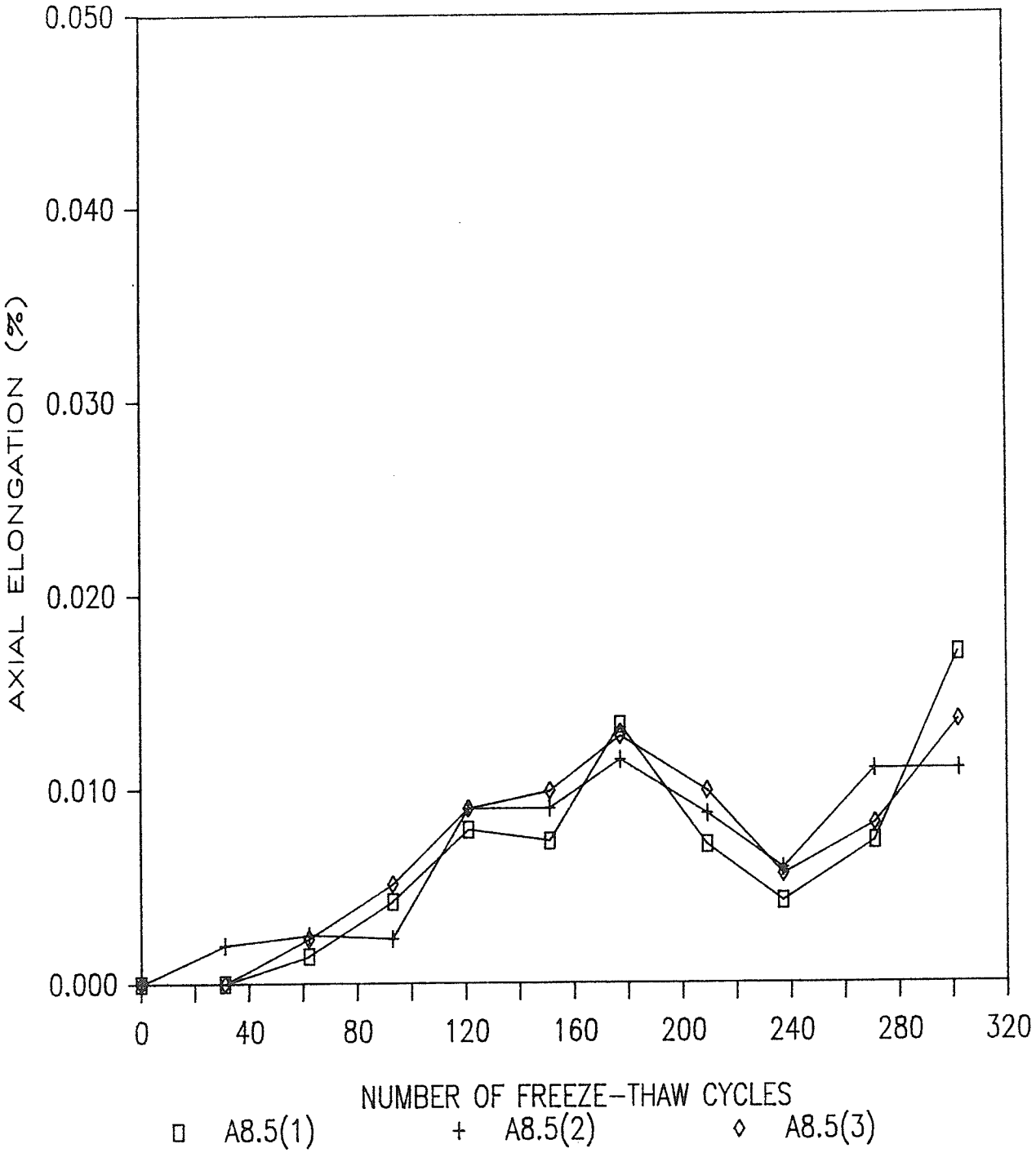

Figure 5.14: Freeze-Thaw Performance of Sealed Specimens Formed from Mix A8.5

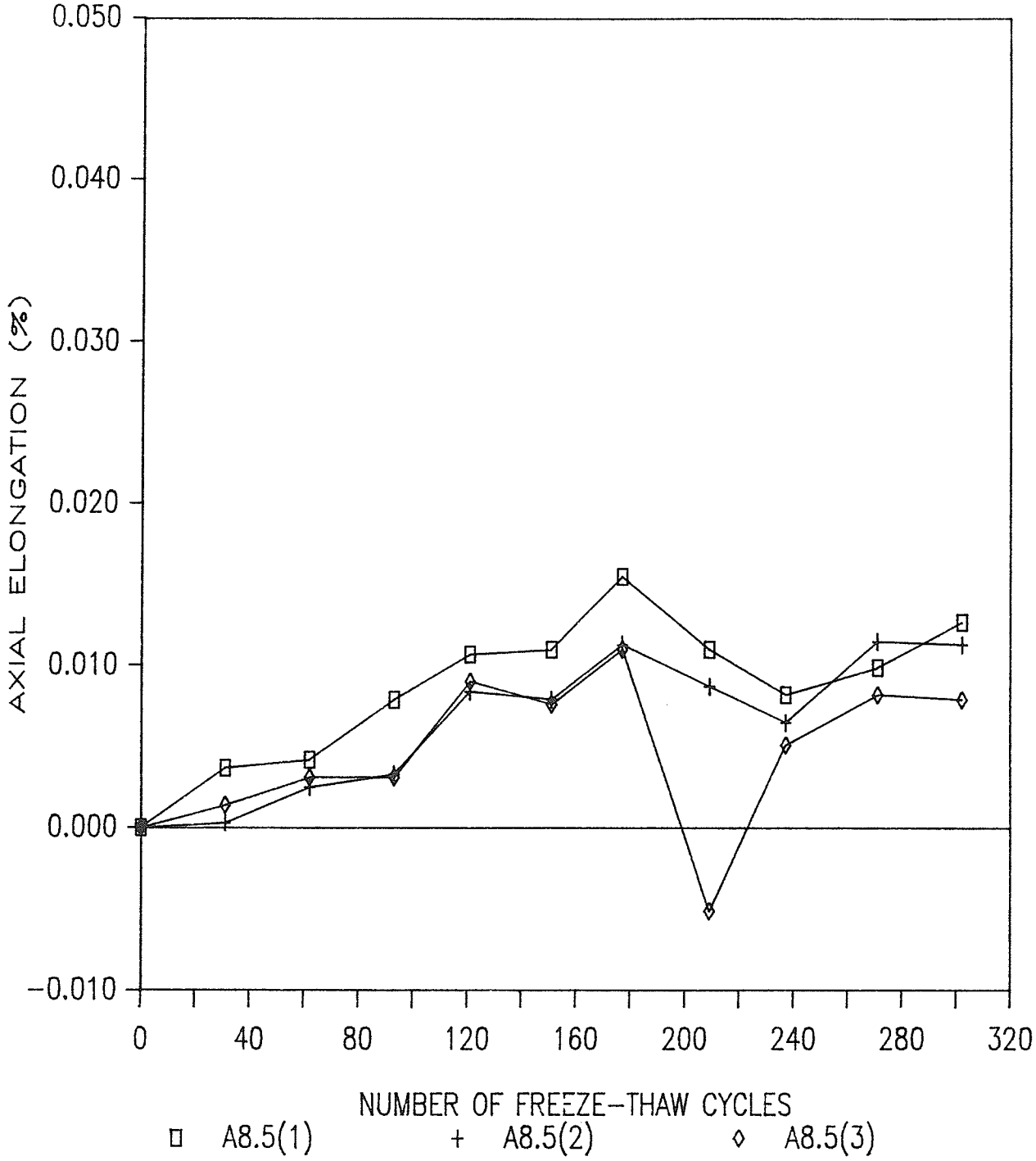

Figure 5.15: Freeze-Thaw Performance of Unsealed Specimens Formed from Mix A8.5

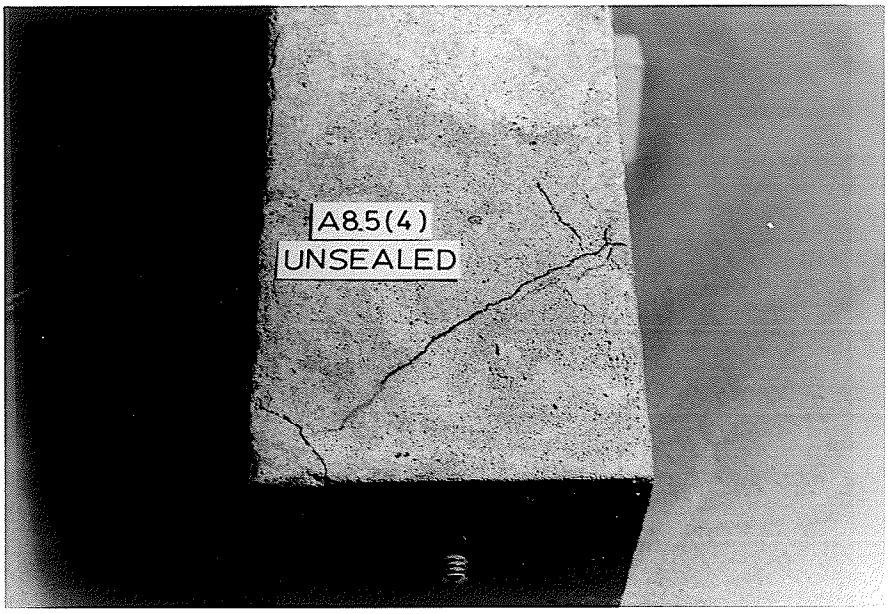

Figure 5.16: Photograph of Specimen A8.5(4) After 300 Cycles of Freeze-Thaw Showing Minor Aggregate Related Distress

Figure 5.17: Photograph of Specimen A8.5(6) After 300 Cycles of Freeze-Thaw Showing Aggregate Fracture

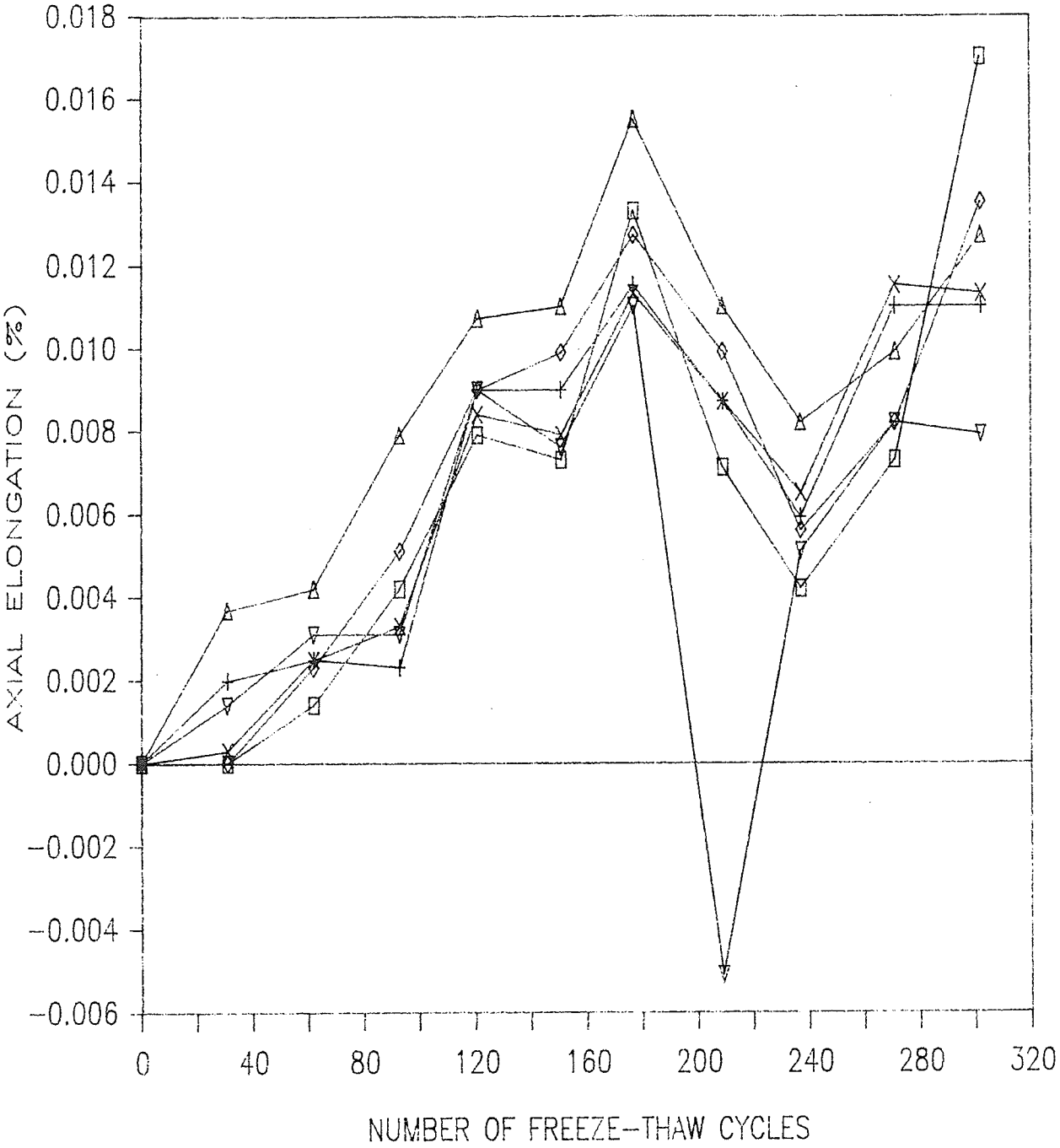

Sealed Specimens		Unsealed Specimens	
□	A8.5(1)	△	A8.5(4)
+	A8.5(2)	×	A8.5(5)
◇	A8.5(3)	▽	A8.5(6)

Figure 5.18 Comparison of the Freeze-Thaw Performance of of Specimens With an Air Content of 8.5 Percent

unsealed specimens, the implication is that air content is of greater significance than availability of moisture. Additional testing would be required to prove this unequivically.

5.6 GENERAL DISCUSSION OF RESULTS

The effect of external water and air content on the freeze-thaw durability and D-Cracking susceptibility of concrete prisms has been documented in the preceding sections. The test results are summarized in this section.

5.6.1 Effect of Air Content

Distress increased with decreasing entrained air content for the unsealed specimens. The effect of air content on durability for sealed and unsealed specimens is shown in Figure 5.19. The plot shows a decrease in durability with decreasing air content. In a general sense the decrease in durability was greater in the unsealed specimens.

This trend is also shown in Figure 5.20, which shows the freeze-thaw performance of the unsealed specimens from all three mixes. The specimens made from the A8.5 mix were the only ones of the unsealed specimens to meet the 300 cycle axial elongation criterion of 0.06 percent. Specimens made from the other two mix designs surpassed this value early in the test and continued to accelerate upward.

Much of the distress experienced by the unsealed specimens was aggregate related as evidenced in Figures 5.6, 5.7, 5.12, 5.16, and 5.17. Since all other mix design factors and environmental conditions were held virtually constant, it would appear that entrained air content of the paste positively affected the durability of the coarse aggregate. Two

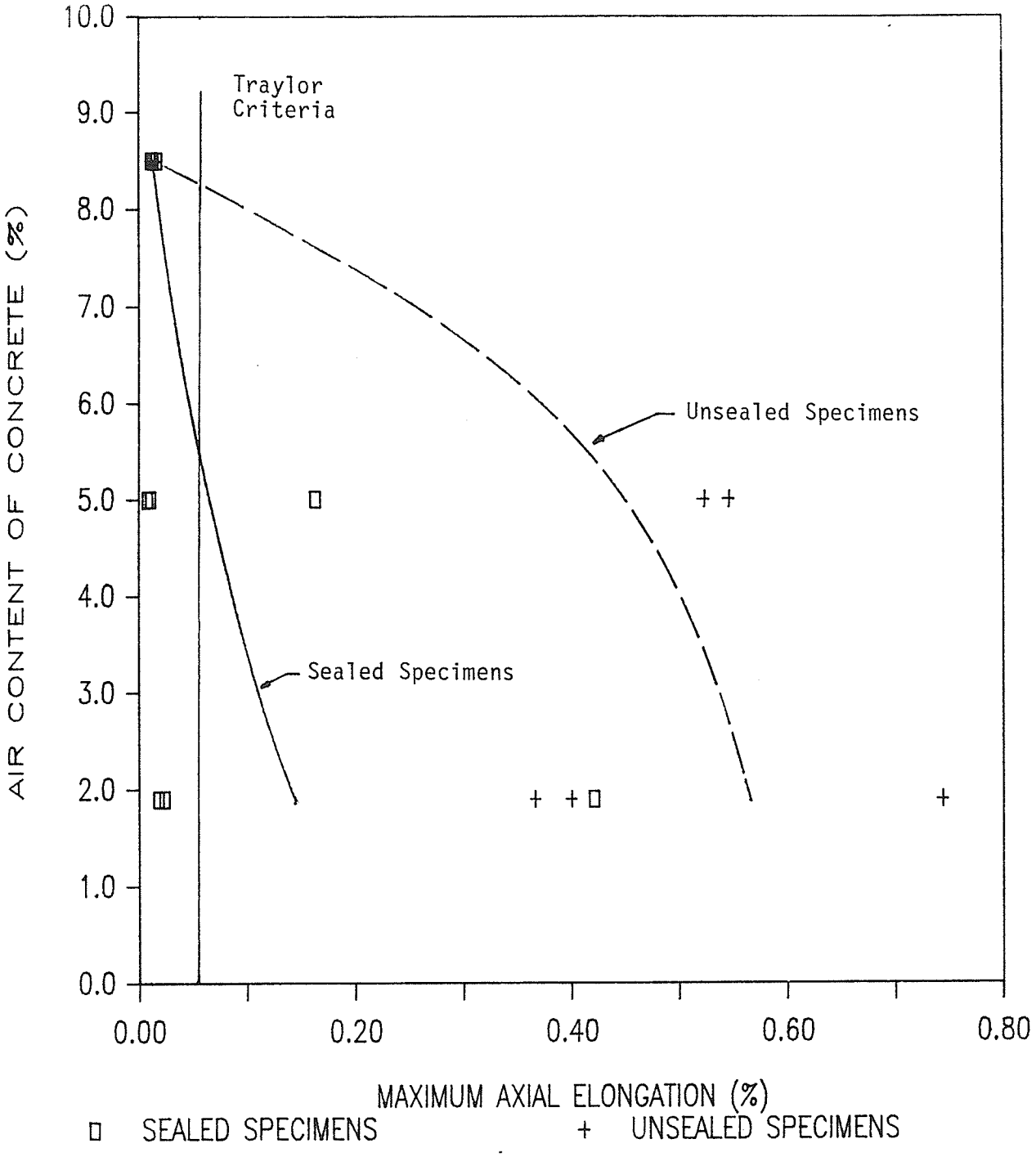

Figure 5.19: Effect of Air Content on Freeze-Thaw Durability of Sealed and Unsealed Specimens From All Mixes

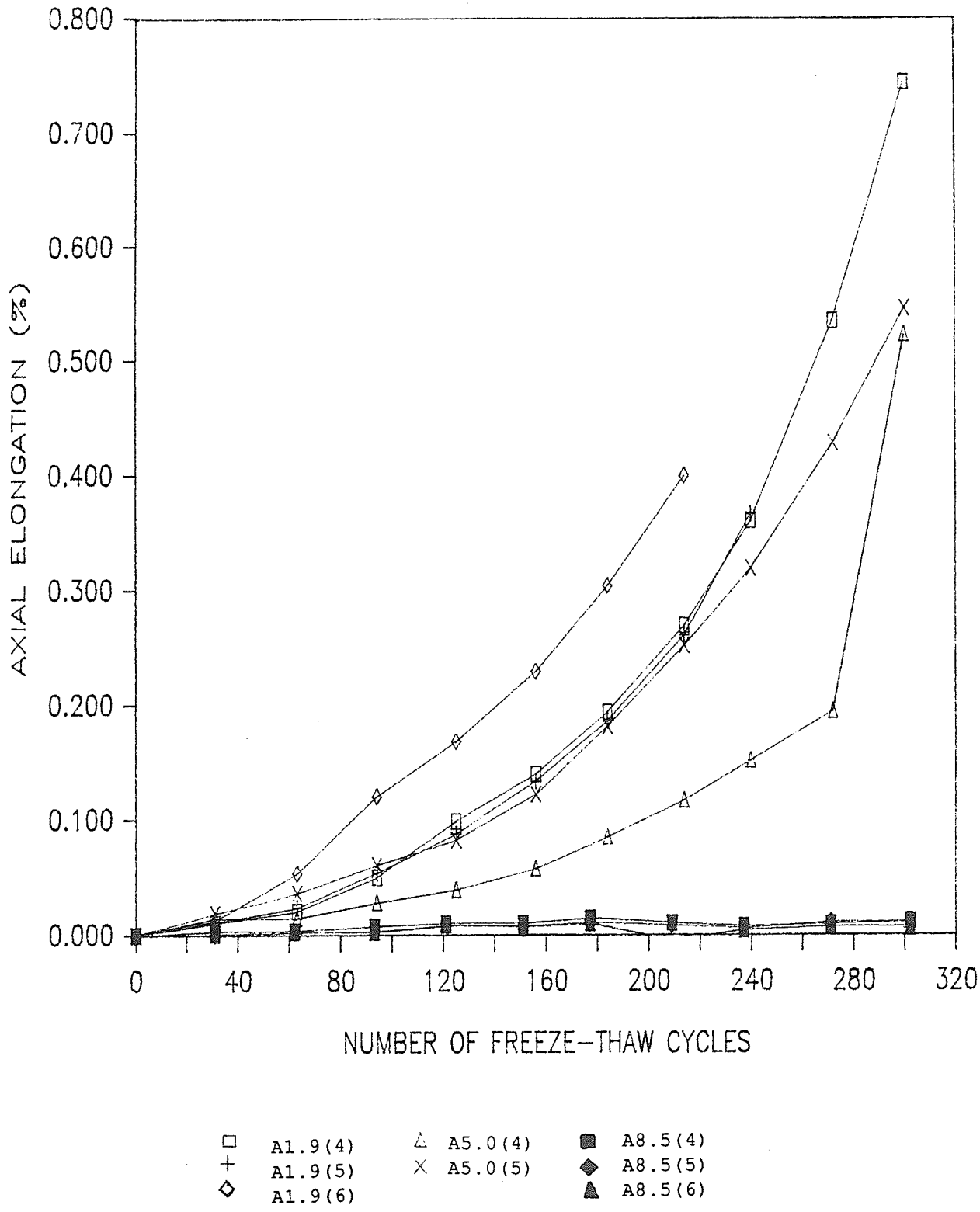

Figure 5.20: Comparison of the Freeze-Thaw Performance of Unsealed Specimens From All Mixes

possible explanations exist. The first possibility, which has been discussed at length in Section 2.3.2.1, relates to the ability of the paste to accommodate the excess volume of water which is extruded from a saturated aggregate upon freezing. An increase in the air content of the paste would increase the its ability to accomodate moisture extruded from the aggregate upon freezing. A non-air entrained paste would be extremely susceptible to this type of failure because it contains no empty voids which could accomodate the excess moisture. This type of failure mechanism woulod be typified by an aggregate/paste bond failure. Since this type of failure was not evident during visual examination of the specimens, this theory must be discarded.

A second possible explanation is that the entrained air bubbles act to control destructive stresses caused by diffusion processes. According to the free energy difference theory discussed in Section 2.4.2, differences in free energy levels of the water in the different types of pores found in concrete after freezing create a flow pattern similar to diffusion. In cement paste, moisture flows from the gel pores to ice formed in the capillary cavities and entrained air voids after a temperature has been reached which is low enough to cause the water held in the capillary pores and entrained air voids to freeze. As water migrates to the capillary cavities it becomes available for freezing. When the capillary becomes full the free energy of the frozen water increases due to the pressure increase caused by the resistance of the pore walls to expansion. At some point in time the free energy of the capillary ice becomes greater than that of the gel water and the flow is reversed, travelling from the capillaries, through the gel pores (where it becomes liquid), and eventually to the entrained air voids (where it becomes solid again).

Since entrained air voids rarely become saturated, the free energy of the ice contained in them does not increase. Flow approaches zero as the free energies of the three phases approach an equal value.

For aggregates encased in cement paste, diffusion processes could theoretically take place across an aggregate/paste interface because the size and shape of the pores in most concrete aggregates are similar to capillary cavities found in cement paste. If the air content of the paste is lowered, then the equilibrium pressure required to reverse flow between the ice in the aggregate pores and the gel water should increase. If the air content is sufficiently low then the pressure required to reverse flow could exceed the tensile strength of the aggregate causing rupture. Also, differences in free energy within the aggregate itself can be harmful provided the aggregate is fine grained (ie. possesses pores with significant freezing point depressions). In this case excessive pressures within the aggregate could also be created due to the large difference in free energy between unfrozen bulk water and capillary ice.

The permeability of cement paste formed with a low w/c ratio is dependent primarily on the properties of the gel. The specimens used in the testing program had a w/c ratio of 0.45. As discussed in Section 2.3.1, this implies that the capillary cavities would not be completely interconnected after hydration. The effect of air entrainment on the permeability of the test specimens would be negligible in this case since the entrained air voids are discreet and would not serve to interconnect the capillaries to an appreciable extent.

Examination of Figure 5.20 leads one to believe that mix design A8.5 is far superior to the other mixes when protection from external moisture is not provided. It should be noted, however, that there may be other

problems associated with the use of a mix with high air entrainment (such as low compressive strength) that are beyond the scope of the current discussion.

5.6.2 Effect of Access to External Moisture

Test results did not unequivically indicate that protection of concrete from external moisture was completely effective in eliminating freeze-thaw deterioration as evidenced by the poor performance of two out of six specimens. Figures 5.3 and 5.4 show that the distress in these specimens was probably caused by a single aggregate which was particularly frost susceptible. The inconsistent performance of the sealed specimens is shown in Figure 5.21, which shows the freeze-thaw performance of the sealed specimens from all three mixes. Only the A8.5 specimens performed satisfactorily throughout the test. Again, while the technique does show some promise, test results do not indicate conclusively that protection from external moisture will prevent deterioration of coarse aggregate exposed to a freeze-thaw environment. Yet prevention of access to external moisture prevented what otherwise would have been excessive elongation of the other four specimens.

As shown in Table 5.1, a 25 mm coarse aggregate gradation calls for 5 percent of the aggregate by weight passing the 37.5 mm sieve be retained on the 25 mm sieve. It appears that the aggregates which caused the distress in specimens A1.9(1) and A5.0(2) fell into this portion of the gradation curve. Because aggregates of this size were relatively rare in the mixes, it is probable that an aggregate of this size was not in every specimen that was formed. This may have been the reason for the inconsistent performance of the sealed specimens. Unfortunately, the above hypothesis is purely speculative at this time and remains a topic for further research.

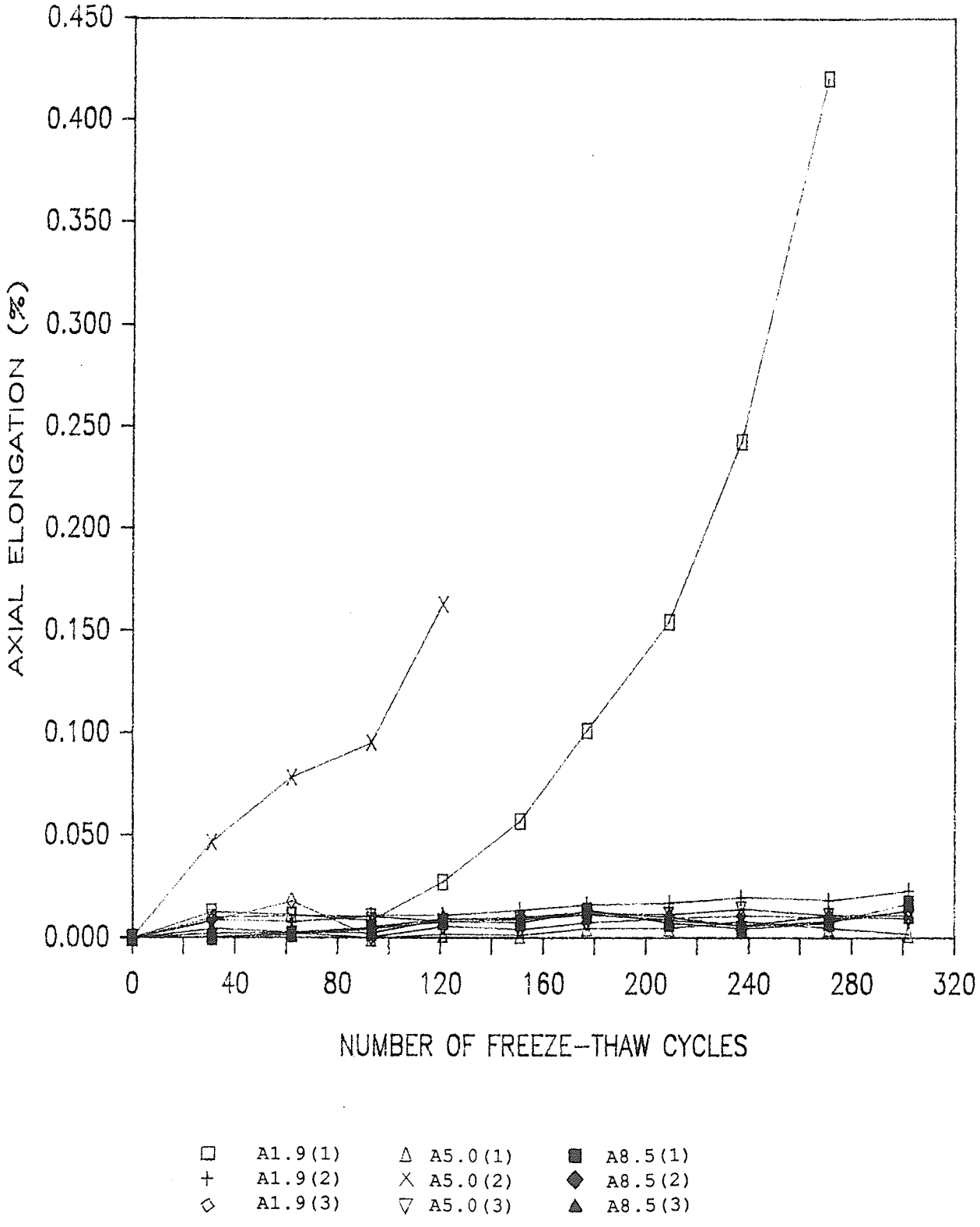

Figure 5.21: Comparison of the Freeze-Thaw Performance of Sealed Specimens From All Mixes

Chapter VI

CONCLUSIONS AND RECOMMENDATIONS FOR FURTHER RESEARCH

6.1 INTRODUCTION

The results and analysis of the results from the testing program were presented in the previous two chapters. This chapter summarizes the findings of the program and provides recommendations for further research. Conclusions from the fly ash test will be summarized first.

6.2 OBSERVATIONS AND CONCLUSIONS FROM THE FLY ASH TEST

1. The addition of fly ash to the mixes led to lower air contents and lower slumps. This was probably due to the presence of carbon black particles which absorbed a portion of the air entraining agent.
2. Compressive strengths of the fly ash mixes were higher than the ordinary PCC mixes. The difference in strength increased as the age of the concrete increased, which illustrated the time dependent effect of fly ash on the strength of the mixes.
3. The freeze-thaw resistance of the ordinary PCC control mixes were superior to that of the fly ash mixes containing the same coarse eggregate. This was the case even though the compressive strengths of the fly ash mixes were higher than the control mixes.

4. Distress present in the ordinary PCC control mixes was coarse aggregate related. A higher air content was associated with improved freeze-thaw durability of the ordinary PCC control specimens.
5. An aggregate/cement paste interfacial failure was responsible for deterioration of the fly ash specimens.
6. A higher entrained air content was associated with improved freeze-thaw resistance of the fly ash specimens.

6.3 OBSERVATIONS AND CONCLUSIONS FROM THE AIR CONTENT AND EXTERNAL MOISTURE TEST

1. As air content increased, the slump of the mixes increased and density decreased, as expected.
2. An inverse relationship existed between compressive strength and and air content of the mixes.
3. The freeze-thaw resistance of sealed specimens was extremely variable.
4. Test results showed that limiting accessibility of concrete specimens to external moisture improved freeze-thaw resistance of four out of six specimens. The other two specimens underwent excessive elongation.
5. In a general sense, the difference in freeze-thaw resistance between the sealed and unsealed specimens was greatest for the n on-air entrained specimens (mix A1.9), less for the mix with 5.0 percent air entrainment (mix A5.0), and nonexistent for the mix with an entrained air content of 8.5 percent (mix A8.5).

6. An increase in the air content of the cement paste improved the freeze-thaw resistance of aggregates encased in the paste. The reason may be due to the fact that an increased entrained air content reduces the magnitude of destructive stresses caused by diffusion processes.

6.4 RECOMMENDATIONS FOR FURTHER RESEARCH

Recommendations for further research are as follows:

1. The effect of the rate of temperature change on the laboratory freeze-thaw performance could be studied. This could shed more light on the mechanisms involved in the deterioration of concrete due to frost action.
2. Length changes in the specimens during freezing and thawing could be monitored continuously during the freeze-thaw cycles using LVDT's and automated data gathering devices. This technique would provide a better understanding of what actually happens to a specimen during a freeze-thaw cycle.
3. The performance of the fly ash specimens showed considerable sensitivity to variations in air content in the 4 to 5 percent range. Additional testing could be carried out with closer controls on the air contents of the fly ash and control mixes to provide more insight into whether a significant difference exists between the structure of ordinary concrete and fly ash concrete which could account for any difference in performance.
4. The effect of composition of fly ash on the freeze-thaw performance of fly ash concrete specimens could be studied. This is particularly important because fly ash is a byproduct of a

relatively uncontrolled process and therefore its properties can vary considerably from plant to plant and with time within a single plant. Results from this testing program could provide information on the relative durability of different types of fly ash concrete when subjected to cyclic freeze-thaw.

5. Additional testing should be undertaken to determine why aggregate performance improved as the entrained air content of the cement paste was increased. If the mechanism is related to a diffusion process involving interaction between both aggregate and paste as previously discussed, then a testing program which would involve slow cooling of concrete specimens to a given temperature and maintaining that temperature for a predetermined length of time could verify this hypothesis. Holding the temperature constant would be necessary to ensure that destructivce forces created during freezing (predicted by the Hydraulic Pressure Theory) would not contribute to the distress experienced by the specimens. This process would be repeated for mixes with different air contents, thus providing insight on the effect of air content of cement paste on destructive forces caused by free energy differences.

6. Additional testing should be undertaken to determine the effect of the moisture condition of the coarse aggregate prior to mixing on the freeze-thaw resistance of the aggregate. The procedure would involve soaking the coarse aggregates for different lengths of time and possibly under different conditions (ie. ordinary soaking, evacuating the pores system of air and then soaking), performing freeze-thaw tests, and comparing the results.

7. A series of tests could be performed to determine the effect of aggregate mineralogy on freeze-thaw durability. The performance of specimens containing aggregate of similar mineralogical composition could be compared to the performance of specimens containing aggregate of different mineralogical compostion. Results from such a testing program could provide information on the degree of frost susceptibility of different aggregate types.

REFERENCES

1. Girard, R.J., Myers, E.W., Manchester, G.D., and Trimm, W.L. (1982), "D-Cracking: Pavement Design and Construction Variables," in Concrete Analysis and Deterioration, Transportation Research Record 853, Transportation Research Board, National Research Council, National Academy of Sciences, Washington, D.C., pp.1-8.

2. Traylor, M.L. (1982), "Efforts to Eliminate D-Cracking in Illinios," in Concrete Analysis and Deterioration, TRR 853, Transportation Research Board, Washington, D.C., pp.9-14.

3. Winslow, D.N., Lindgren, M.K., and Dolch, W.L. (1982), "Relation Between Pavement D-Cracking and Aggregate Pore Structure," in Concrete Analysis and Deterioration, TRR 853, Transportation Research Board, Washington, D.C., pp.17-20.

4. Marks, V.J., and Dubberke, W. (1982), "Durability of Concrete and the Iowa Pore Index Test," in Concrete Analysis and Deterioration, TRR 853, Transportation Research Board, Washington, D.C., pp.25-30.

5. Stark, D. (1976), "Characteristics and Utilization of Coarse Aggregates Associated with D-Cracking," in Living with Marginal Aggregates, American Society for Testing and Materials Special Technical Publication No. 597, Philadelphia, Pa., pp.44-58.

6. Bukovatz, J.E., Crumpton, C.F., and Worley, H.E. (1974), "Kansas Concrete Pavement Performance as Related to D-Cracking," in Cement-Aggregate Reactions, TRR 525, Transportation Research Board, Washington, D.C., pp.1-8.

7. Stark, D. and Klieger, P. (1973), "Effects of Maximum Size of Coarse Aggregate on D-Cracking in Concrete Pavements," in Grading of Concrete Aggregtes, Highway Research Record 441, Highway Research Board, National Research Council, National Academy of Sciences, Washington, D.C., pp.33-43.

8. Powers, T.C. (1955), "Basic Considerations Pertaining to Freezing and Thawing Tests," ASTM Proceedings, Vol. 55, pp.1132-1155.

9. Verbeck, G., and Langdren, R. (1960), "Influence of Physical Characteristics of Aggregtes on Frost Resistance of Concrete," ASTM Proceedings, Vol. 60, pp.1063-1079.

10. Stark, D. (1970), "Field and Laboratory Studieson the Effect of Subbase Type on the Development of D-Cracking," in Environmental Effects on Concrete, HRR 342, Highway Research Board, Washington, D.C., pp.27-38.

11. Axon, E.O., Murray, L.T., and Rucker, R.M., (1969), "Laboratory Freeze-Thaw Tests vs Outdoor Exposure Tests," HRR 268, Highway Research Board, Washington, D.C., pp.35-47.

12. Powers, T.C. (1945), "A Working Hypothesis fdr Further Studies of Frost Resistance of Concrete," American Concrete Institute Proceedings, Vol. 41, pp.245-272.

13. Litvan, G.G. (1972), "Phase Transitions of Adsorbates IV. Mechanism of Frost Action in Hardened Cement Paste," Research Paper No. 499 of the Division of Building Research, National Research Council of Canada. Reprinted from the Journal of the American Ceramic Society, Vol. 55, pp.38-42.

14. Litvan, G.G. (1978), "Absorptive Systems at Temperatures Below the Freezing Point of the Adsorptive," DBR Paper No. 781, NRCC. Reprinted from Advances in Colloid and Interface Science, Vol. 9, pp.253-297.

15. Powers, T.C., and Helmuth, R.A. (1953), "Theory of Volume Changes in Hardened Portland Cement Paste During Freezing," HRB Proceedings, Vol. 32, pp.285-297.

16. Larson, T.D., and Cady, P.D. (1969), "Identification of Frost Susceptible Particles in Concrete Aggregates," National Cooperative Highway Research Program, Report No. 66, Washington, D.C.

17. Neville, A.M. (1963), Properties of Concrete, Sir Issac Pitman and Sons, London.

18. Cordon, W.A. (1966), Freezing and Thawing of Concrete-Mechanisms and Control, ACI Monograph No. 3, Detroit.

19. Thomson, S.R., Olsen, M.P.J., and Dempsey, B.J. (1980), "Synthesis Report: D-Cracking in Portland Cement Concrete Pavements," Transportation Engineering Series No.29, Illinios Cooperative Highway and Transportation Series No. 187, University of Illinios, Urbana, Illinios.

20. Verbeck, G. (1956), "Pore Structure," ASTM STP No. 169, pp.137-142.

21. Dolch, W.L. (1956), "Porosity," ASTM STP No. 169, pp.443-461.

22. Dunn, J.R., and Hudec, P.P. (1972), "Frost and Sorption Effects in Argillaceous Rocks," in Frost Action in Soils HRR 393, Highway Research Board, Washington, D.C., pp.65-78.

23. Powers, T.C. (1975), "Freezing Effects in Concrete," in Durability of Concrete, ACI Special Publication No. 47, Detriot, pp.1-12.

24. Powers, T.C. (1949), "The Air requirement of Frost Resistant Concrete," HBR Proceedings, Vol. 29, pp.184-203.

25. Popovics, S. (1968), "What Should an Engineer Know About the Nature of Admixtures?" Concrete, Vol. 2, pp.272-277.

124

26. Klieger, P. (1952), "Effect of Entrained Air on Strength and Durability of Concrete with Various Sizes of Aggregates," HRB Proceedings, pp.1-17.

27. Axon, E.O., Willis, T.F., and Reagel, F.V. (1943), "Effect of Air Entrapping Cement on the Resistance to Freezing and Thawing of Concrete Containing Inferior Coarse Aggregate," ASTM Proceedings, Vol. 43, pp.981-1000.

28. Bugg, S.L. (1947), "Effect of Air Entrainment on the Durability Characteristics of Concrete Aggregates." HRB Proceedings, Vol. 27, pp.156-170.

29. Berry, E.E., and Malhotra, V.M. (1980), "Fly Ash in Concrete - A Critical Review," ACI Journal, pp.59-73.

30. "Standard Specification for Fly Ash and Raw or Calcinated Natural Pozzolan for Use as a Mineral Admixture in Portland Cement Concrete," (ASTM C618-85), 1985 Book of ASTM Standards, Section 4.02, ASTM, Philadelphia, Pa., pp.382-385.

31. Pasko, T.J., and Larson, T.D. (1962), "Some Statistical Analysis of the Strength and Durability of Fly Ash Concrete," ASTM Proceedings, Vol.62, pp.1054-1067.

32. Higginson, E.C. (1956), "Mineral Admixtures," ASTM STP No. 169A, pp.543-551.

33. Washa, G.W., and Withey, N.H. (1953), "Strength and Durability of Concrete Containing Chicago Fly Ash," ACI Proceedings, Vol. 24, pp.701-712.

34. Abdun-nur, E.A. (1961), "Fly Ash in Concrete - An Evaluation," HRB Bulletin 284, Washington, D.C.

35. Committee MC-B5(7) (1971), "Use of Pozzolans in Highway Concrete," in Admixtures in Concrete, HRB Special Report 119, pp.21-28.

36. Larson, T.D. (1964), "Air Entrainment and Durability Aspects of Fly Ash Concrete," ASTM Proceedings, Vol. 64, pp.866-886.

37. Larson, G.H. (1953), "Effect of Substitutions of Fly Ash for Portions of Cement in Air Entrained Concrete," HRB Proceedings, Vol. 32, pp.328-335.

38. Bollen, R.E., and Sutton, C.A. (19??), "Pozzolans in Sand-Gravel Aggregate Concrete," HRB Proceedings, Vol. 32, pp.317-328

39. Klieger, P., and Langdren, R. (1969), "Performance of Concrete Slabs in Outdoor Exposure," HHR 268, Highway Research Board, Washington, D.C., pp.62-79.

40. "Standard Test Method for Resistance of Concrete to Rapid Freezing and Thawing," (ASTM C666-84), 1984 Book of ASTM Standards, Section 4.02, ASTM, Philadelphia, Pa., pp.403-410.

41. "Standard Test Method for Unit Weight and Voids in Aggregate," (C29-78), 1984 Book of ASTM Standards, Section 4.02, ASTM, Philadelphia, Pa.,pp.1-4.

42. "Standard Test Method for Specific Gravity and Absorption of Coarse Aggregate," (C127-84), 1984 Book of ASTM Standards, Section 4.02, ASTM, Philadelphia, Pa.,pp.82-87.

43. "Standard Test Method for Specific Gravity and Absorption of Fine Aggregate," (C128-84), 1984 Book of ASTM Standards, Section 4.02, ASTM, Philadelphia, Pa.,pp.88-93.

44. "Domaschuk, L., and Hermanson, G. (1984), "D-Cracking of Concrete Pavements Progress Report No. 3, Freeze-Thaw Testing Using a Modified ASTM C666 Proceedure," Unpublished Report to Transport Canada (Winnipeg Branch).

45. "Standard Method of Making and Curing Concrete Test Specimens in the Laboratory," (C192-81), 1984 Book of ASTM Standards, Section 4.02, ASTM, Philadelphia, Pa.,pp.141-150.

46. "Standard Specification for Apparatus for Use in Measurement of Length Changes in Hardened Cement Paste, Mortar, and Concrete," (C490-83a), 1984 Book of ASTM Standards, Section 4.02, Philadelphia, Pa.,pp.315-321.

47. Mysyk, W.K. Personal Communication.

48. Mysyk, W.K., and Edwards, R.J. (1985), "Mineralogical Analysis and Literature Review of Limestone Aggregate Porosity/Permeability From Apron 1, Winnipeg International Airport, Winnipeg, Manitoba," Final Report to Transport Canada, Contract No. CCB-CON-84-24.

49. Domaschuk, L. (1986), "A Preliminary Study of D-Cracking of Concrete Pavements in Manitoba," Report to Transport Canada.

ANNOTATED BIBLEOGRAPHY

1. Hiltrop, C.L., and Lemish, J. (1960), "Relationship of Pore Size Distribution and Other Rock Properties to Serviceability of Some Carbonate Aggregates," Highway Research Board Bulletin, No.239, Washington, D.C., pp.1-23.

2. Shakoor, A., West, T.R., and Scholer, C.F. (1982), "Physical Characteristics of Some Indiana Argillaceous Carbonates Regarding Their Freeze-Thaw Resistance in Concrete," Bulletin of the Association of Engineering Geologists, Vol. 19, pp.371-384.

3. Dolch, W.L. (1980), "Porosity," Chapter 37, ASTM STP 169B, ASTM, Philadelphia, Pa., pp.646-656.

4. Kaneuji, M., Winslow, D.N., and Dolch, W.L. (1980), "The Relationship Between an Aggregate's Pore Size Distribution and its Freeze-Thaw Durability in Concrete," Cement and Concrete Research, Vol. 10, pp.433-441.

5. Alford, N.McN., and Rahman, A.A. (1981), "An Assessment of Porosity And Pore Sizes in Hardened Cement Pastes," Journal of Materials Science, Vol. 16, pp.3105-3114.

6. Havens, J.H. and Deen, R.C. (1977), "Possible Explanation of Concrete Pop-Outs," in Concrete, Aggregates, Marking Materials, Corrosion, and Joint Seals TRR 651, Transportation Research Board, Washington, D.C., pp.16-24.

7. Larson, T., Cady, P., Franzen, M., and Reed, J. (1964), "A Critical Review of Literature Treating Methods of Identifying Aggregates Subject to Destructive Volume Change When Frozen in Concrete and a Proposed Program of Research," Highway Research Board Special Report 80, Washington, D.C.

8. Larson, T.D. Boettcher, A., Cady, P., Franzen, M., and Reed, J. (1965), "Identification of Concrete Aggregates Exhibiting Frost Susceptibility," NCHRP, Report 15, Highway Research Board, Washington, D.C.

APPENDIX A

PROPERTIES OF FLY ASH USED IN THE TESTING PROGRAM

MAY 13 1 -

COAL BY-PRODUCTS UTILIZATION INSTITUTE

Engineering Experiment Station
University of North Dakota
8115 University Station
Grand Forks, ND 58202
Phone: (701) 777-4222 or 3779

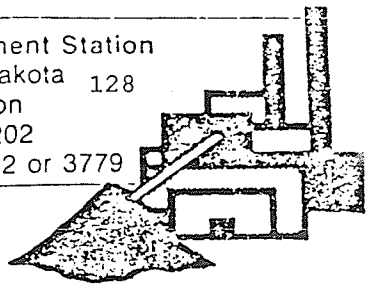

CHEMICAL AND PHYSICAL ANALYSES OF FLY ASH

REPORT TO: Saskatchewan Power Corp. DATE: 4/4/85

Laboratory No. 85-9

Sample Identification: Boundary Dam #6

Date Received: 1/15/85

			ASTM: C 618 SPECIFICATIONS CLASS F		ASTM: C 618 SPECIFICATIONS CLASS C	
CHEMICAL COMPOSITION(%):						
Silicon Dioxide (SiO_2)	43.8					
Aluminum Oxide (Al_2O_3)	22.6					
Iron Oxide (Fe_2O_3)	3.4					
Total ($SiO_2 + Al_2O_3 + Fe_2O_3$)		69.8	70.0	Min	50.0	Min
Sulfur Trioxide (SO_3)		.65	5.0	Max	5.0	Max
Calcium Oxide (CaO)		13.6				
Moisture Content		.10	3.0	Max	3.0	Max
Loss of Ignition		1.89	6.0	Max	6.0	Max
Available Alkalies as Na_2O*		2.93	1.5	Max	1.5	Max
PHYSICAL TEST RESULTS:						
Fineness						
Retained on #325 sieve, (%)		29.00	34	Max	34	Max
Pozzolanic Activity Index						
With Portland Cement (%)						
Ratio to Control @ 28 days		94	75	Min	75	Min
With Lime @ 7 days (psi)		812	800	Min	800	Min
Water Requirement, % of Control		94	105	Max	105	Max
Soundness						
Autoclave Expansion (%)		.07	0.8	Max	0.8	Max
Drying Shrinkage						
Increase at 28 days (%)*			0.03	Max	0.03	Max
Specific Gravity		2.31				

*These optional limits apply only when specifically requested.

REMARKS:

Na_2O	7.3
K_2O	.6

Coal By-Products Utilization Institute

Oscar E. Manz, Director

COAL BY-PRODUCTS UTILIZATION INSTITUTE

Engineering Experiment Station
University of North Dakota
8115 University Station
Grand Forks, ND 58202
Phone: (701) 777-4222 or 3779

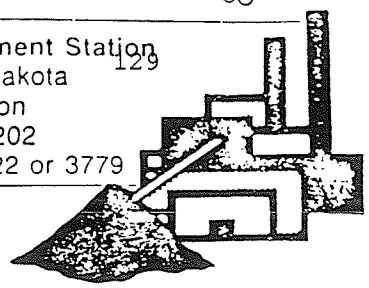

CHEMICAL AND PHYSICAL ANALYSES OF FLY ASH

REPORT TO: Saskatchewan Power Company DATE: 4/8/85

Laboratory No. 85-69

Sample Identification: Boundary Dam #6

Date Received: 2/19/85

			ASTM: C 618 SPECIFICATIONS CLASS F	CLASS C
CHEMICAL COMPOSITION(%):				
Silicon Dioxide (SiO_2)	45.8			
Aluminum Oxide (Al_2O_3)	21.8			
Iron Oxide (Fe_2O_3)	3.6			
Total ($SiO_2 + Al_2O_3 + Fe_2O_3$)		71.2	70.0 Min	50.0 Min
Sulfur Trioxide (SO_3)		.50	5.0 Max	5.0 Max
Calcium Oxide (CaO)		12.2		
Moisture Content		.08	3.0 Max	3.0 Max
Loss of Ignition		.62	6.0 Max	6.0 Max
Available Alkalies as Na_2O*			1.5 Max	1.5 Max
PHYSICAL TEST RESULTS:				
Fineness				
Retained on #325 sieve, (%)		30.69	34 Max	34 Max
Pozzolanic Activity Index				
With Portland Cement (%)				
Ratio to Control @ 28 days			75 Min	75 Min
With Lime @ 7 days (psi)		1138	800 Min	800 Min
Water Requirement, % of Control		96	105 Max	105 Max
Soundness				
Autoclave Expansion (%)		.13	0.8 Max	0.8 Max
Drying Shrinkage				
Increase at 28 days (%)*			0.03 Max	0.03 Max
Specific Gravity		2.29		

*These optional limits apply only when specifically requested.

REMARKS:

Na_2O	6.6
K_2O	0.8

Coal By-Products Utilization Institute

Oscar E. Manz, Director

APPENDIX B

DETERMINATION OF AGGREGATE PROPERTIES AND MIX DESIGNS FOR THE EXTERNAL MOISTURE AND AIR CONTENT TEST

B.1 DRY RODDED DENSITY OF COARSE AGGREGATE

Source: ASTM C29-78

Weight of container = 2.651 kg
Weight of container and soil = 7.736 kg
Weight of container and water = 5.457 kg (at 21°C.)

Density of water at 21°C = 988.42 kg/m^3

Net weight aggregate = 5.085 kg
Net weight of water = 2.806 kg

Density of coarse aggregate = (A/B) * C

where:
A = Weight of aggregate (kg)
B = Weight of water (kg)
C = Density of water at temperature of test (kg/m^3)

Therefore, Density = (5.085/2.806) * 988.42 = 1792 kg/m^3

B.2 RELATIVE DENSITY AND ABSORPTION OF FINE AGGREGATE

Source: ASTM C128-84

A = Mass of oven dry fine aggregate in air = 493.12 g
B = Mass of pycnometer filled with water = 672.46 g
C = Mass of pycnometer with fine aggregate and water to calibration mark = 982.36 g

Mass of fine aggregate in the Saturated Surface Dry (SSD) condition = 500.00 g

Bulk Relative Density = A/(B + 500 - C)
= 493.12/(672.46 + 500.00 - 982.36) = 2.594

Bulk Relative Density = 500.00/(B + 500 -C)
(SSD Basis) = 500.00/(672.46 + 500.00 - 982.36) = 2.630

Apparent Rel. Density = A/(B + A - C)
= 493.12/(672.46 + 493.12 - 982.36) = 2.691

Absorption (%) = [(500.00 - A)/A] * 100
= [(500.00 - 493.12)/493.12] * 100 = 1.395

For any given type of relative density, the mean value of the entire gradation is given by:

$$G = \frac{1}{\frac{P_1}{100G_1} + \frac{P_2}{100G_2} + \ldots + \frac{P_n}{100G_n}}$$

Similarly, the mean absorption value for any given gradation is given by:

$$A = (P_1A_1/100) + (P_2A_2/100) + \ldots + (P_nA_n/100)$$

The coarse aggregate gradation used for mix designs in the air content and external moisture test is as follows:

Sieve Size	Percent Passing
37.5 mm	100
25.0 mm	95
12.5 mm	45
4.8 mm	0

The Bulk Relative Density (SSD basis) is usually used in calculations pertaining to concrete mix design. Therefore, for mix design purposes, the following values were used:

$$\text{Bulk Relative Density SSD Basis} = \frac{1}{\frac{5}{100(2.679)} + \frac{50}{100(2.675)} + \frac{45}{100(2.677)}}$$

$$= \underline{2.676}$$

$$\text{Absorption (\%)} = \frac{5(1.421)}{100} + \frac{50(1.615)}{100} + \frac{45(1.173)}{100}$$

$$= \underline{1.658}$$

B.3 DETERMINATION OF COARSE AGGREGATE ABSORPTION AND RELATIVE DENSITY

Source: ASTM C127-84

Weight of Samples in Different Conditions (g)	Sample Size Limits (in.)		
	1.5 - 1	1 - 0.5	0.5 - No.4
SSD weight	6031.5	5349.0	2347.5
Submerged weight	3780.0	3349.5	1470.5
Oven dry weight	5947.0	5264.0	2307.5

Bulk Relative Density = A/(B - C)

Bulk Relative Density = B/(B - C)
(SSD Basis)

Apparent Rel. Density = A/(A - C)

Absorption (%) = [(B - A)/A] * 100

where:
A = Weight of oven dry specimen in air (g)
B = Weight of saturated surface dry (SSD) specimen in air (g)
C = Weight of saturated specimen in water (g)

Test Results

Type of Relative Density	Particle Size Range (in.)		
	1.5 - 1	1 - 0.5	0.5 - No.4
Bulk	2.641	2.632	2.631
Bulk (SSD)	2.679	2.675	2.677
Apparent	2.744	2.750	2.757
Absorption	1.421	1.615	1.733

B.4 PRELIMINARY MIX DESIGN FOR THE AIR CONTENT/EXTERNAL MOISTURE TEST MIX DESIGN NO. 1 (NO AIR ENTRAINMENT)

Properties of the Materials and Desired Mix Characteristics

Cement :Type 10 Normal

Coarse Aggregate: Max. nominal size = 25 mm (5% Retained on sieve)
Relative Density (SSD) = 2.68
24 hour absorption = 1.66%
Dry Rodded Mass (SSD) = 1792 kg/m^3

Fine Aggregate : Relative Density (SSD) = 2.630
24 hour absorption = 1.395%
Moisture Content = 0% (oven dry)
Fineness Modulus = 2.98

Concrete Desired: Frequently exposed to freeze-thaw
28 day compressive strength = 25 MPa

Air Content : As close to 0% as possible

Slump :50 mm + 10 mm

C.4.1 Mix Design No. 1 (No Air Entrainment)

Methodology based on the procedure outlined in the Canadian Portland Cement Association CPCA handbook.

Step 1 Select slump = 50 mm

Step 2 Maximum aggregate size = 25 mm

Step 3 Mixing water requirement depends on maximum size, particle shape, grading of the aggregates, and the amount of entrained air. From Table 7.6 (CPCA Handbook) estimate the amount of mixing water for non-air entrained concrete with a slump of 50 mm and 25 mm aggregate.

Estimated amount of mixing water = 180kg/m^3

Step 4 The required w/c ratio is determined by strength requirements, durability requirements, and finishing properties.
a) For f'_c = 25 MPa, the average strength required is equal to the specified strength plus 1.4 times the expected standard deviation (when the standard deviation is not more than 35 MPa).

$$f'_c = 25 + (1.4 * 2.8) = 29 \text{ MPa}.$$

Therefore from Table 7.1 of the CPCA handbook, w/c =0.54

b) For exposure conditions, The CPCA recommends a maximum w/c

ratio of 0.5. Note: Class B exposure conditions: Frequent freeze-thaw when saturated in fresh water or infrequent wetting by seawater, or complete, continuous immersion in seawater.

However, a ratio w/c = 0.45 was selected so that comparison to the results of the previous test results would be possible if desired.

Step 5 The required cement content is:

Cement content = 180 (kg/m^3)/ 0.45 = 400 kg/m^3

Step 6 Estimate the quantity of coarse aggregate needed for a fineness modulus of 2.96 and 25 mm maximum particle size.

From CPCA handbook:
Quantity of coarse
aggregate required = 0.63 m^3/m^3 of concrete

Therefore the required mass = 0.63 * 1792 = 1129kg (dry)/m^3

Step 7 The quantities of all the ingredients of the mix have been estimated except the fine aggregate. The amount of fine material required can now be determined on the basis of either mass or absolute volume.

Using the mass basis:

From the CPCA handbook, the estimated mass of a cubic metre on non-air entrained concrete containing 25 mm aggregate = 2365 kg

Masses already known:

Mixing Water	=	180 kg
Cement	=	400 kg
Coarse Aggregate	=	1129 kg
Total		1709 kg

Therefore:

Mass of fine material = 2365 - 1709 = 656 kg (dry)

Step 8 Corrections are needed to compensate for moisture in the aggregates. The coarse aggregate were in the SSD condition. Therefore, any free water on the surface of the aggreates must be subtracted from the amount of mix water added to the mix. This amount can only be determined just prior to mixing when the weight of the coarse aggregate is determined. Fine aggregate will be in an oven dry state so extra water (equal to the amount that the fine aggregate will absorb during mixing) must be added to the mix water. This value can be assummed to be 80 percent of the 24 hour absorption value.

Therefore coarse aggregate 1129 * (1.0166) = 1148 kg
(1.66% absorption)

Therefore fine aggregate weight = 656 kg
(Oven dry)

Water to be added as mix water:

180 + 656(0.01395) - free water on coarse aggregate =
189 - free water on coarse aggregate

The new estimated batch quantities for 1 m^3 of concrete are as follows:

Mixing Water	= 189 kg - free water on coarse aggregate
Cement	= 400 kg
Coarse Aggregate (SSD)	= 1148 kg
Fine Aggregate (0% MC)	= 656 kg

Step 9 Calculate batch quantities for a trial batch 0.03 m^3 in size:

Mixing Water	= 5.67 kg - free water on coarse aggregate
Cement	= 12.00 kg
Coarse Aggregate (SSD)	= 34.44 kg
Fine Aggregate (0% MC)	= 19.68 kg

B.4.1.1 Trial Mix (No Air Entrainment)

Date: 22 July 1985

Mix Size: 0.03 m^3

Mix Design:

	Total Water[1] (kg)	Cement Type 10 (kg)	Coarse Aggregate (kg)	Fine Aggregate (kg)	Air Entraining Agent (ml)
Called for:	5.67	12.00	34.44	19.68	0
Used:	5.12	12.00	34.44	19.68	0

Results: Entrapped Air: 1.6%
Slump: 75 mm

In the above mix design, it was assumed that the fine aggregate would absorb a certain amount of the water based on its 24 hour absorption value. In accordance with ASTM C192-84 it was assumed that 80 percent of the 24 hour value will be absorbed during the time the concrete is in the mixer. Putting this clause into action lowers the "called for" water content to:

$$5.67 - (19.68 * 0.80 * 0.1395) = 5.36 \text{ kg}$$

Therefore, the amount of excess water is now 5.36 - 5.12 = 0.24 kg.

To compensate, more fine sand was added to the mix. If 1 kg is added to the 0.03 m^3 trial mix, the required water content will be:

$$5.12 + (1 * 0.80 * 0.01395) = 5.13 \text{ kg}$$

The new cement content to maintain a w/c ratio of 0.45 is:

$$5.13 - (20.68 * 0.80 * 0.1395)/0.45 = 10.89 \text{ kg}$$

[1]Total Water = All water added to the mix except that required to create an "SSD" condition for the coarse aggregate. Note that this value must compensate for the amount of water absorbed by the fine aggregate (80 percent of the 24 hour absorption value).

The new estimated batch quantities for 1 m^3 of concrete are as follows:

Mixing Water = 167.3 kg - free water on coarse aggregate
Cement = 355.6 kg
Coarse Aggregate (SSD) = 1147.7 kg
Fine Aggregate (0% MC) = 655.4 kg

Step 9 Calculate batch quantities for a trial batch 0.03 m^3 in size:

Mixing Water = 5.02 kg - free water on coarse aggregate
Cement = 10.67 kg
Coarse Aggregate (SSD) = 34.43 kg
Fine Aggregate (0% MC) = 21.66 kg

Note:
The following rule of thumb was employed: 50 ml/100kg cement should approximately lead to an air content of 5 percent. Therefore, since this mix requires 10.67 kg of cement,the amount of AEA required for 5 percent air entrainment should be:

$$\frac{50 \text{ ml}}{100 \text{ kg}} = \frac{X}{10.67 \text{kg}}$$

Therefore X = AEA to be added = 5.3 ml

B.4.1.2 Second Trail Mix (No Air Entrainment)

	Total Water (kg)	Cement Type 10 (kg)	Coarse Aggregate (kg)	Fine Aggregate (kg)	Air Entraining Agent (ml)
Called for:	5.13	10.89	33.87 (Dry)	20.68 +2.50 23.18	0
Used:	5.13	10.89	33.87	23.18	

An extra 2.50 kg of fine aggregate was required to bring the slump into an acceptable range.

Check w/c ratio:

Water available for hydration 5.13 -(23.18 * 0.8 * 0.01395) = 4.87 kg

w/c = 4.87/10.89 =0.447 =0.45

Results:

w/c	= 0.45
C/F (Dry)	= 1.46
Slump	= 60 mm
Air Content (Entrapped)	= 2.0 %
Density	= 2441 kg/m^3
Volume Produced	= 0.0302 m^3
Yield	= 2.77E-03 m^3/kg cement
Relative Yield	= 1.003
Cement Factor	= 361 kg cement/m^3

These "fresh" characteristics meet all requirements. Therefore, use the following quantities (per m^3).

Total Water (kg)	Cement Type 10 (kg)	Coarse Aggregate (kg)	Fine Aggregate (kg)	Air Entraining Agent (ml)
171	361	1140 (1121 dry)	768	0

[1]Total Water = All water added to the mix except that required to create an "SSD" condition for the coarse aggregate. Note that this value must compensate for the amount of water absorbed by the fine aggregate (80 percent of the 24 hour absorption value).

B.5 PRELIMINARY MIX DESIGNS FOR THE AIR CONTENT/EXTERNAL MOISTURE TEST MIX DESIGN NO. 2 (5 PERCENT AIR ENTRAINMENT)

Properties of the Materials and Desired Mix Characteristics

Cement : Type 10 (normal)

Coarse Aggregate: Max. nominal size = 25 mm (5% retained on sieve)
Relative density (SSD) = 2.68
24 hour absorption = 1.66%
Dry rodded mass (SSD) = 1792 kg/m^3

Fine Aggregate : Relative Density (SSD) = 2.630
24 hour absorption = 1.395%
Moisture content = 0% (oven dry)
Fineness Modulus = 2.98

Concrete Desired: Frequently exposed to freeze-thaw
28 day compressive strength = 25 MPa

Air Content : As close to 5% as possible

B.5.1 Mix Design No. 2 (5 Percent Air Content)

Methodology based on the procedure outlined in the Canadian Portland Cement Association CPCA handbook.

Step 1 Select slump = 50 mm

Step 2 Maximum aggregate size = 25 mm

Step 3 From CPCA handbook Table 7.6 (air entrained concrete), select mix water requirement (kg/m^3)

Water requirement = 160 kg/m^3

Step 4 Select w/c ratio:
a.) For f_c' = 25MPa

$f_c' = 25 + (1.4 * 2.8) = 29$ MPa
from Figure 7.1, w/c = 0.45

b.) Class B durability minimum w/c = 0.50

Therefore, select w/c ratio of 0.45. This value would have been selected regardless of the above requirements in order to allow comparisons to be made to the nonair entrained mix design.

Step 5 The required cement content is:

Cement content = 160 (kg/m^3)/ 0.45 = 355.6 kg/m^3

Step 6 Estimate the quantity of coarse aggregate needed for a fineness modulus of 2.96 and 25 mm maximum particle size.

From Table 7.7 in CPCA handbook:
Quantity of coarse
aggregate required = 0.63 m^3/m^3 of concrete

Therefore the required mass = 0.63 * 1792 = 1129kg (dry)/m^3

Step 7 The quantities of all the ingredients of the mix have been estimated except the fine aggregate. The amount of fine material required can now be determined on the basis of either mass or absolute volume.

Using the mass basis:

From the CPCA handbook, the estimated mass of a cubic metre on air entrained concrete containing 25 mm aggregate = 2300 kg

Masses already known:

Mixing Water	=	160.0 kg
Cement	=	355.6 kg
Coarse Aggregate	=	1129.0 kg
Total		1644.6 kg

Therefore:

Mass of fine material = 2300 - 1644.6 = 655.4 kg (dry)

Step 8 Corrections are needed to compensate for moisture in the aggregates. The coarse aggregate were in the SSD condition. Therefore, any free water on the surface of the aggreates must be subtracted from the amount of mix water added to the mix. This amount can only be determined just prior to mixing when the weight of the coarse aggregate is determined. Fine aggregate will be in an oven dry state so extra water (equal to the amount that the fine aggregate will absorb during mixing) must be added to the mix water. This value can be assummed to be 80 percent of the 24 hour absorption value.

Therefore coarse aggregate 1129 * (1.0166) = 1147.7 kg SSD (1.66% absorption)
Therefore fine aggregate weight = 656 kg (Oven dry)

Water to be added as mix water:

160 + 656(0.80 * 0.01395) - free water on coarse aggregate =
167.3 - free water on coarse aggregate

B.5.1.1 Trial Mix (5 Percent Air Entrainment)

Date: 25 July 1985

Mix Size: 0.03 m^3

Mix Design:

	Total Water[1] (kg)	Cement Type 10 (kg)	Coarse Aggregate (kg)	Fine Aggregate (kg)	Air Entraining Agent (ml)
Called for:	5.02	10.67	34.43	21.66	5.3
Used:	5.02	10.67	34.43	21.66	5.3

Characteristics of the Fresh Concrete:

Slump: 55 mm
Air Content: 4.4%
Density: 2379 kg/m^3

Slump was in the proper range but air content was too low by 0.6 percent. Rule of thumb (CPCA handbook): reduce or increase the mixing water content by 3 kg for each 1 % by which the air content is to be increased or decreased.

Reduce water to retain slump when increasing air content (but first subtract water absorbed by the fine aggregate):

Mix water required = 167.3 - 0.8 *0.01395 * 655.4 = 160.0 kg

Therefore, water content reduced to 160.0 - 3 * 0.6 = 158.2 kg

Therefore, less cement is needed to maintain w/c = 0.45; and the new cement content is:

$$\frac{158.2}{0.45} = 351.6 \text{ kg}$$

The new estimated density of concrete with 0.6 percent more air is:

$$\frac{2379}{1.006} = 2365 \text{ kg/m}^3$$

[1]Total Water = All water added to the mix except that required to create an "SSD" condition for the coarse aggregate. Note that this value must compensate for the amount of water absorbed by the fine aggregate (80 percent of the 24 hour absorption value).

Calculate new batch masses based on new density value:

Workability satisfactory, therefore mass of coarse aggregate remains unchanged at 1147.7 kg SSD (per m^3).

The amount of sand required is:

2365.0
158.2
351.6
1147.7
707.5 SSD or $\frac{707.5}{1.014}$ = 697.7 kg (Dry)

B.5.1.2 Second Trial Mix (5 Percent Air Entrainment)

Size: 0.02 m^3

	Total[1] Water (kg)	Cement Type 10 (kg)	Coarse Aggregate (kg)	Fine Aggregate (kg)	Air Entraining Agent (ml)
Called for:	3.32	7.03	22.95 (Dry)?	13.95	4.0
Used:[2]	----	----	-----	-----	---

Determination of AEA requirement:

Originally $\frac{50 \text{ ml}}{100 \text{ kg}} = \frac{X}{7.03}$ Implies X = 3.5 which resulted in 4.4% air entrainment

Again assumming a linear relationship:

Therefore, $\frac{3.5 \text{ ml}}{4.4\%} = \frac{X}{5.0\%}$

X = AEA required = 4.0 ml

[1]Total Water = All water added to the mix except that required to create an "SSD" condition for the coarse aggregate. Note that this value must compensate for the amount of water absorbed by the fine aggregate (80 percent of the 24 hour absorption value).

[2]Due to a shortage of materials it was assummed that the small changes incorporated above would produce concrete with the desired characteristics.

B.6 PRELIMINARY MIX DESIGNS FOR THE AIR CONTENT/EXTERNAL MOISTURE TEST MIX DESIGN NO. 3 (8 PERCENT AIR ENTRAINMENT)

Properties of the Materials

See Mix Design No.2 for details. The only difference between these two mixes was the entrained air requirement. Because entrained air works to increase the workability of a mix, slight variations in sand content (and hence the C/F ratio) will likely occur. In essence, however, the mixes are identical. From Mix No.2, the initial design gives the following values for a trial batch approximately 0.02 m^3 in size:

Total Water (kg)	Cement (Type 10) (kg)	Coarse Aggregate (kg)	Fine Aggregate (kg)	AEA (ml)
3.35	7.06	22.95 SSD	14.44 +1.00 15.44 Dry	12.5

It was found that an extra 1.00 kg of sand was necessary to bring the slump down to the desired level.

Again, the amount of Darex air entraining agent was approximated from the following rule of thumb:

$$\frac{50 \text{ ml AEA}}{100 \text{ kg cement}} = 5.0\% \text{ air entrainment}$$

and also from the fact that a previous mix with 10.2 ml of AEA resulted in an air content of 6.2 percent.

Characteristics of Fresh Concrete

w/c = 0.45
C/F (Dry) = 1.46
Slump = 50 mm
Density = 2287 kg/m^3
Volume Produced = 0.0214 m^3
Yield = 0.00305 m^3/kg cement
Relative Yield = 1.07
Cement Factor = 332 kg cement/m^3

Since the properties of the fresh concrete from the trial mix satisfies all requirements, the following masses for 1 m^3 of concrete for Mix Design No.3 should be used:

Total[1] Water (kg)	Cement (Type 10) (kg)	Coarse Aggregate (kg)	Fine Aggregate (kg)	AEA (ml)
156.5	332.2	1072.4 SSD	721.5 Dry	584.0

Therefore, for a mix of 0.05 m^3, use the following proportions:

Total[1] Water (kg)	Cement (Type 10) (kg)	Coarse Aggregate (kg)	Fine Aggregate (kg)	AEA[2] (ml)
7.83 +0.80 8.63	16.61 +0.50 17.11	53.62 SSD 52.76 Dry	36.08 Dry	29.2

Note: An error was made in scaling the trial batch of 0.02 m^3 up to the 1 m^3 quantity. This error was passed to the mix proportions for the actual from which the specimens and cylinders were made. However, as can be seen in the final mix design summary, the characteristics of the fresh concrete give satisfactory results. The only problem is with the w/c ratio which is 0.48. See correction in next section.

[1] See Mix Design No.1.

[2] Calculated from $\frac{12.5 \text{ ml}}{7.11 \text{ kg}} = \frac{X}{332.2 \text{ kg}}$

B 7.0 FINAL MIX DESIGNS

C 7.1 Mix Design No.1 (No Air Entrainment)

The following masses (in kg) were determined by trial mixes for 1 m^3 are as follows:

Total[1] Water (kg)	Cement (Type 10) (kg)	Coarse Aggregate (kg)	Fine Aggregate (kg)	AEA (ml)
171	361	1140 SSD 1211 Dry	768 Dry	0

The amount of concrete required for the specimen molds and compression test cylinders was approximately 0.04 m^4. Therefore 0.05 m^3 will be batched in order to ensure that all test specimens and test cylinders would be homogeneous.

Total[1] Water (kg)	Cement (Type 10) (kg)	Coarse Aggregate (kg)	Fine Aggregate (kg)	AEA (ml)
8.55	18.05	57.00 SSD 56.05 Dry	38.40 Dry	0

Characteristics of Fresh Concrete

w/c = 0.45
C/F (Dry) = 1.46

Slump = 45 mm
Density = 2441 kg/m^3
Volume Produced = 0.0499 m^3
Yield = 0.00277 m^3/kg cement
Relative Yield = 1.00
Cement Factor = 361 kg cement/m^3

[1]Total Water = All water added to the mix except that used to create an SSD condition for the coarse aggregate. Note that this value must compensate for the amount of water absorbed by the fine aggregate (80 percent of 24 hour value).

B 7.2 Mix Design No.2 (5 Percent Air Content)

The following masses (in kg) were determined by trial mixes for 1 m^3 are as follows:

Total[1] Water (kg)	Cement (Type 10) (kg)	Coarse Aggregate (kg)	Fine Aggregate (kg)	AEA (ml)
160	351.5	1147.5 SSD 1129.0 Dry	697.5 Dry	200

The amount of concrete required for the specimen molds and compression test cylinders is approximately 0.04 m^4. Therefore 0.05 m^3 will be batched in order to assure homogeneity between specimens and samples.

Total[1] Water (kg)	Cement (Type 10) (kg)	Coarse Aggregate (kg)	Fine Aggregate (kg)	AEA (ml)
8.30	17.58	57.38 SSD 56.05 Dry	38.88 Dry	10.0

Characteristics of Fresh Concrete

w/c	= 0.45
C/F (Dry)	= 1.62
Slump	= 50 mm
Density	= 2389 kg/m^3
Volume Produced	= 0.0491 m^3
Yield	= 0.00279 m^3/kg cement
Relative Yield	= 0.98
Cement Factor	= 358 kg cement/m^3

[1]Total Water = All water added to the mix except that used to create an SSD condition for the coarse aggregate. Note that this value must compensate for the amount of water absorbed by the fine aggregate (80 percent of 24 hour value).

B 7.3 Mix Design No.3 (8.5 Percent Air Content)

The original version (see trial mix section) produced fresh concrete with a w/c ratio of 0.48 that met all other demands. However, when produced on a larger scale these characteristics could not be duplicated.

The amount of concrete required for the specimen molds and compression test cylinders is approximately 0.04 m^4. Therefore 0.05 m^3 will be batched in order to assure homogeneity between specimens and samples.

The following masses (in kg) for a mix of 0.05 m^3 were used:

Total[1] Water (kg)	Cement (Type 10) (kg)	Coarse Aggregate (kg)	Fine Aggregate (kg)	AEA (ml)
8.40	17.65	60.43 SSD 59.45 Dry	41.60 Dry	25.0

Note: Added 3 kg coarse and 3 kg fine in an effort to adjust slump to the desired value.

Characteristics of Fresh Concrete

w/c	= 0.45
C/F (Dry)	= 1.62
Slump	= 50 mm
Density	= 2389 kg/m^3
Volume Produced	= 0.0491 m^3
Yield	= 0.00279 m^3/kg cement
Relative Yield	= 0.98
Cement Factor	= 358 kg cement/m^3

Because the volume produced is known, for 1 m^3 we have:

Total[1] Water (kg)	Cement (Type 10) (kg)	Coarse Aggregate (kg)	Fine Aggregate (kg)	AEA (ml)
160	351.5	1147.5 SSD 1129.0 Dry	697.5 Dry	200

[1]Total Water = All water added to the mix except that used to create an SSD condition for the coarse aggregate. Note that this value must compensate for the amount of water absorbed by the fine aggregate (80 percent of 24 hour value).

B 8.0 SAMPLE CALCULATIONS FOR FRESH CONCRETE CHARACTERISTICS

1. Slump: Measured by a standard test. No calculations.

2. Air Content: Measured using a air pressure meter. No calculations.

3. Density: Use the bowl of the air content measuring device. Compact concrete as instructed in CSA standards. Strike off with a glass plate. Determine weight.

   The volume of the container is given by:

   Volume = V = $(3.142 * 4^2) * 8.375 = 420.973$ in^3

   Density of the concrete is given by:

   Density = D = W/V = $(38.11$ lbs$)/(420.973$ in$^3) = 0.0905$ lbs/in^3

   D = $0.0905 * 39^3/2.2 =$ 2441 kg/m^3

4. Volume Produced: $S = \dfrac{W_a + W_f + W_c + W_w}{D}$

   where:
   - D = density of concrete
   - Numerator = sum of weights of all components in the mix
   - S = volume of concrete produced

   $S = \dfrac{8.55 + 18.05 + 57.00 + 38.40}{2441}$

   S = 0.04998 m^3

5. Yield: Y = S/N

   where:
   - Y = yield of concrete per kg of cement (alternatively per 40 kg bag of cement
   - S = volume produced
   - N = weight of cement in the batch

   $Y = \dfrac{0.04998}{18.05} * 40$

   Y = 0.111 m^3/bag cement

   Y = 0.00277 m^3/kg cement

6. Relative Yield: The ratio of actual volume obtained to the volume for which the batch was designed.

$$R_y = S/V_d$$

where:

R_y = relative yield
S = volume produced
V_d = design volume

$R_y = 0.04998/0.05 = 0.9996$

$R_y = \underline{1.0}$

7. Cement Factor:

$$N_1 = 1/Y = 1/0.111 = 9.01 \text{ bags of cement/m}^3$$

$N_1 = \underline{361 \text{ kg cement/m}^3}$

B 8.1 FLY ASH/ NORMAL PCC STRENGTH COMPARISON TEST

The object of this test was to observe the effect of the fly ash admixture on the compressive strength of concrete over time. The results of this test were used to verify two things. First, that the air entrainment values measured in the test specimens were valid, and secondly, that the fly ash admixture was contributing to the development of additional compressive strength. Mix Design No. 2 from the external moisture and air content test (air content approximately 5.0 percent) was employed for this test. In order to create the fly ash specimens, 20 percent of the cement by weight was replaced with fly ash as was the case for the mixes formed with the fly ash test. The procedure used for the test is as follows:

1. Form 15 compression test cylinders formed with normal concrete proportioned in accordance with Mix Design No. 2. Record slump, air content, and density of concrete.

2. Form 15 compresion test cylinders formed from fly ash concrete proportioned in accordance with Mix Design No. 2 with a 20 percent replacement of cement with fly ash as was done in the durability of fly ash test. Replace water content accordingly. Keep the amount of AEA added to the mix constant and record the air content, slump, and density of the concrete.

3. Perform compression tests using a constant strain rate loading apparatus according to the following schedule and record results.

Test Schedule

Days After Pour	Fly Ash Cylinders	Ordinary PCC Cylinders	Total
1	3	3	6
7	3	3	6
14	3	3	6
28	3	3	6
35	3	3	6

B 8.2 Mix Designs for Fly Ash/Ordinary PCC Comparison Test

B 8.2.1 Ordinary PCC Mix (5.0 % Air Entrainment)

The following masses for 0.03 m^3 of concrete were as follows:

Total[1] Water (kg)	Cement (Type 10) (kg)	Coarse Aggregate (kg)	Fine Aggregate (kg)	AEA (ml)
4.74	10.55	36.86 SSD[2] 36.30 Dry	22.43 Dry[2]	6.0

Characteristics of Fresh Concrete

w/c	= 0.45
C/F (Dry)	= 1.64
Slump	= 50 mm
Air Content	= 5.1%
Density	= 2387 kg/m^3
Volume Produced	= 0.0316 m^3
Yield	= 0.002996 m^3/kg cement
Relative Yield	= 1.05
Cement Factor	= 333.8 kg cement/m^3

[1]Total Water = All water added to the mix except that used to create an SSD condition for the coarse aggregate. Note that this value must compensate for the amount of water absorbed by the fine aggregate (80 percent of 24 hour value).

[2]These mixes were modelled after Mix Design No.2 in the external moisture and air content test. It was necessary, however, to add 1.5 kg of fine aggregate and 2.43 kg coarse aggregate to control slump value measured for the ordinary PCC mix. These amounts were also added to the fly ash concrete mix.

B 8.2.2 Fly Ash Concrete Mix (5.0 % Air Entrainment)

The following masses for 0.03 m^3 of concrete were as follows:

Total[1] Water (kg)	Cement (Type 10) (kg)	Fly Ash (kg)	Coarse Aggregate (kg)	Fine Aggregate (kg)	AEA (ml)
3.80	8.44	2.11	36.86 SSD[2] 36.30 Dry	22.43 Dry[2]	6.0

Characteristics of Fresh Concrete

w/c	= 0.45
C/F (Dry)	= 1.64
Slump	= 50 mm
Air Content	= 2.6%
Density	= 2443 kg/m^3
Volume Produced	= 0.0301 m^3
Yield	= 0.00357 m^3/kg cement
Relative Yield	= 1.00
Cement Factor	= 280.0 kg cement/m^3

[1]Total Water = All water added to the mix except that used to create an SSD condition for the coarse aggregate. Note that this value must compensate for the amount of water absorbed by the fine aggregate (80 percent of 24 hour value).

[2]These mixes were modelled after Mix Design No.2 in the external moisture and air content test. It was necessary, however, to add 1.5 kg of fine aggregate and 2.43 kg coarse aggregate to control slump value measured for the ordinary PCC mix. These amounts were also added to the fly ash concrete mix.

B 8.3 Test Results

Results of Fly Ash/ Ordinary PCC Comparison Test

Age of Concrete	Compressive Strength Ordinary PCC Mix (MPa)		Fly Ash Concrete Mix (MPa)	
24 hours	10.21 10.21 10.21	mean 10.21	11.66 11.42 11.42	mean 11.50
7 days	26.01 26.01 21.39	mean 24.47	31.02 29.79 32.49	mean 31.10
14 days	30.86 31.59 29.65	mean 30.70	34.51 37.67[2]	mean 36.09
31 PCC 32 Fly Ash	31.83 31.83 31.11	mean 31.59	42.28 42.72 34.51	mean 40.40

[1]Third cylinder broken.

APPENDIX C

TIME-TEMPERATURE PLOTS

FLY ASH TEST

Number of Cycles
Completed: 32

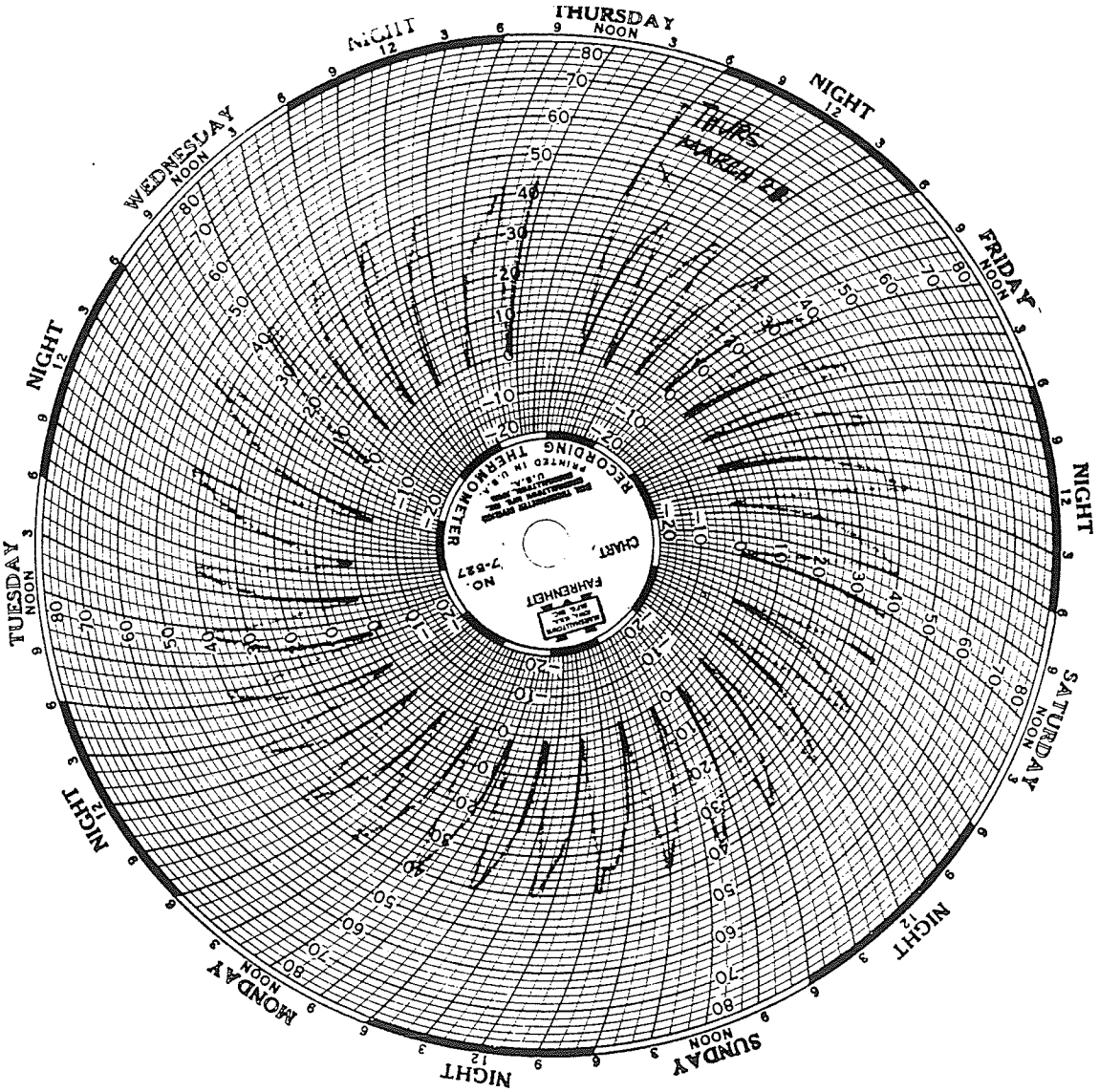

Figure A3.1: Time Against Temperature Inside the Temperature Control Specimen From 0 to 32 Cycles

FLY ASH TEST

Number of Cycles
Completed: 60

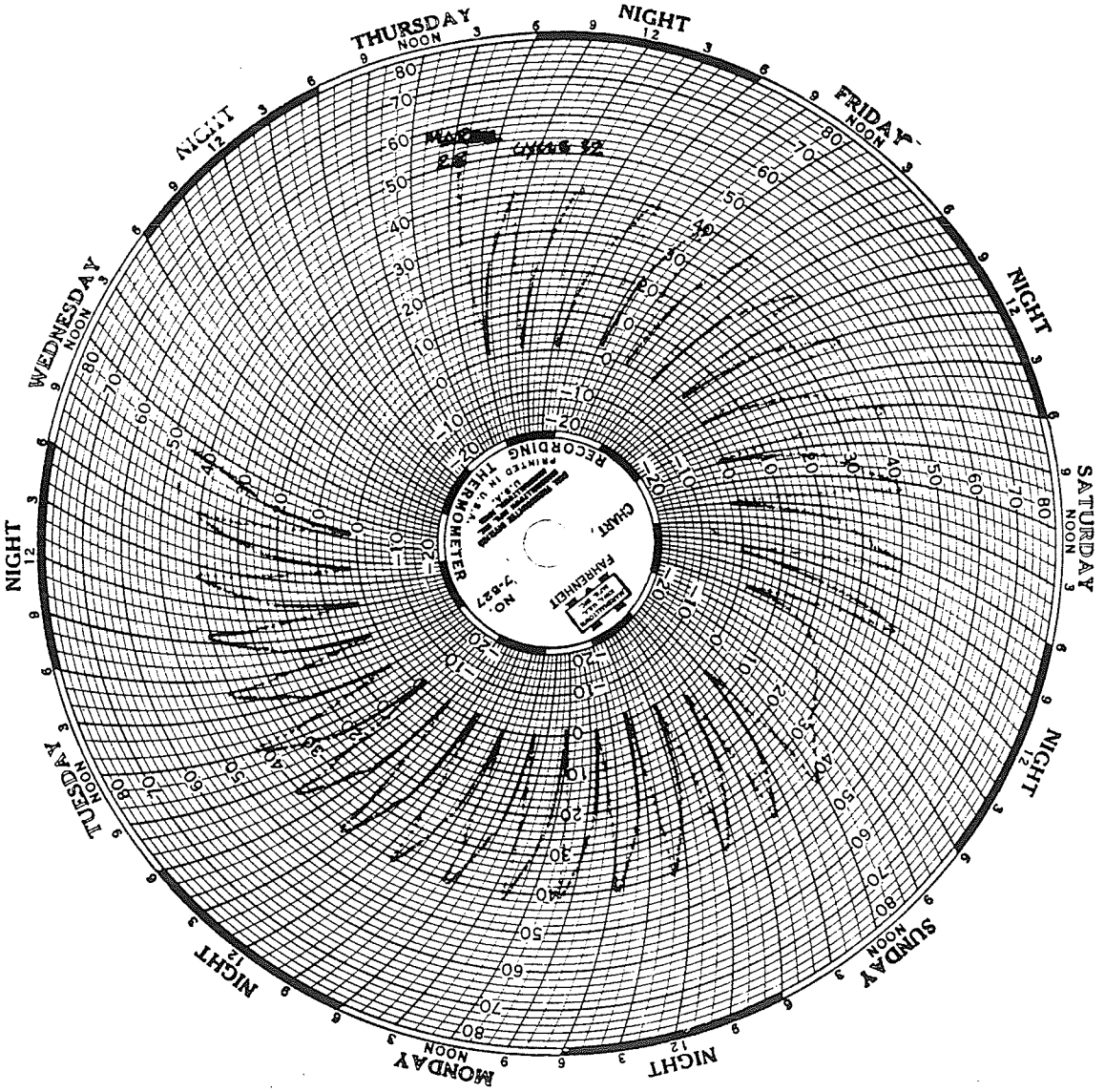

Figure A3.2: Time Against Temperature Inside the Temperature Control Specimen From 32 to 60 Cycles

FLY ASH TEST

Number of Cycles
Completed: 91

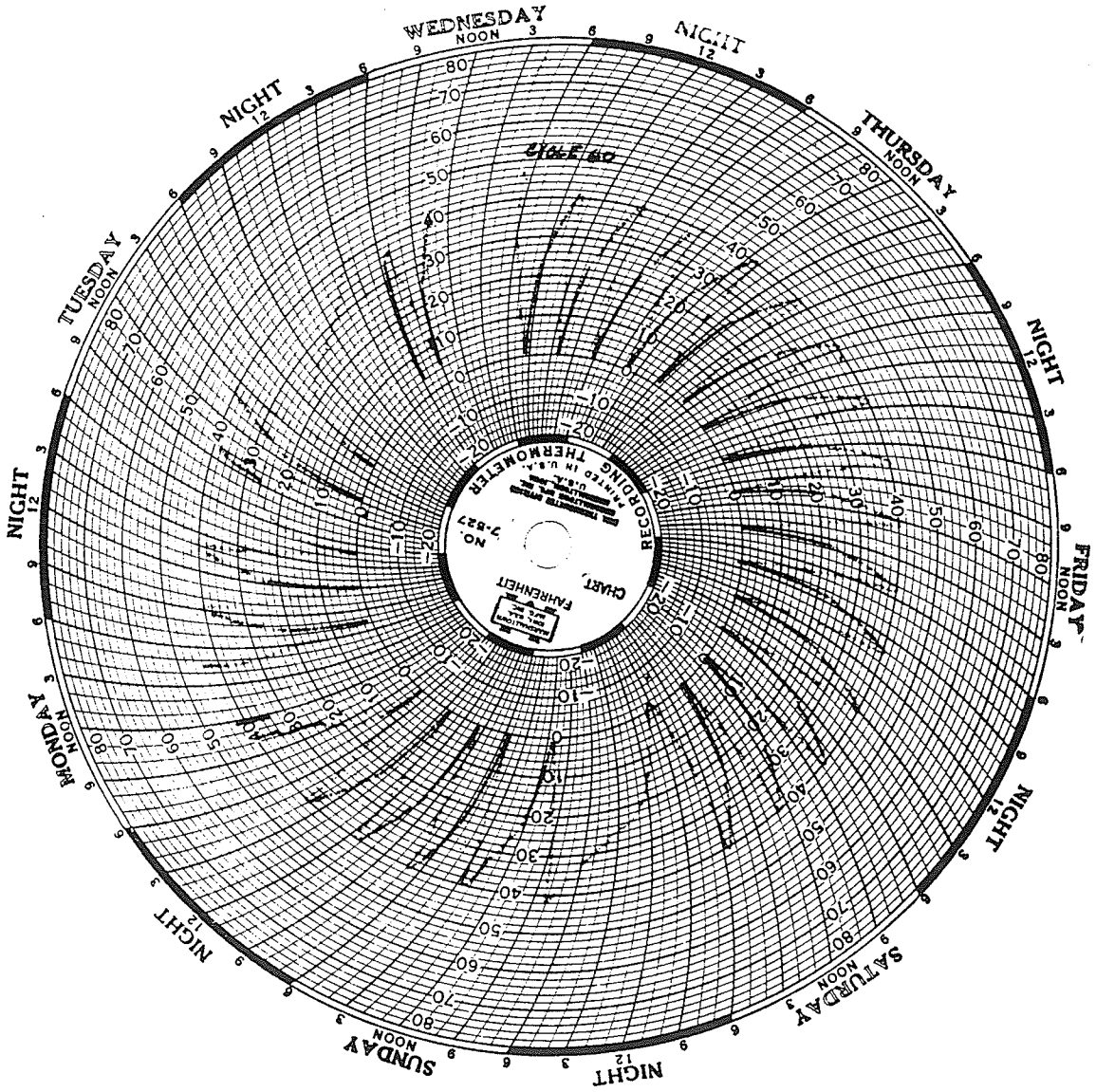

Figure A3.3: Time Against Temperature Inside the Temperature Control Specimen From 60 to 91 Cycles

FLY ASH TEST

Number of Cycles
Completed: 117

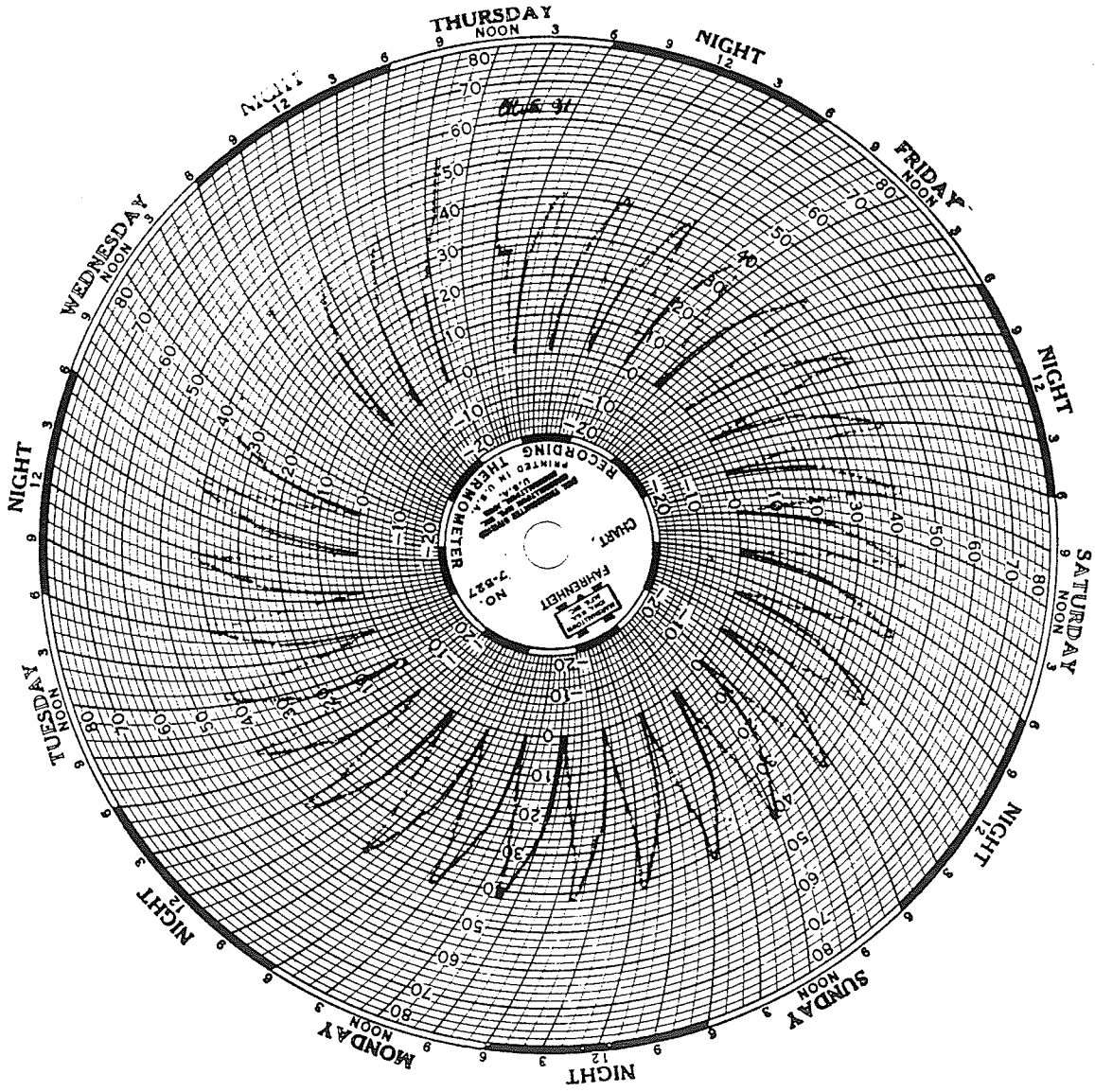

Figure A3.4: Time Against Temperature Inside the Temperature Control Specimen From 91 to 117 Cycles

FLY ASH TEST

Number of Cycles
Completed: 145

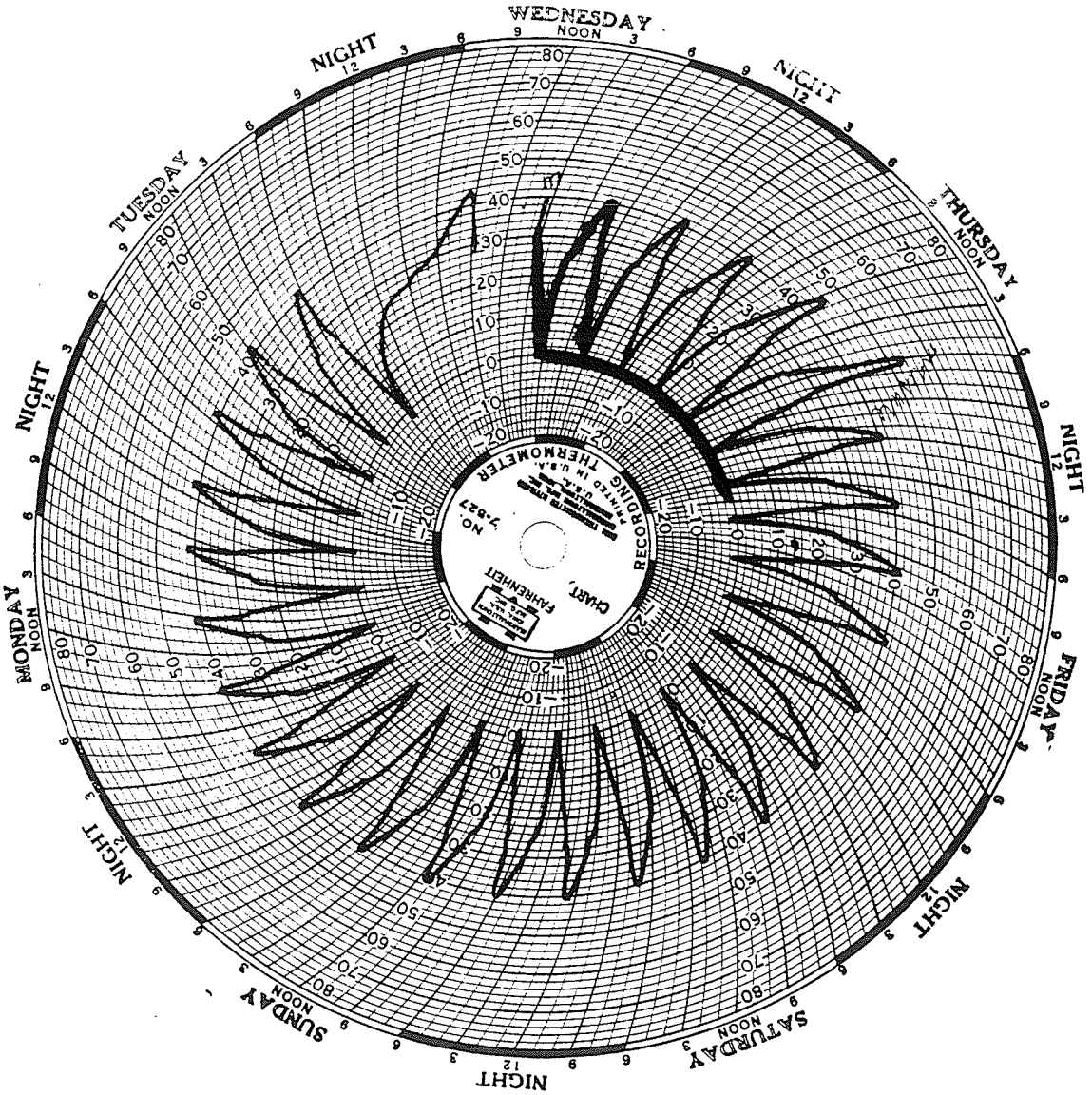

Figure A3.5: Time Against Temperature Inside the Temperature Control Specimen From 117 to 145 Cycles

FLY ASH TEST

Number of Cycles
Completed: 174

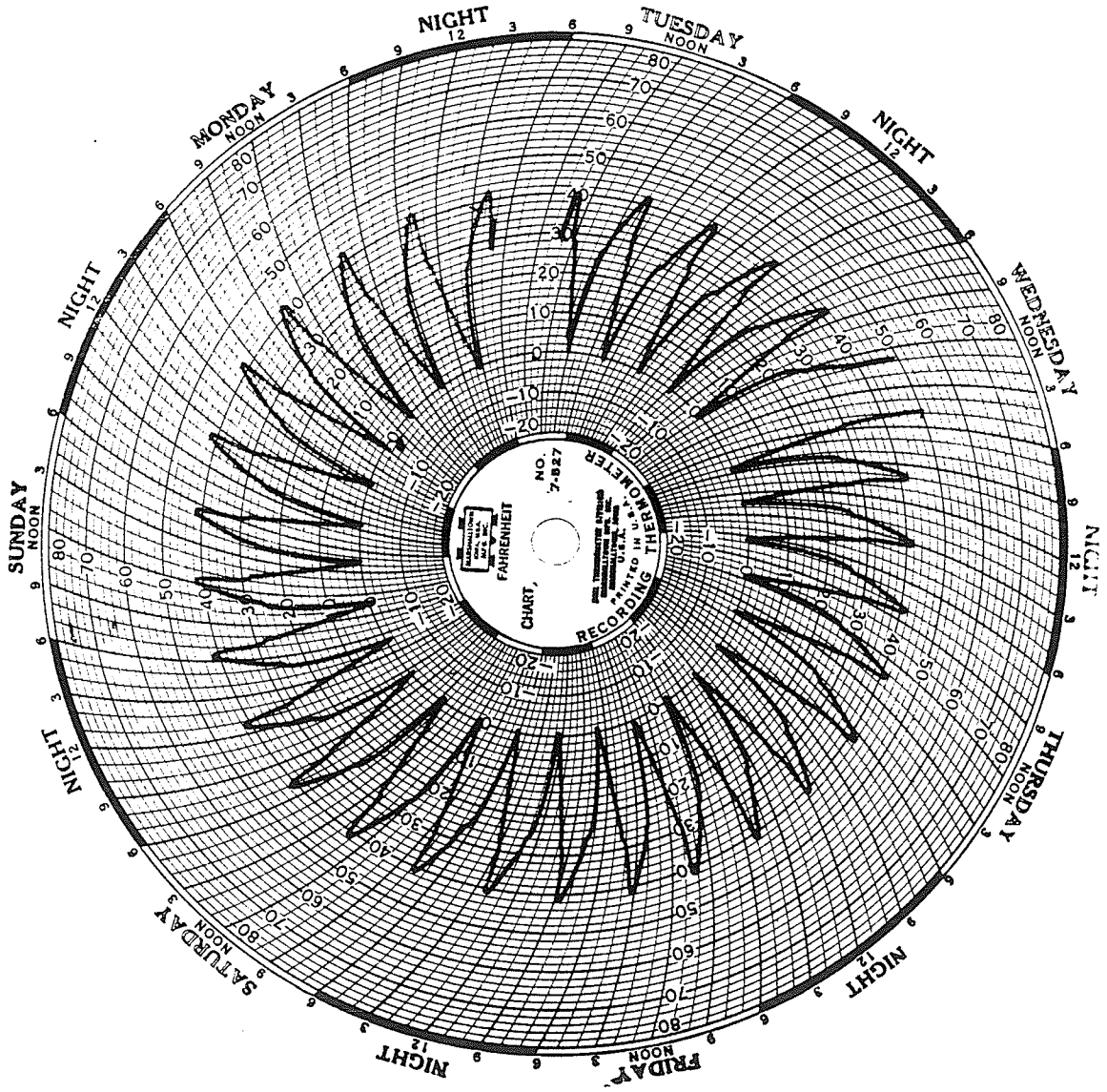

Figure A3.6: Time Against Temperature Inside the Temperature Control Specimen From 145 to 174 Cycles

FLY ASH TEST

Number of Cycles
Completed: 198

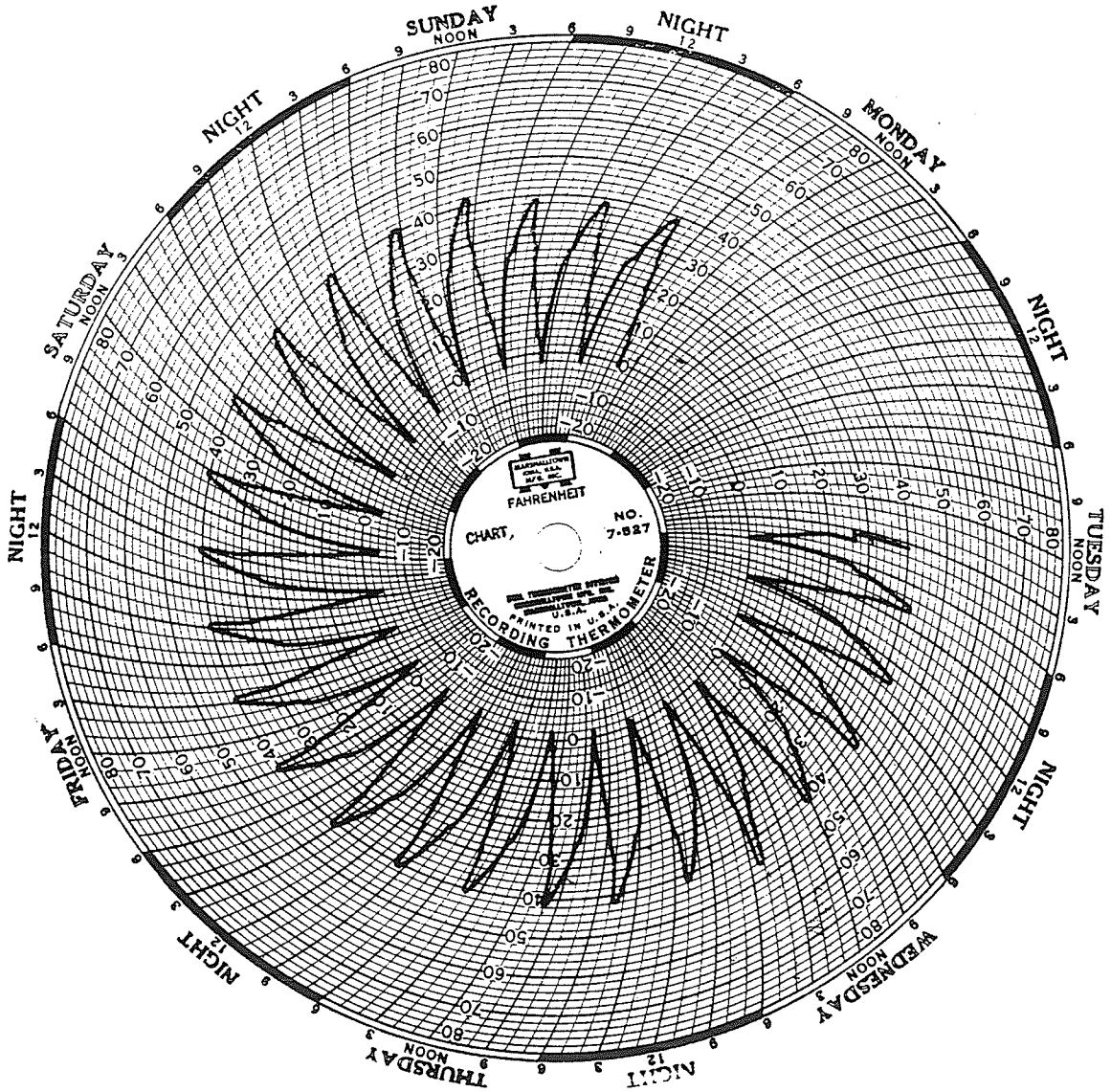

Figure A3.7: Time Against Temperature Inside the Temperature Control Specimen From 174 to 198 Cycles

FLY ASH TEST

Number of Cycles
Completed: 224

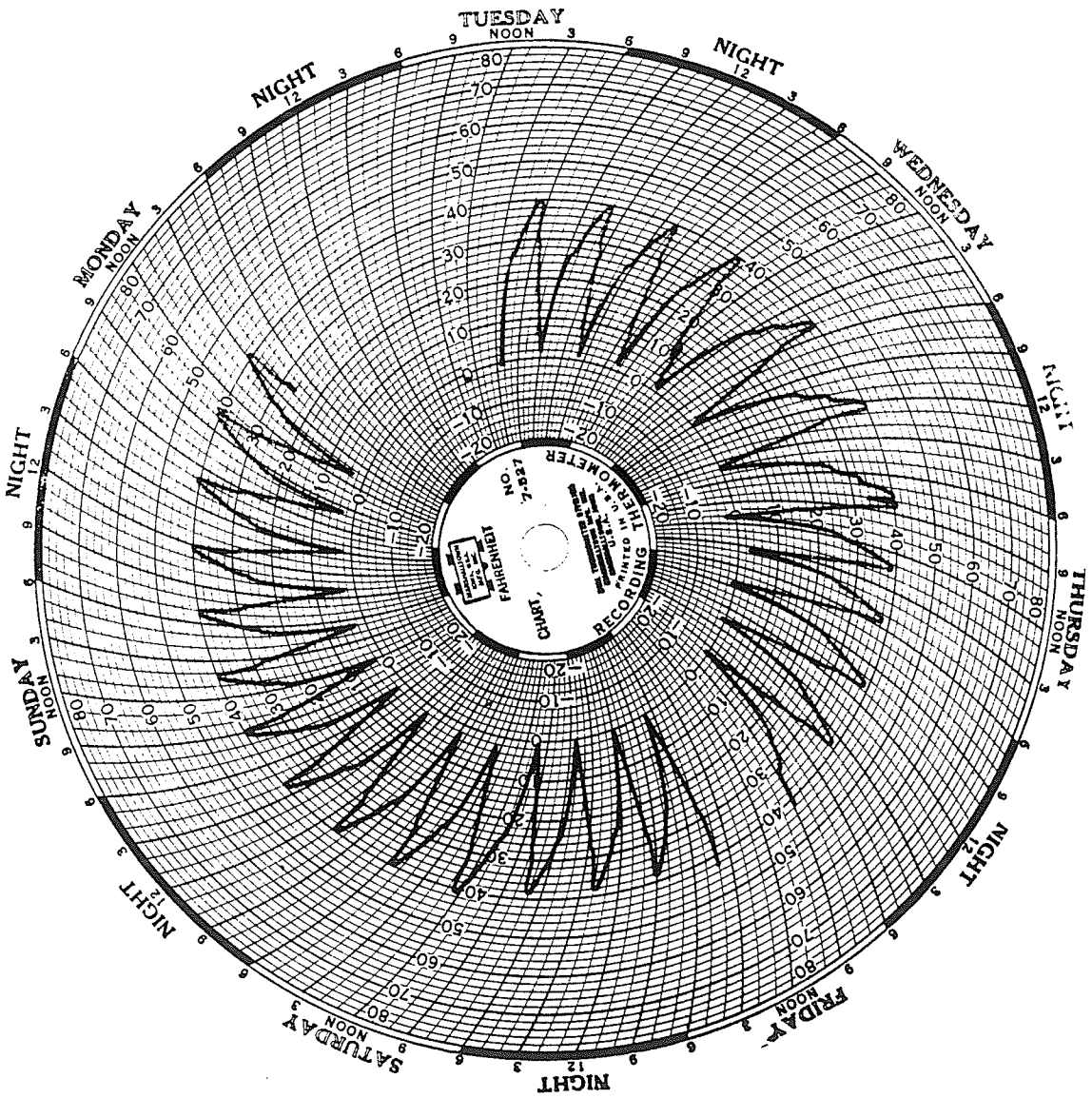

Figure A3.8: Time Against Temperature Inside the Temperature Control Specimen From 198 to 224 Cycles

FLY ASH TEST

Number of Cycles
Completed: 240

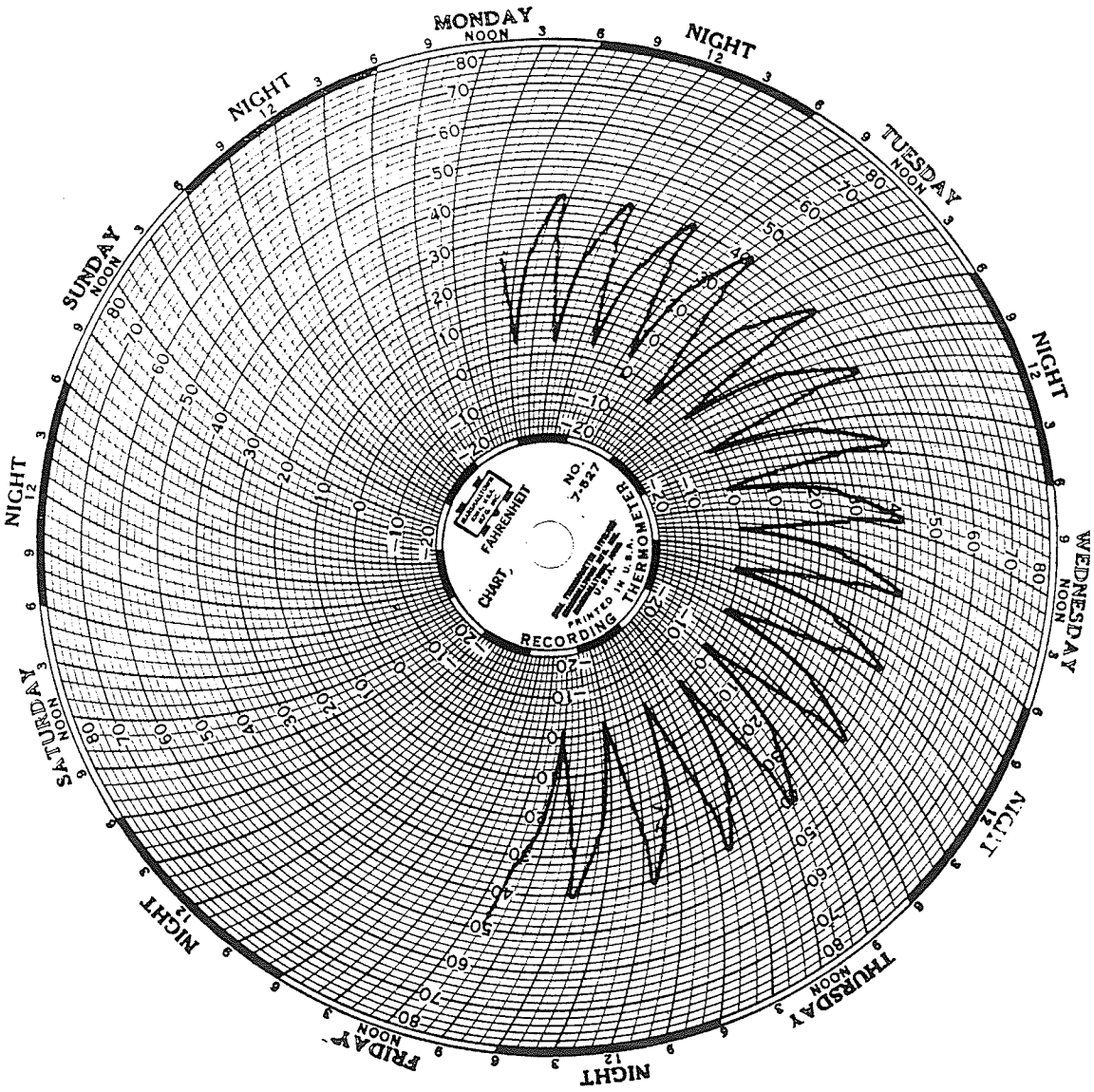

Figure A3.9: Time Against Temperature Inside the Temperature Control Specimen From 224 to 240 Cycles

FLY ASH TEST

Number of Cycles
Completed: 262

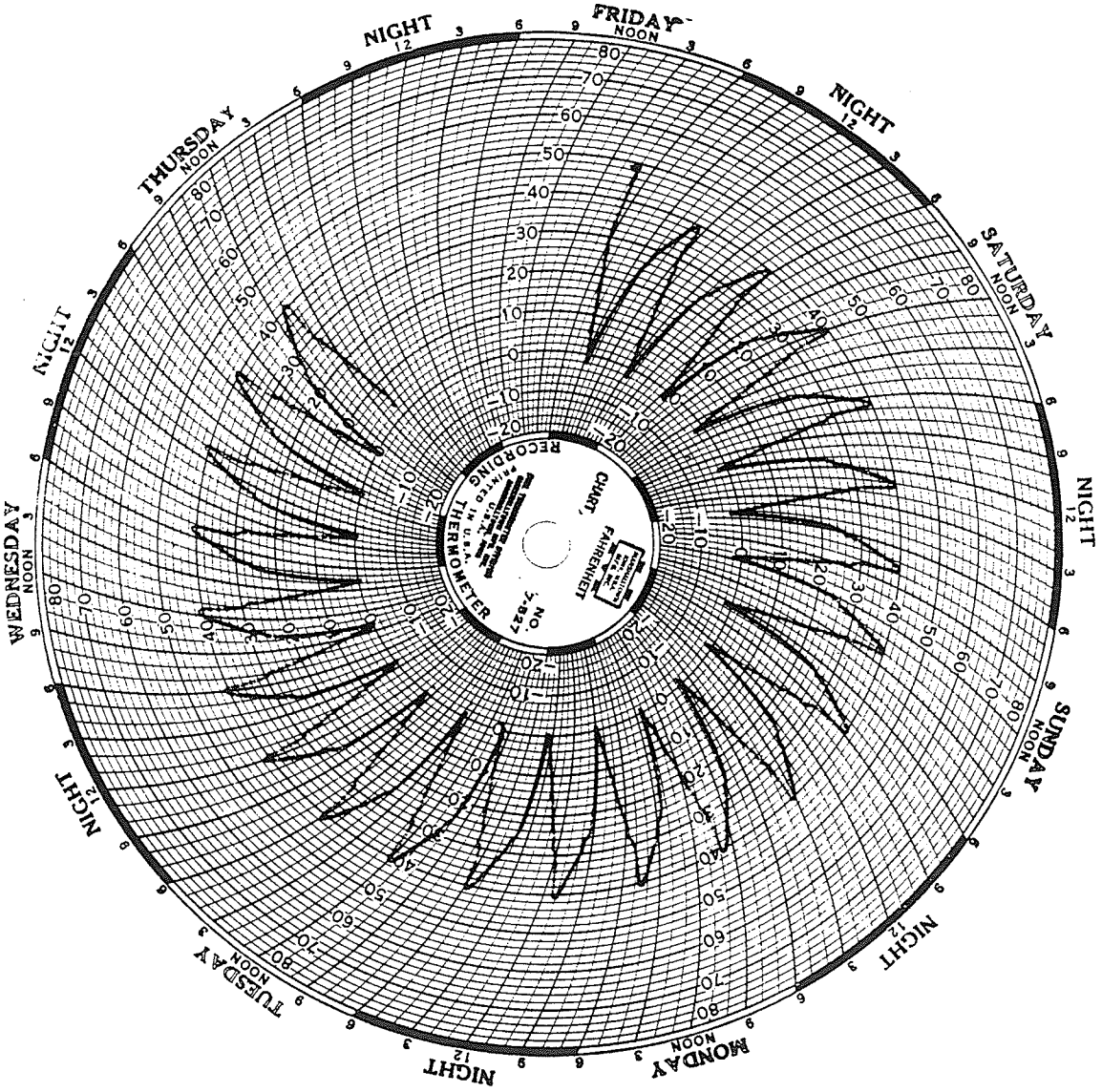

Figure A3.10: Time Against Temperature Inside the Temperature Control Specimen From 240 to 262 Cycles

FLY ASH TEST

Number of Cycles
Completed: 283

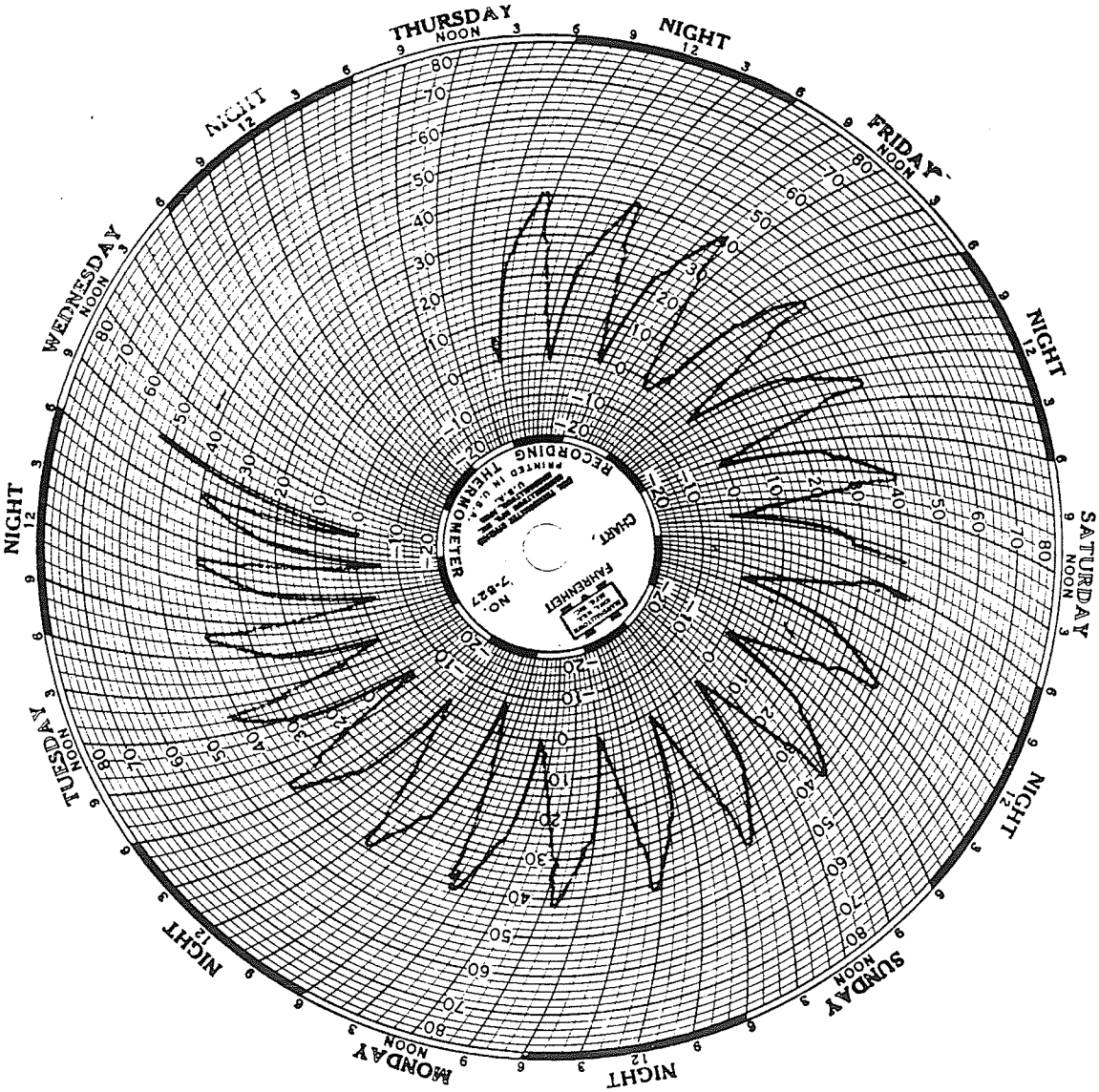

Figure A3.11: Time Against Temperature Inside the Temperature Control Specimen From 262 to 283 Cycles

FLY ASH TEST

Number of Cycles
Completed: 303

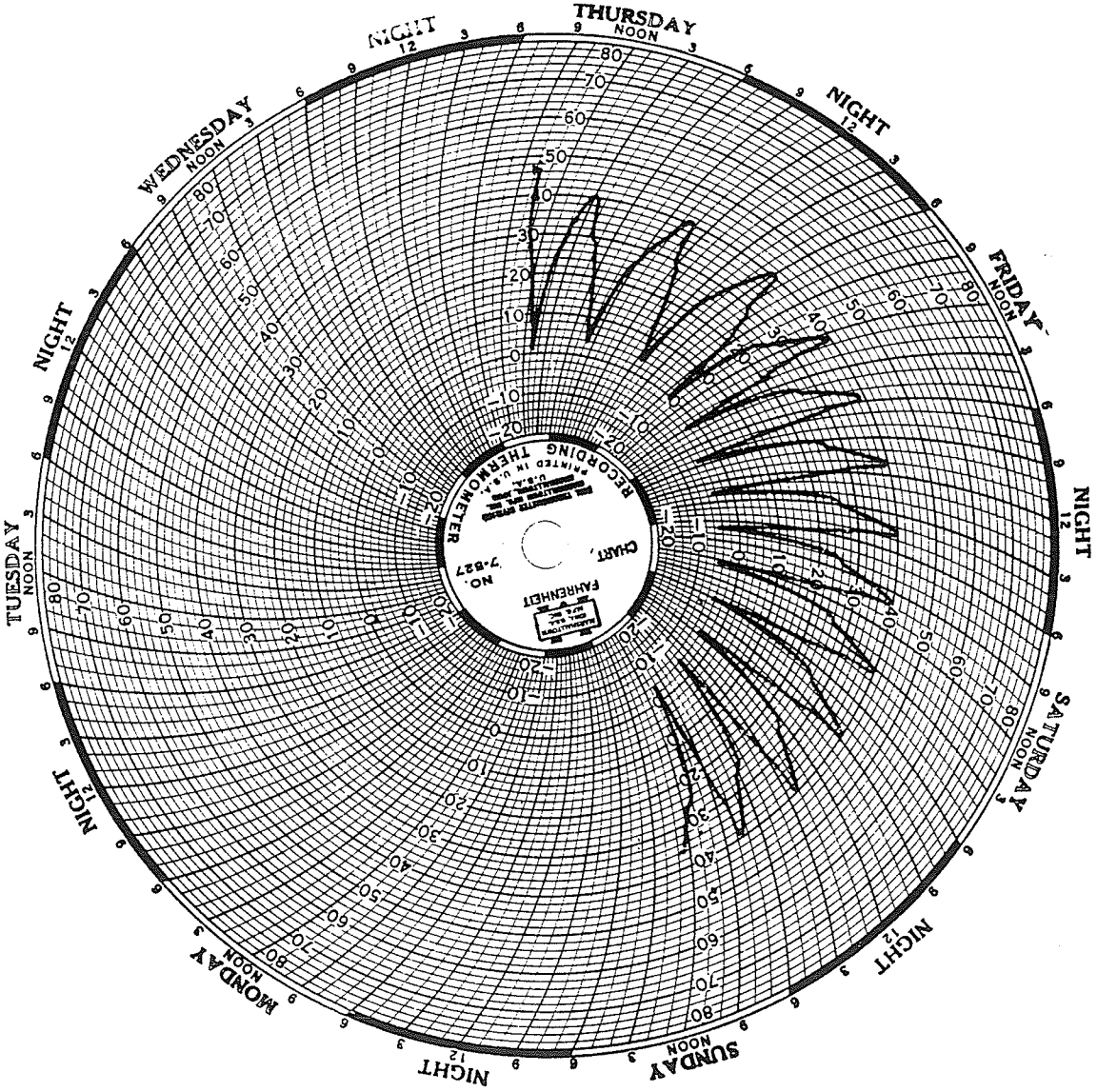

Figure A3.12: Time Against Temperature Inside the Temperature Control Specimen From 283 to 303 Cycles

EXTERNAL MOISTURE AND AIR CONTENT TEST

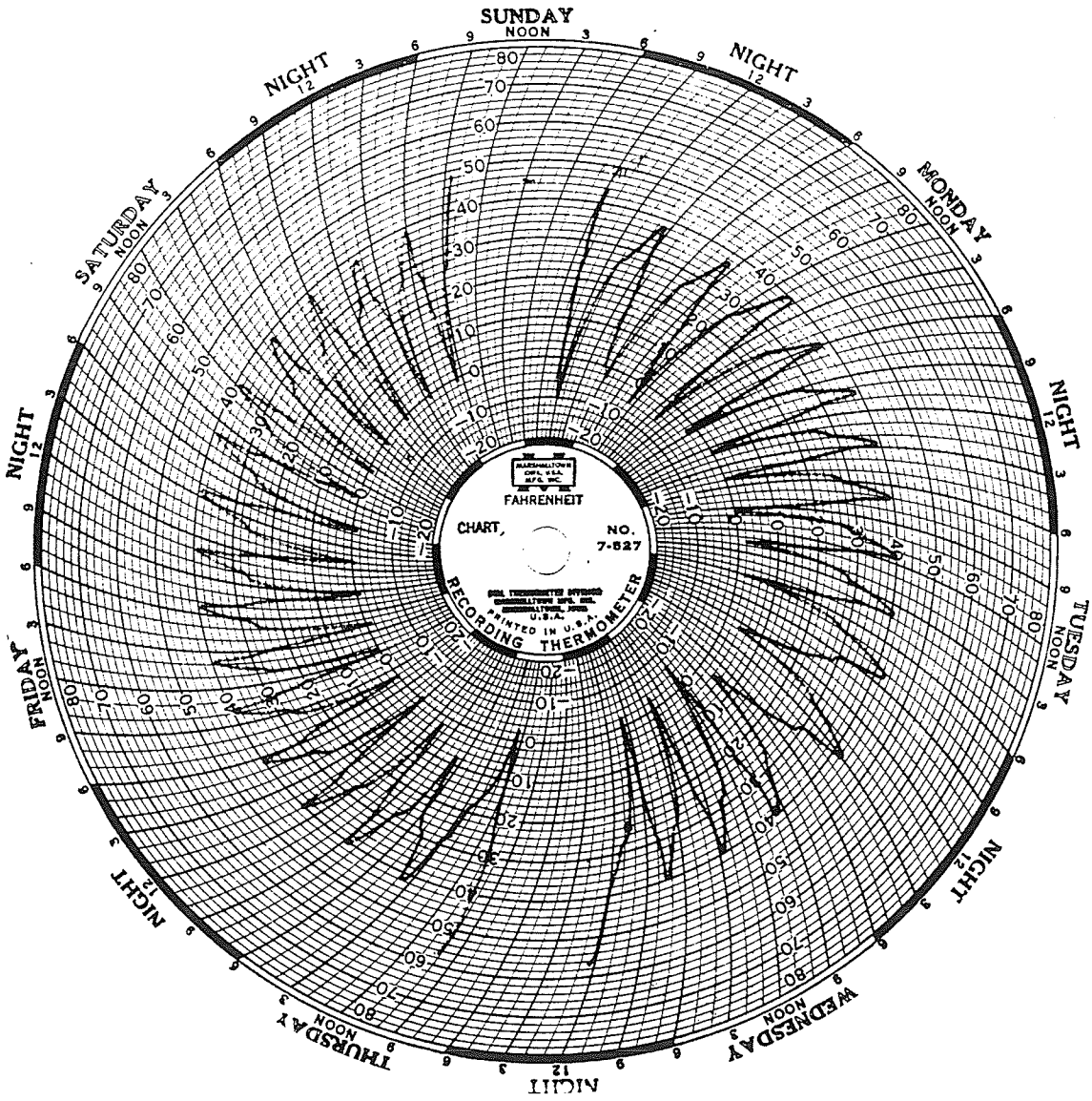

Figure A3.13: Time Against Temperature Inside the Temperature Control Specimen From 0 to 32 Cycles for A1.9 and A5.0 Specimens

EXTERNAL MOISTURE AND AIR CONTENT TEST

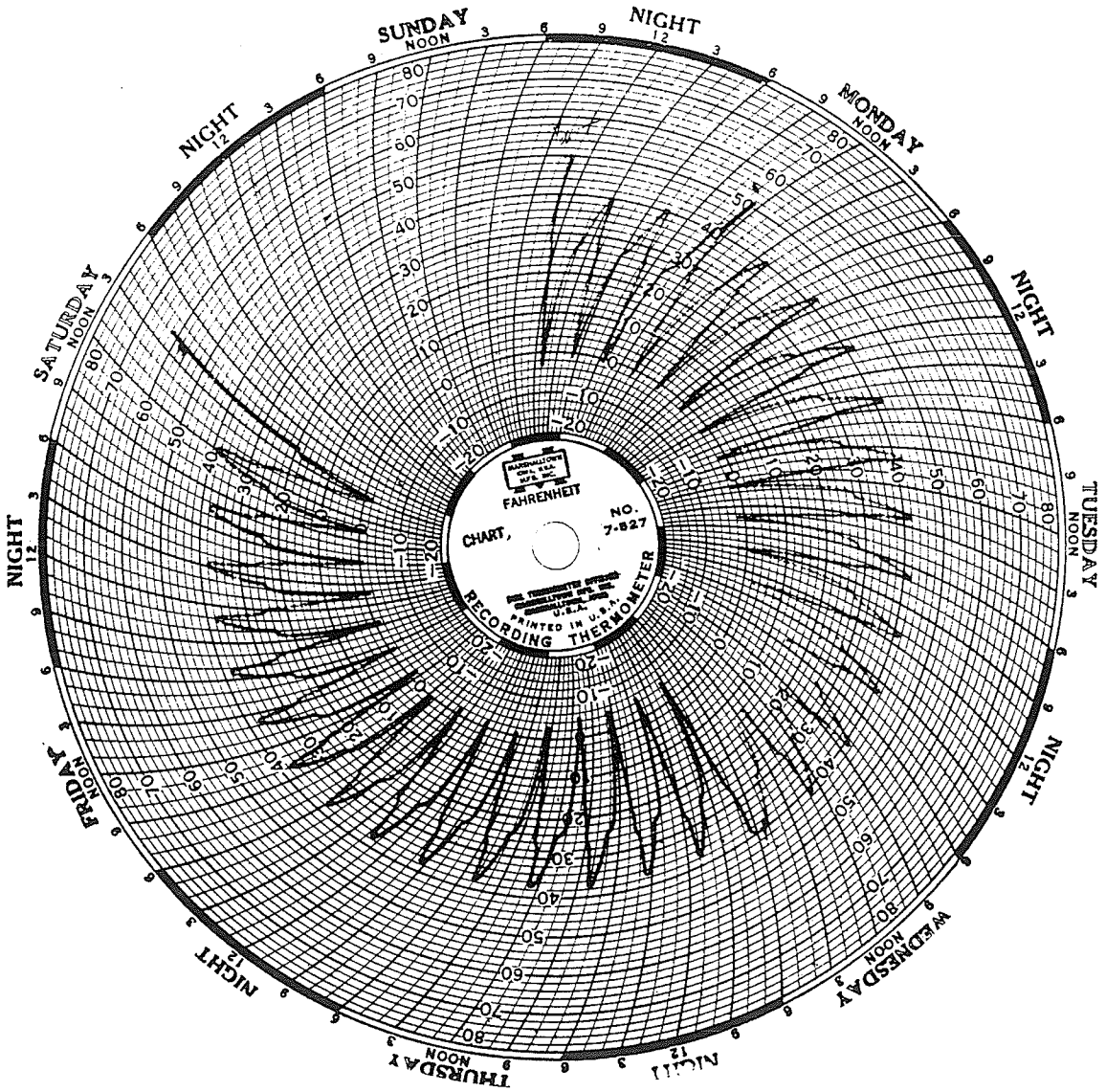

Figure A3.14: Time Against Temperature Inside the Temperature Specimen From 33 to 63 Cycles for A1.9 and A5.0 Specimens

EXTERNAL MOISTURE AND AIR CONTENT TEST

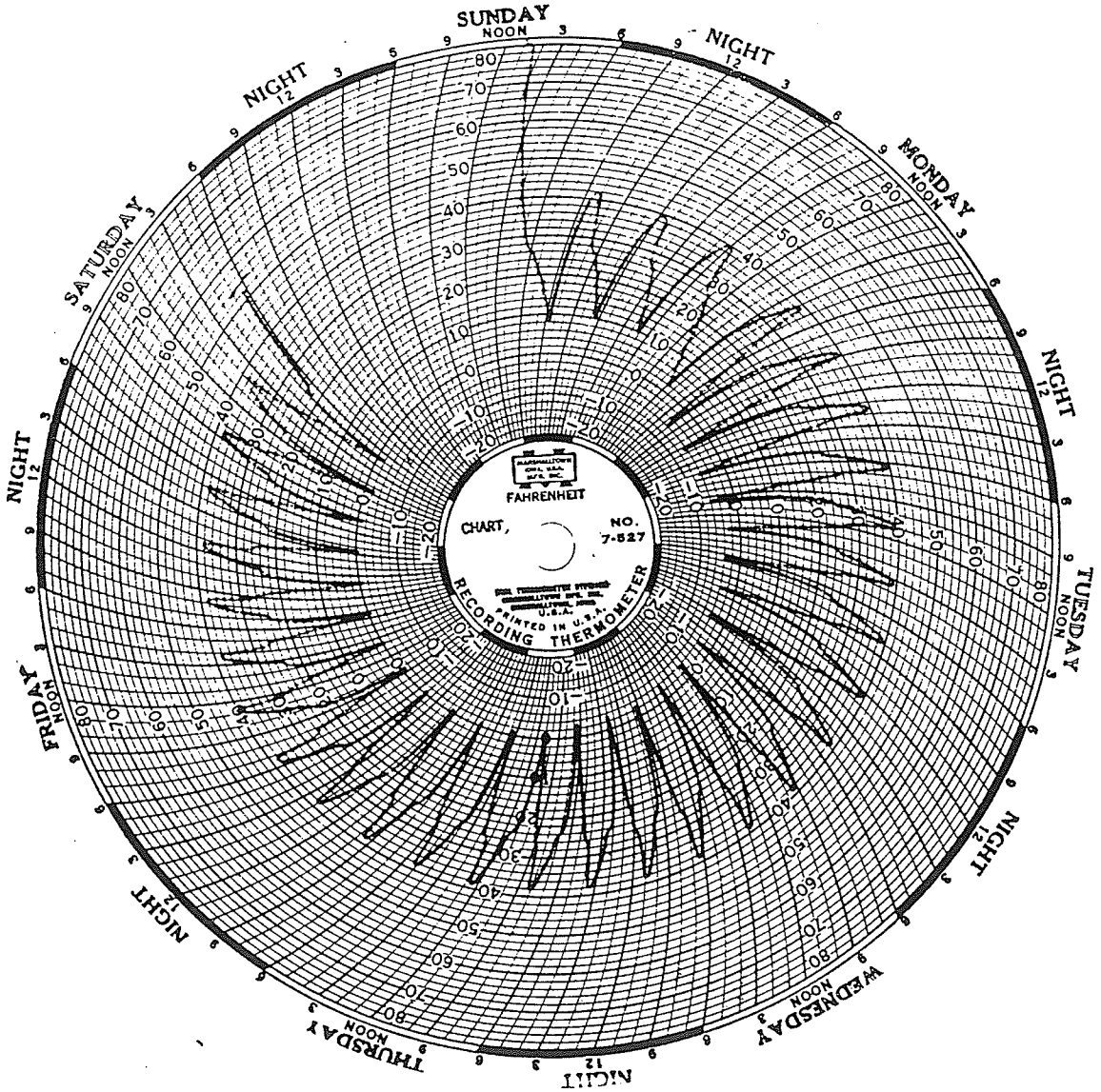

Figure A3.15: Time Against Temperature Inside the Temperature Control Specimen From 64 to 94 Cycles for A1.9 and A5.0 Specimens; 0 to 31 Cycles for A8.5 Specimens

EXTERNAL MOISTURE AND AIR CONTENT TEST

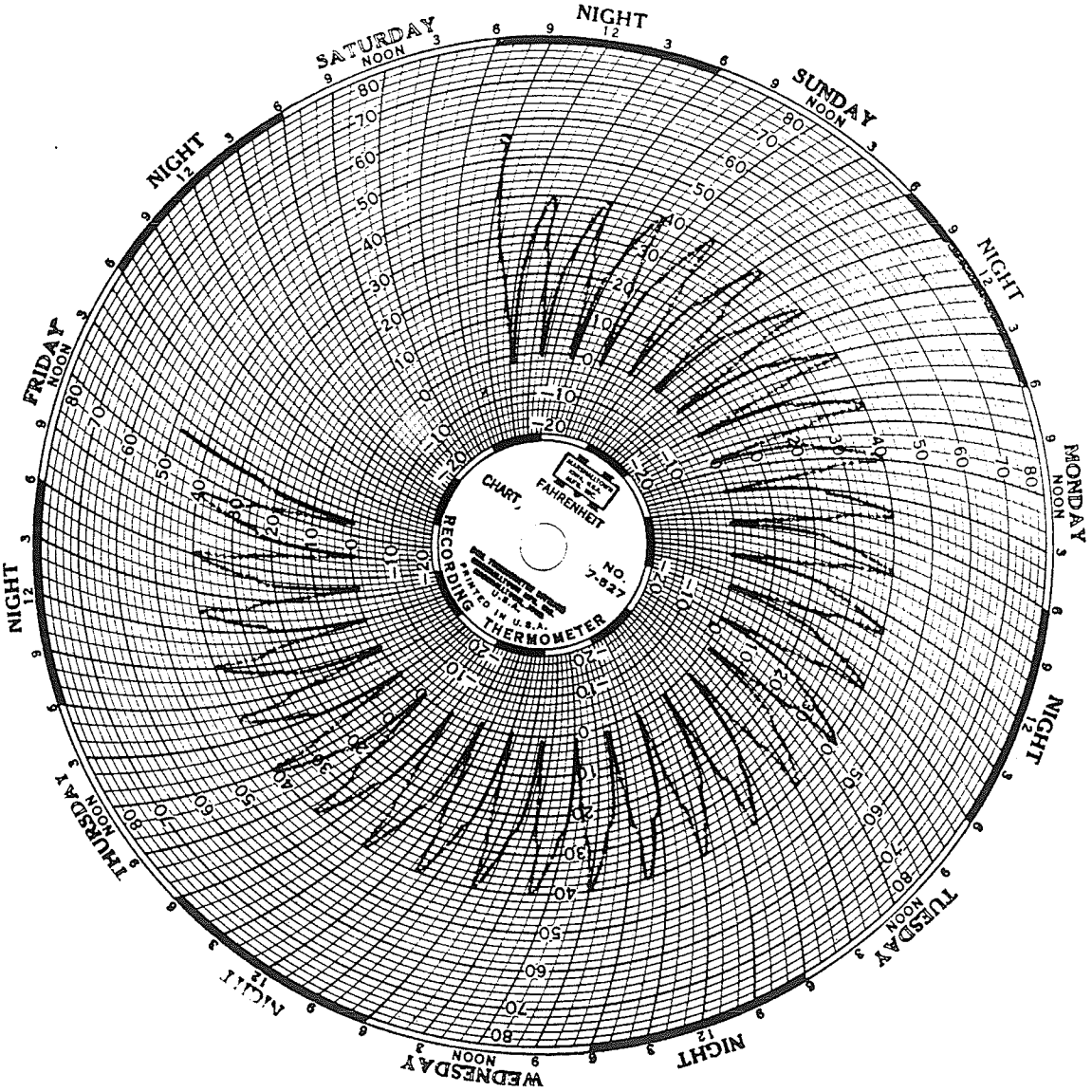

Figure A3.16: Time Against Temperature Inside the Temperature Control Specimen From 95 to 125 Cycles for A1.9 and A5.0 Specimens; 32 to 62 Cycles for A8.5 Specimens

EXTERNAL MOISTURE AND AIR CONTENT TEST

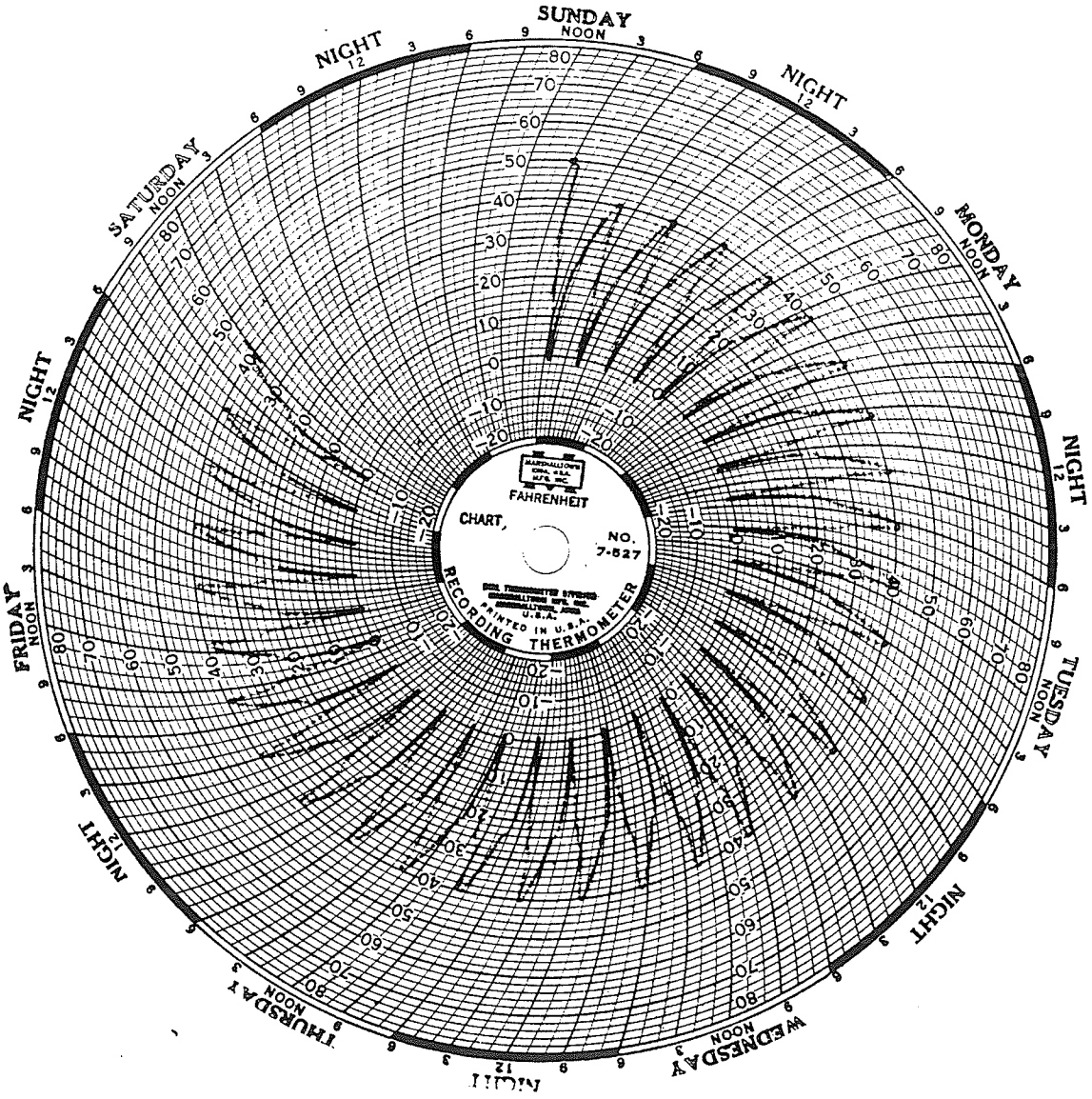

Figure A3.17: Time Against Temperature Inside the Temperature Control Specimen From 126 to 156 Cycles for A1.9 and A5.0 Specimens; 63 to 93 Cycles for A8.5 Specimens

EXTERNAL MOISTURE AND AIR CONTENT TEST

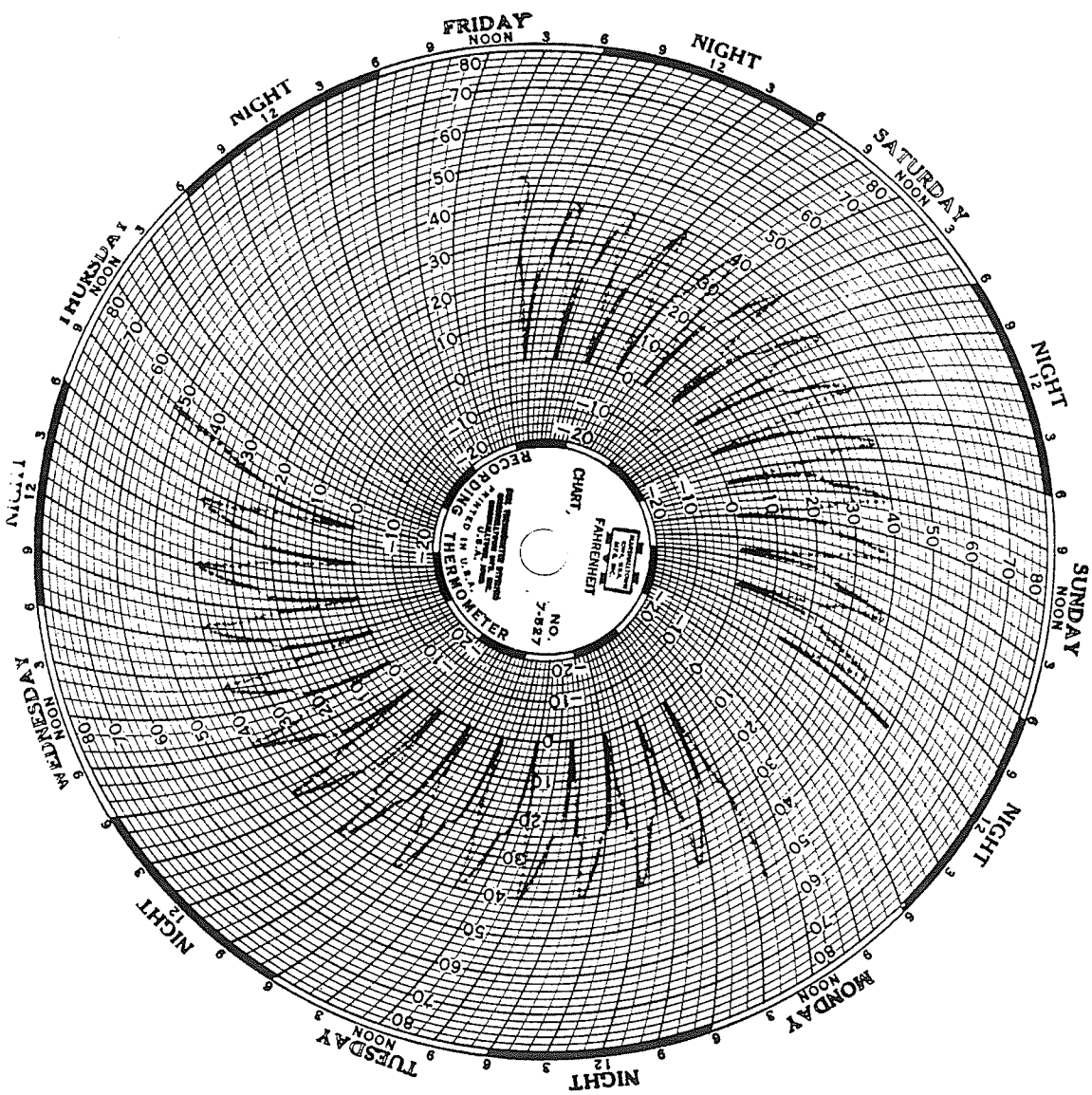

Figure A3.18: Time Against Temperature Inside the Temperature Control Specimen From 157 to 184 Cycles for A1.9 and A5.0 Specimens; 94 to 121 Cycles for A8.5 Specimens

EXTERNAL MOISTURE AND AIR CONTENT TEST

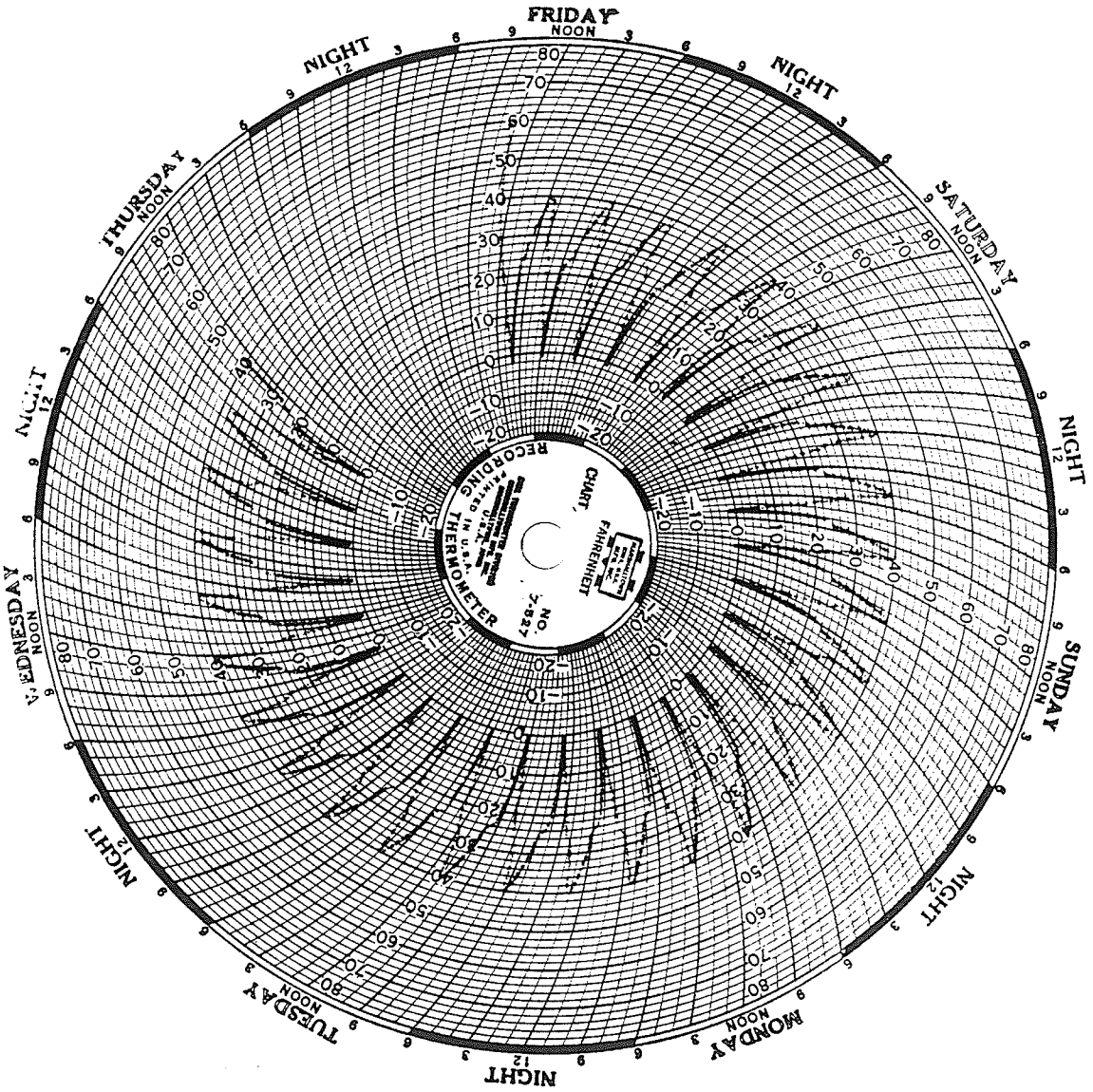

Figure A3.19: Time Against Temperature Inside the Temperature Control Specimen From 185 to 214 Cycles for A1.9 and A5.0 Specimens; 122 to 151 Cycles for A8.5 Specimens

EXTERNAL MOISTURE AND AIR CONTENT TEST

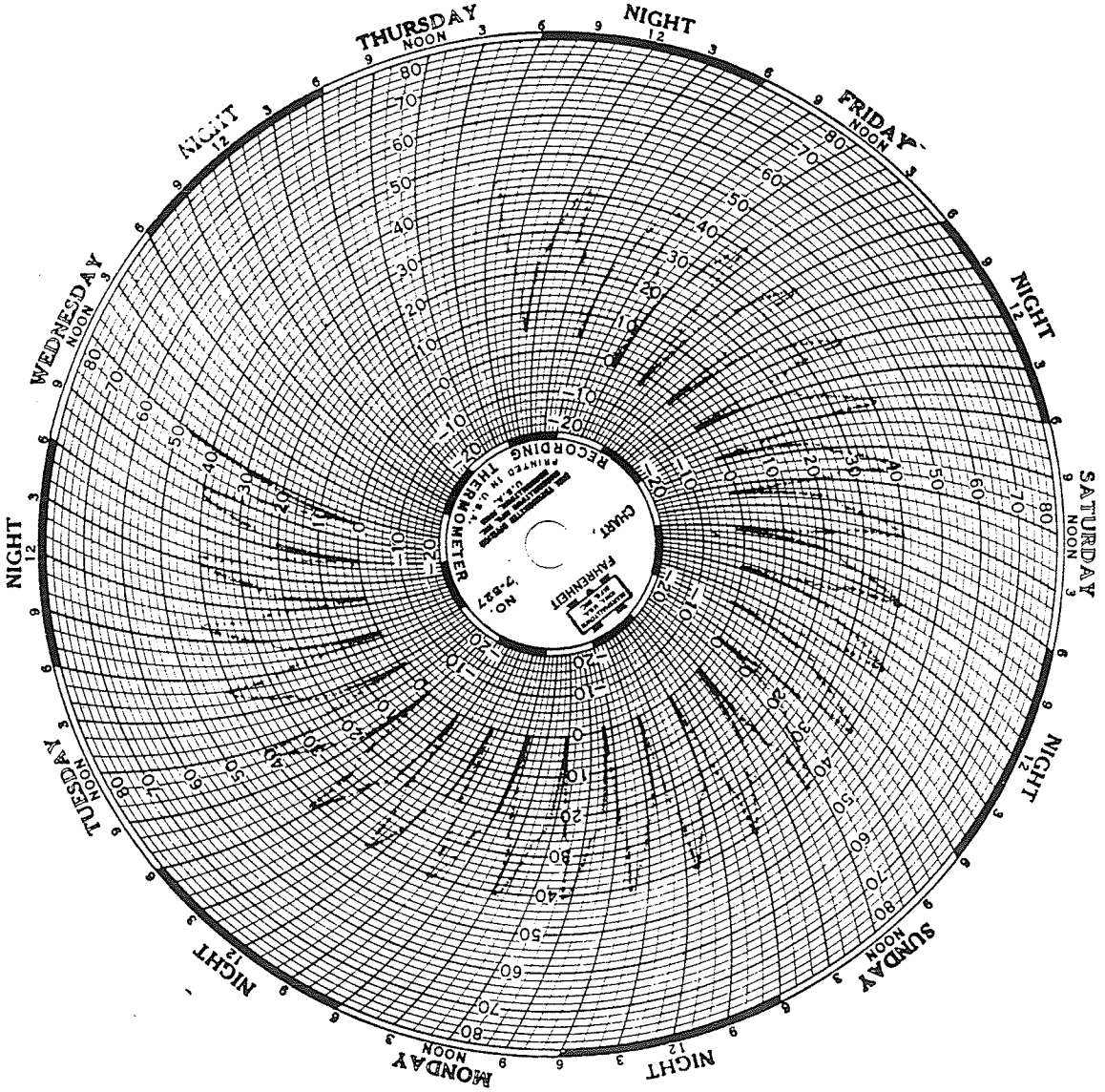

Figure A3.20: Time Against Temperature Inside the Temperature Control Specimen From 215 to 240 Cycles for A1.9 and A5.0 Specimens; 152 to 177 Cycles for A8.5 Specimens

EXTERNAL MOISTURE AND AIR CONTENT TEST

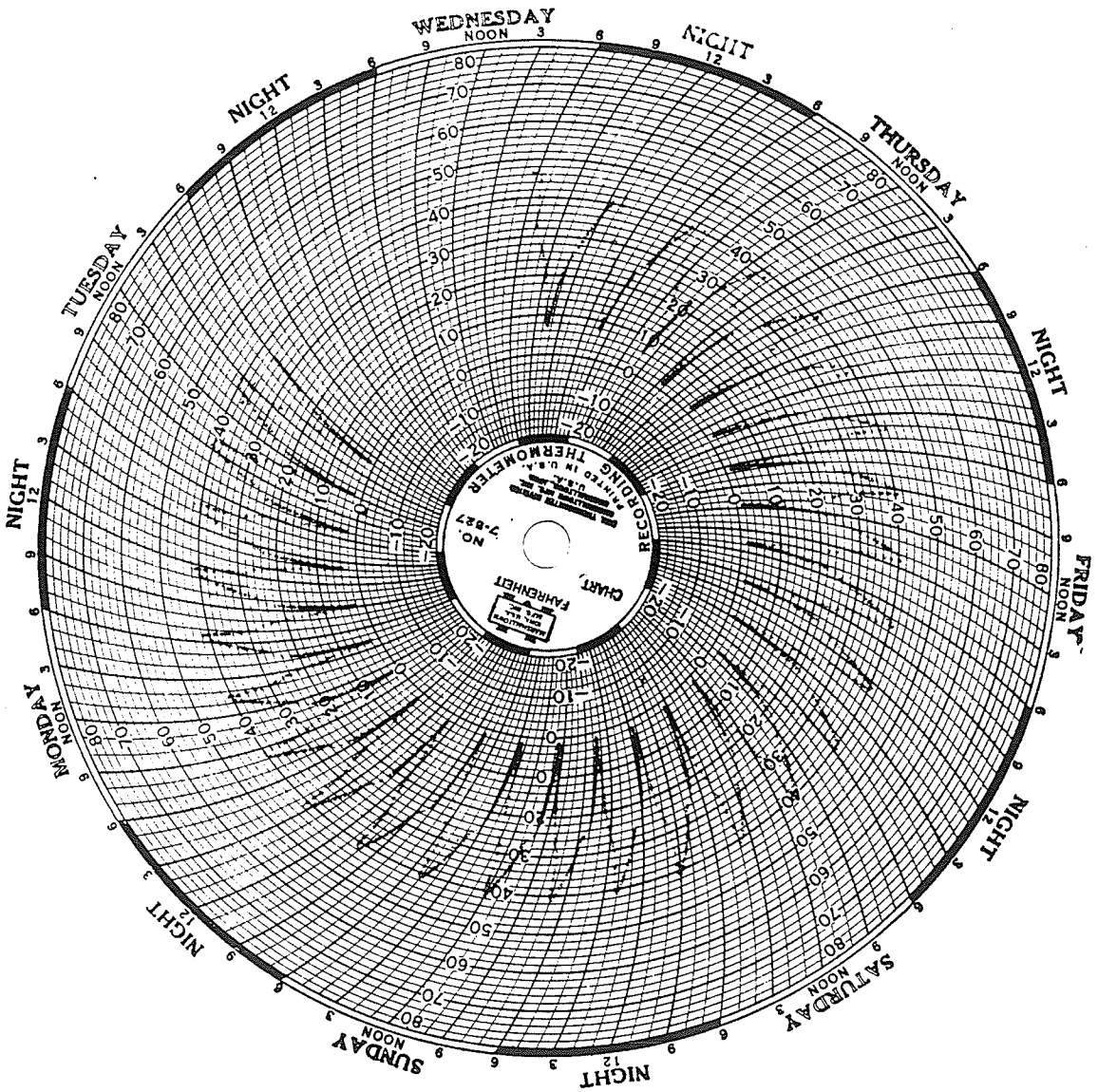

Figure A3.21: Time Against Temperature Inside the Temperature Control Specimen From 241 to 272 Cycles for A1.9 and A5.0 Specimens; 178 to 209 Cycles for A8.5 Specimens

EXTERNAL MOISTURE AND AIR CONTENT TEST

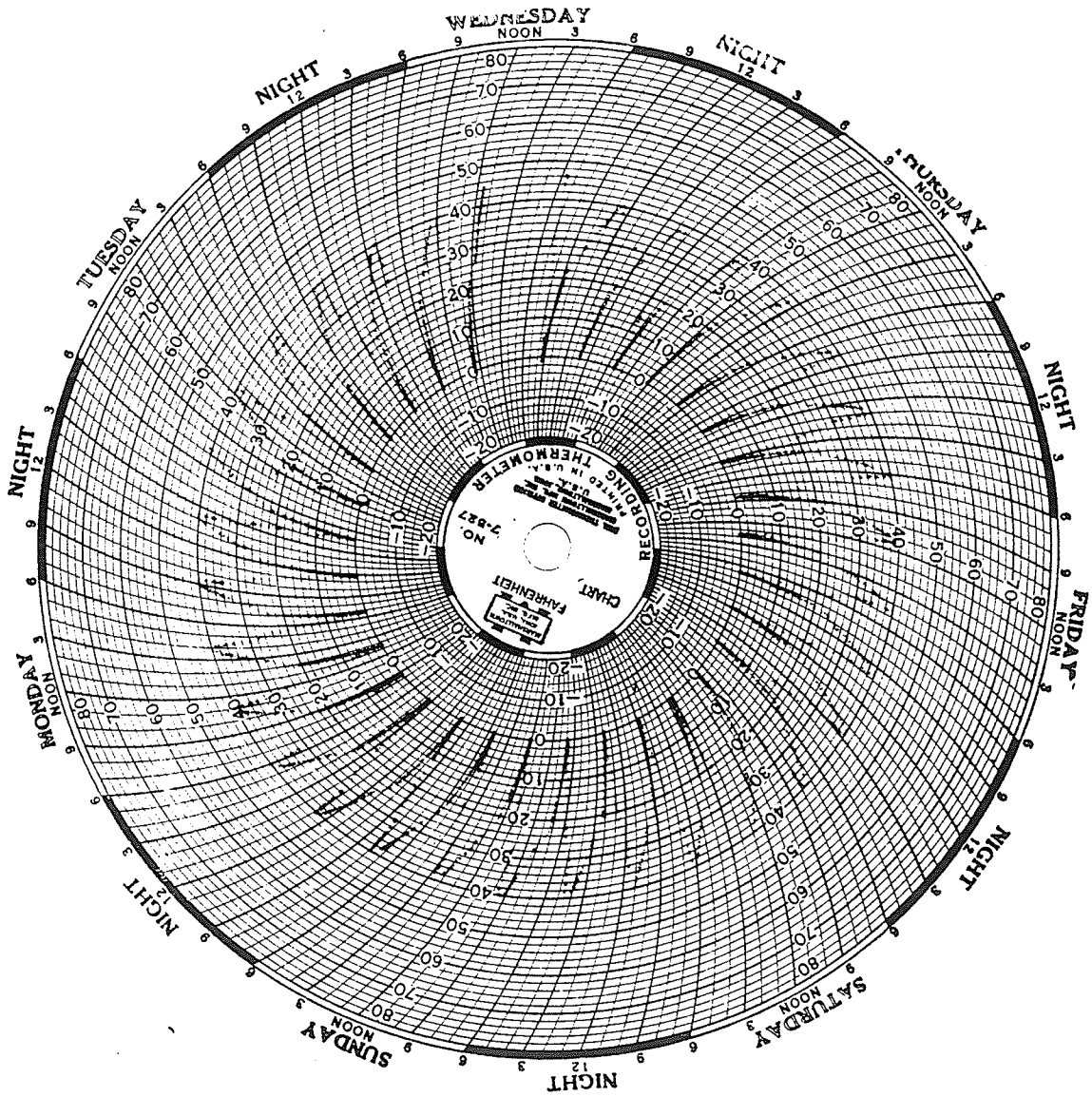

Figure A3.22: Time Against Temperature Inside the Temperature Control Specimen 273 to 300 Cycles for A1.9 and A5.0 Specimens; 210 to 237 Cycles for A8.5 Specimens

EXTERNAL MOISTURE AND AIR CONTENT TEST

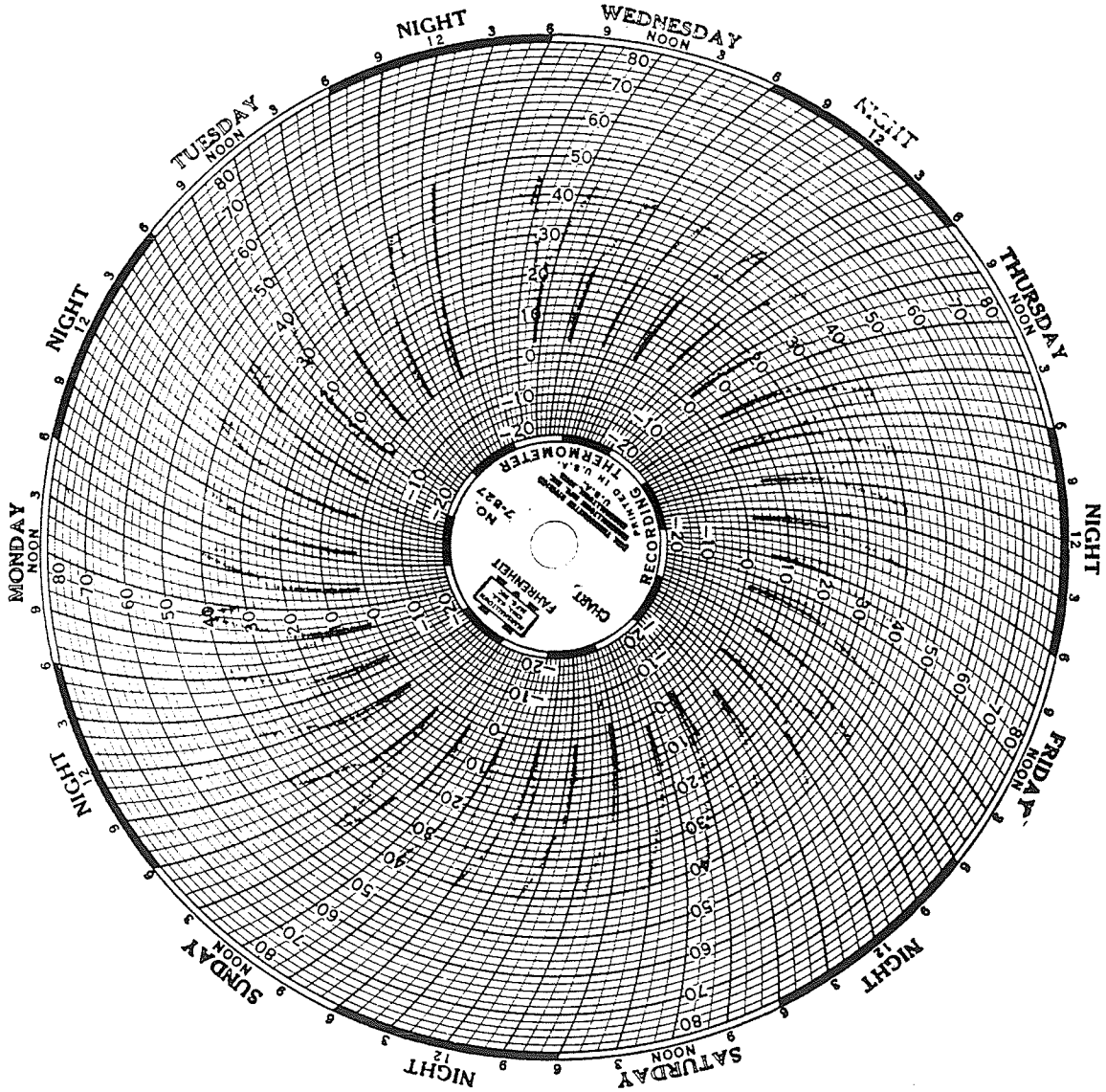

Figure A3.23: Time Against Temperature Inside the Temperature Control Specimen 238 to 271 Cycles for A8.5 Specimens

EXTERNAL MOISTURE AND AIR CONTENT TEST

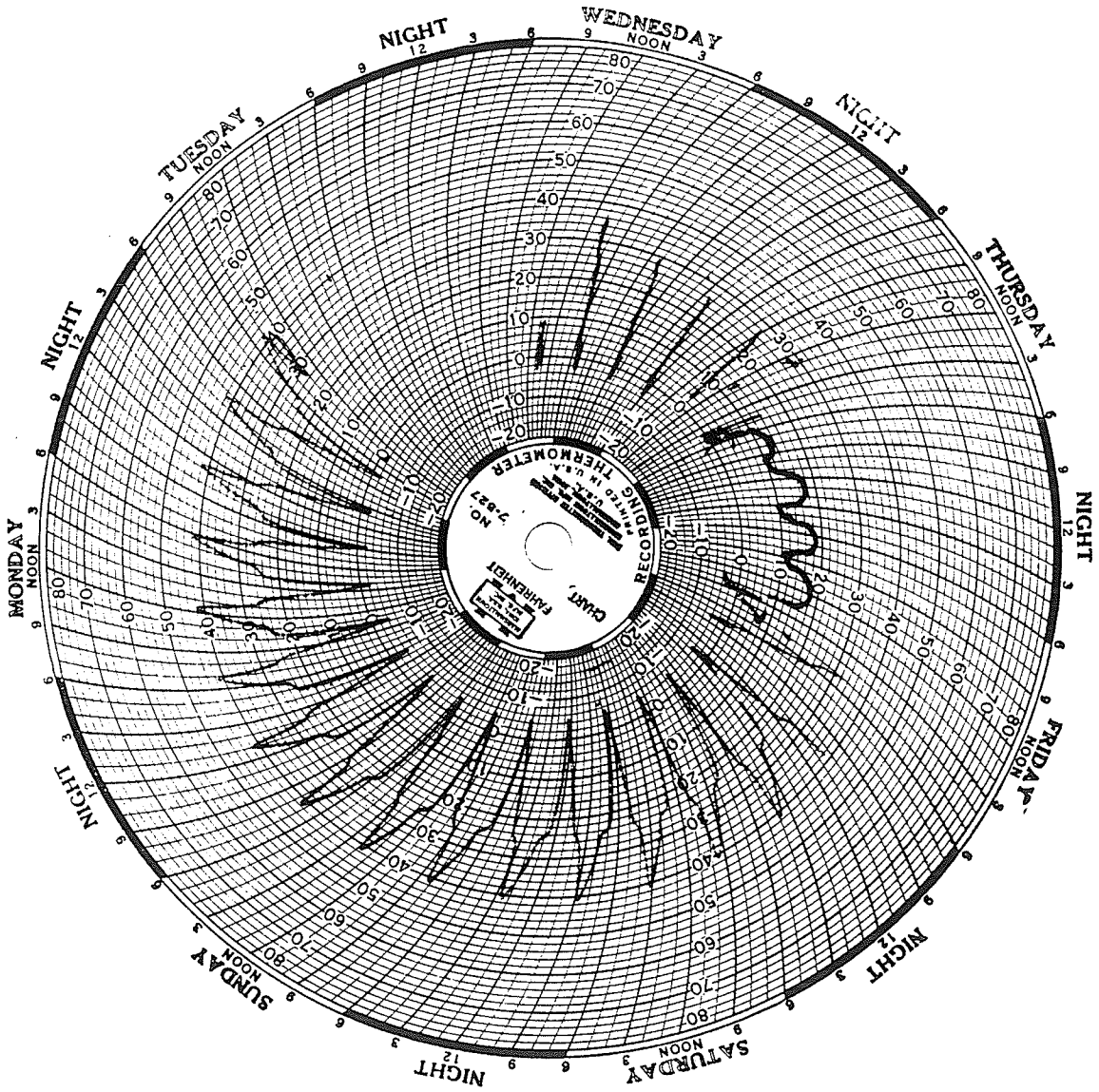

Figure A3.24: Time Against Temperature Inside the Temperature Control Specimen 272 to 302 Cycles for A8.5 Specimens

APPENDIX D

ELONGATION MEASUREMENTS AND DOCUMENTATION OF DISTRESSES

FLY ASH TEST

Number of Cycles Completed: 0

Date: 20 March 1985

Specimen Designation	Percent Axial Elongation	Specimen Condition/Description
BP1(1)	0.0	No deterioration.
BP1(2)	0.0	No deterioration.
BP1(3)	0.0	No deterioration.
BP1FA(1)	0.0	No deterioration.
BP1FA(2)	0.0	No deterioration.
BP1FA(3)	0.0	No deterioration.
S1(1)	0.0	No deterioration.
S1(2)	0.0	No deterioration.
S1(3)	0.0	No deterioration.
S1FA(1)	0.0	No deterioration.
S1FA(2)	0.0	No deterioration.
S1FA(3)	0.0	No deterioration.
S2(1)	0.0	No deterioration.
S2(2)	0.0	No deterioration.
S2FA(1)	0.0	No deterioration.
S2FA(2)	0.0	No deterioration.
S2FA(3)	0.0	No deterioration.

FLY ASH TEST

Number of Cycles Completed: 32

Date: 27 March 1985

Specimen Designation	Percent Axial Elongation	Specimen Condition/Description
BP1(1)	0.0214	Three small popouts approximately 5 mm deep.
BP1(2)	0.0189	No deterioration.
BP1(3)	0.0180	Two small popouts approximately 5 mm deep.
BP1FA(1)	0.0312	One small popout approx. 5 mm deep.
BP1FA(2)	0.0137	One small popout approx. 5 mm deep.
BP1FA(3)	0.0411	One small popout approx. 5 mm deep.
S1(1)	0.0079	No deterioration.
S1(2)	0.0099	No deterioration.
S1(3)	0.0104	One small popout approx. 5 mm deep.
S1FA(1)	0.0180	No deterioration.
S1FA(2)	0.0114	No deterioration.
S1FA(3)	0.0152	No deterioration.
S2(1)	0.0051	No deterioration.
S2(2)	0.0054	Small popout imminent.
S2FA(1)	0.0850	No deterioration.
S2FA(2)	0.0578	No deterioration.
S2FA(3)	0.0812	No deterioration.

FLY ASH TEST

Number of Cycles Completed: 60

Date: 3 April 1985

Specimen Designation	Percent Axial Elongation	Specimen Condition/Description
BP1(1)	0.0279	Continued popouts; no hairline cracks.
BP1(2)	0.0208	Continued popouts; no hairline cracks.
BP1(3)	0.0236	Continued popouts; no hairline cracks.
BP1FA(1)	0.0398	Continued popouts; no hairline cracks.
BP1FA(2)	0.0240	Continued popouts; no hairline cracks.
BP1FA(3)	0.0543	Continued popouts; small hairline cracks.
S1(1)	0.0223	No deterioration.
S1(2)	0.0246	No deterioration.
S1(3)	0.0217	No additional deterioration.
S1FA(1)	0.0391	No deterioration.
S1FA(2)	0.0285	No deterioration.
S1FA(3)	0.0298	Developing a few hairline cracks.
S2(1)	0.0094	No deterioration.
S2(2)	0.0091	Small popout.
S2FA(1)	0.1644	Developing a network of fine cracks.
S2FA(2)	0.1097	Developing a network of fine cracks.
S2FA(3)	0.1531	Developing a network of fine cracks.

FLY ASH TEST

Number of Cycles Completed: 91

Date: 11 April 1985

Specimen Designation	Percent Axial Elongation	Specimen Condition/Description
BP1(1)	0.0262	Continued small popouts; no hairline cracks.
BP1(2)	0.0253	One additional large popout; no hairline cracks.
BP1(3)	0.0245	No further deterioration.
BP1FA(1)	0.0535	No further deterioration.
BP1FA(2)	0.0385	No further deterioration.
BP1FA(3)	0.0754	Small hairline cracks developing.
S1(1)	0.0248	No sign of deterioration.
S1(2)	0.0257	No sign of deterioration.
S1(3)	0.0242	No additional deterioration.
S1FA(1)	0.0616	No deterioration.
S1FA(2)	0.0579	No deterioration.
S1FA(3)	0.0432	No additional deterioration.
S2(1)	0.0071	No deterioration.
S2(2)	0.0087	Two popouts approx. 12 mm deep; no hairline cracks.
S2FA(1)	0.2723	Crack network continuing to develop.
S2FA(2)	0.1895	Signs of internal failure; radial cracks.
S2FA(3)	0.2423	Crack pattern extensive and widening.

FLY ASH TEST

Number of Cycles Completed: 122

Date: 18 April 1985

Specimen Designation	Percent Axial Elongation	Specimen Condition/Description
BP1(1)	0.0301	More popouts; becoming deeper.
BP1(2)	0.0262	No further deterioration.
BP1(3)	0.0262	No further deterioration.
BP1FA(1)	0.0897	Radial cracking; signs of internal failure.
BP1FA(2)	0.0399	No further deterioration.
BP1FA(3)	0.1013	Crack network developing.
S1(1)	0.0274	No deterioration.
S1(2)	0.0274	No deterioration.
S1(3)	0.0273	No further deterioration.
S1FA(1)	0.0872	No deterioration.
S1FA(2)	0.0807	No deterioration.
S1FA(3)	0.0581	No further deterioration.
S2(1)	0.0094	No deterioration.
S2(2)	0.0071	No further deterioration.
S2FA(1)	0.3669	Extensive cracking; cracks widening.
S2FA(2)	0.2647	Extensive cracking; cracks widening.
S2FA(3)	0.3318	Extensive cracking; cracks widening.

FLY ASH TEST

Number of Cycles Completed: 150

Date: 25 April 1985

Specimen Designation	Percent Axial Elongation	Specimen Condition/Description
BP1(1)	0.0296	Large corner failure.
BP1(2)	0.0293	No further deterioration.
BP1(3)	0.0254	No further deterioration.
BP1FA(1)	0.1248	Crack network well established.
BP1FA(2)	0.0630	A few minor cracks.
BP1FA(3)	0.1418	Large crack in middle of specimen.
S1(1)	0.0297	No deterioration.
S1(2)	0.0299	No deterioration.
S1(3)	0.0287	No further deterioration.
S1FA(1)	0.1128	Crack network begining to develop.
S1FA(2)	0.0939	Crack network begining to develop.
S1FA(3)	0.0798	Crack network begining to develop; small popout.
S2(1)	0.0168	No deterioration.
S2(2)	0.0100	No further deterioration.
S2FA(1)	0.4717	Major distress; extensive, widening cracks.
S2FA(2)	0.3362	Major distress; extensive, widening cracks.
S2FA(3)	0.4085	Major distress; extensive, widening cracks.

FLY ASH TEST

Number of Cycles Completed: 179

Date: 2 May 1985

Specimen Designation	Percent Axial Elongation	Specimen Condition/Description
BP1(1)	0.0301	No further deterioration.
BP1(2)	0.0312	No further deterioration.
BP1(3)	0.0216	No further deterioration.
BP1FA(1)	0.1745	Crack network increasing in size and width.
BP1FA(2)	0.0810	Minor cracking and popouts.
BP1FA(3)	0.1942	Crack network increasing in size and width.
S1(1)	0.0274	No deterioration.
S1(2)	0.0291	Some minor cracking.
S1(3)	0.0296	Some minor cracking.
S1FA(1)	0.1403	Crack network developing.
S1FA(2)	0.1223	Crack network developing.
S1FA(3)	0.0989	Crack network developing.
S2(1)	0.0157	No deterioration.
S2(2)	0.0120	One large popout.
S2FA(1)	0.5831	Major distress; extensive, widening cracks.
S2FA(2)	0.4047	Major distress; extensive, widening cracks.
S2FA(3)	0.4899	Major distress; extensive, widening cracks.

FLY ASH TEST

Number of Cycles Completed: 210

Date: 10 May 1985

Specimen Designation	Percent Axial Elongation	Specimen Condition/Description
BP1(1)	0.0321	No further deterioration.
BP1(2)	0.0322	Popout about to occur.
BP1(3)	0.0310	No further deterioration.
BP1FA(1)	0.2387	Well defined, deep seated cracking.
BP1FA(2)	0.1074	Some deep radial cracking.
BP1FA(3)	0.2621	Crack network increasing in size and depth.
S1(1)	0.0286	No deterioration.
S1(2)	0.0280	No further deterioration.
S1(3)	0.0324	No further deterioration.
S1FA(1)	0.1765	Crack network developing.
S1FA(2)	0.1545	Crack network developing.
S1FA(3)	0.1224	Crack network developing.
S2(1)	0.0083	No deterioration.
S2(2)	0.0097	No further deterioration.
S2FA(1)	0.7417	Major distress; extensive, widening cracks.
S2FA(2)	0.5013	Major distress; extensive, widening cracks.
S2FA(3)	0.6289	Major distress; extensive, widening cracks.

FLY ASH TEST

Number of Cycles Completed: 240

Date: 17 May 1985

Specimen Designation	Percent Axial Elongation	Specimen Condition/Description
BP1(1)	0.0341	No further deterioration.
BP1(2)	0.0346	Corners deteriorating.
BP1(3)	0.0304	No further deterioration.
BP1FA(1)	0.3204	Crack network becoming larger.
BP1FA(2)	0.1419	Deep radial cracking.
BP1FA(3)	0.3567	One large crack progressing rapidly.
S1(1)	0.0280	No further deterioration.
S1(2)	0.0336	No further deterioration.
S1(3)	0.0329	No further deterioration.
S1FA(1)	0.1933	Crack network slowly developing.
S1FA(2)	0.1750	Crack network slowly developing.
S1FA(3)	0.1435	Crack network slowly developing.
S2(1)	0.0060	No deterioration.
S2(2)	0.0117	No further deterioration.
S2FA(1)	----	Failure at 240 cycles.
S2FA(2)	0.6296	Severe deterioration.
S2FA(3)	1.0269	Severe deterioration.

FLY ASH TEST

Number of Cycles Completed: 269

Date: 25 May 1985.

Specimen Designation	Percent Axial Elongation	Specimen Condition/Description
BP1(1)	0.0411	No further deterioration.
BP1(2)	0.0369	No further deterioration.
BP1(3)	0.0349	Two additional small popouts.
BP1FA(1)	0.4419	Rapid deterioration.
BP1FA(2)	0.1814	Crack pattern continuing to develop.
BP1FA(3)	0.5769	Close to failure.
S1(1)	0.0308	No further deterioration.
S1(2)	0.0331	No further deterioration.
S1(3)	0.0343	No further deterioration.
S1FA(1)	0.2454	Crack network continuing to develop.
S1FA(2)	0.2089	Crack network continuing to develop.
S1FA(3)	0.1840	Crack network continuing to develop.
S2(1)	0.0057	No deterioration.
S2(2)	0.0077	No further deterioration.
S2FA(1)	----	--------
S2FA(2)	0.9794	Severe deterioration.
S2FA(3)	----	Failed at 257 cycles.

FLY ASH TEST

Number of Cycles Completed: 303

Date: 2 June 1985

Specimen Designation	Percent Axial Elongation	Specimen Condition/Description
BP1(1)	0.0493	No further deterioration.
BP1(2)	0.0447	No further deterioration.
BP1(3)	0.0397	No further deterioration.
BP1FA(1)	0.6013	Accelerated deterioration over the last 30 cycles.
BP1FA(2)	0.2621	Moderate cracking.
BP1FA(3)	----	Specimen failed at 290 cycles.
S1(1)	0.0545	Slight hairline cracks.
S1(2)	0.0435	No further deterioration.
S1(3)	0.0380	No further deterioration.
S1FA(1)	0.3132	Deterioration accelerating.
S1FA(2)	0.2674	Deterioration accelerating.
S1FA(3)	0.2410	Deterioration accelerating.
S2(1)	0.0086	No deterioration.
S2(2)	0.0114	No further deterioration.
S2FA(1)	----	-------
S2FA(2)	----	Specimen failed at 290 cycles.
S2FA(3)	----	-------

AIR CONTENT AND EXTERNAL MOISTURE TEST

Specimen Designation[1]	Percent Axial Elongation	Specimen Condition/Description
Number of Cycles Completed: 0		Date: 29 Sept 1985
A1.9(1)	0.0	No deterioration.
A1.9(2)	0.0	No deterioration.
A1.9(3)	0.0	No deterioration.
A1.9(4)	0.0	No deterioration.
A1.9(5)	0.0	No deterioration.
A1.9(6)	0.0	No deterioration.
A5.0(1)	0.0	No deterioration.
A5.0(2)	0.0	No deterioration.
A5.0(3)	0.0	No deterioration.
A5.0(4)	0.0	No deterioration.
A5.0(5)	0.0	No deterioration.
Number of Cycles Completed: 0		Date: 16 October 1985
A8.5(1)	0.0	No deterioration.
A8.5(2)	0.0	No deterioration.
A8.5(3)	0.0	No deterioration.
A8.5(4)	0.0	No deterioration
A8.5(5)	0.0	No deterioration.
A8.5(6)	0.0	No deterioration.

[1]Specimens 1, 2, and 3 of mixes A1.9 and A8.5 were sealed. Specimens 1 and 2 were sealed from mix A5.0.

AIR CONTENT AND EXTERNAL MOISTURE TEST

Specimen Designation[1]	Percent Axial Elongation	Specimen Condition/Description
Cycles Completed: 31		Date: 6 October 1985
A1.9(1)	0.0130	------[2]
A1.9(2)	0.0090	------
A1.9(3)	0.0085	------
A1.9(4)	0.0104	No deterioration.
A1.9(5)	0.0113	No deterioration.
A1.9(6)	0.0127	No deterioration.
A5.0(1)	0.0048	No deterioration.
A5.0(2)	0.0469	Deep seated cracking developing; can be seen through sealant.
A5.0(3)	0.0101	No deterioration.
A5.0(4)	0.0144	Small popout; minor cracking.
A5.0(5)	0.0189	Two small cracks.
Cycles 1985 Completed: 31		Date: 28 October
A8.5(1)	0.0000	------
A8.5(2)	0.0020	------
A8.5(3)	0.0000	------
A8.5(4)	0.0037	No deterioration.
A8.5(5)	0.0003	No deterioration.
A8.5(6)	0.0014	No deterioration.

[1]Specimens 1, 2, and 3 of mixes A1.9 and A8.5 were sealed. Specimens 1 and 2 were sealed from mix A5.0.
[2]Comments on state of distress of sealed specimens was not possible because the translucent epoxy sealant covered any cracking that occurred.

AIR CONTENT AND EXTERNAL MOISTURE TEST

Specimen Designation[1]	Percent Axial Elongation	Specimen Condition/Description
Cycles Completed:63		Date: 16 October 1985
A1.9(1)	0.0113	------[2]
A1.9(2)	0.0082	------
A1.9(3)	0.0181	------
A1.9(4)	0.0206	No deterioration.
A1.9(5)	0.0236	Some cracking around ends of specimens.
A1.9(6)	0.0534	Deep cracking initiated on "north" end of specimen.
A5.0(1)	0.0028	------
A5.0(2)	0.0787	Crack visible through sealant.
A5.0(3)	0.0110	------
A5.0(4)	0.0147	Minor cracking.
A5.0(5)	0.0366	Crack network developing.
Cycles Completed:62		Date: 2 November 1985
A8.5(1)	0.0014	------
A8.5(2)	0.0025	------
A8.5(3)	0.0023	------
A8.5(4)	0.0042	No deterioration.
A8.5(5)	0.0025	No deterioration.
A8.5(6)	0.0031	No deterioration.

[1]Specimens 1, 2, and 3 of mixes A1.9 and A8.5 were sealed. Specimens 1 and 2 were sealed from mix A5.0.
[2]Comments on state of distress of sealed specimens was not possible because the translucent epoxy sealant covered any cracking that occurred.

AIR CONTENT AND EXTERNAL MOISTURE TEST

Specimen Designation[1]	Percent Axial Elongation	Specimen Condition/Description
Cycles Completed:94		Date: 28 October 1985
A1.9(1)	0.0085	------[2]
A1.9(2)	0.0110	------
A1.9(3)	0.0004	------
A1.9(4)	0.0504	Some cracking; becoming more pronounced.
A1.9(5)	0.0543	Bulging and cracking; subsurface aggregate failure.
A1.9(6)	0.1203	Large corner chip due to aggregate failure; pronounced cracking.
A5.0(1)	0.0000	------
A5.0(2)	0.0956	Cracks under epoxy.
A5.0(3)	0.0107	------
A5.0(4)	0.0285	Two popouts; minor cracking.
A5.0(5)	0.0611	One large shallow popout; crack network expanding.
Cycles Completed:93		Date: 8 November 1985
A8.5(1)	0.0042	------
A8.5(2)	0.0023	------
A8.5(3)	0.0051	------
A8.5(4)	0.0079	Some very minor cracking.
A8.5(5)	0.0033	Some staining.
A8.5(6)	0.0031	Some staining.

[1]Specimens 1, 2, and 3 of mixes A1.9 and A8.0 were sealed. Specimens 1 and 2 were sealed from mix A5.0.
[2]Comments on state of distress of sealed specimens was not possible because the translucent epoxy sealant covered any cracking that occurred.

AIR CONTENT AND EXTERNAL MOISTURE TEST

Specimen Designation[1]	Percent Axial Elongation	Specimen Condition/Description
Cycles Completed:125		Date: 2 November 1985
A1.9(1)	0.0276	------[2]
A1.9(2)	0.0113	------
A1.9(3)	0.0059	------
A1.9(4)	0.0988	Fine network of cracks developing.
A1.9(5)	0.0883	Fine network of cracks; pronounced on "north" end.
A1.9(6)	0.1680	Cracking very pronounced.
A5.0(1)	0.0020	------
A5.0(2)	0.1632	Large cracks visible under epoxy coating.
A5.0(3)	0.0082	------
A5.0(4)	0.0395	Little further deterioration.
A5.0(5)	0.0825	Crack pattern propogating.
Cycles Completed:121		Date: 15 November 1985
A8.5(1)	0.0079	------
A8.5(2)	0.0090	------
A8.5(3)	0.0090	------
A8.5(4)	0.0107	Some very minor cracking.
A8.5(5)	0.0084	Some staining.
A8.5(6)	0.0090	Some very minor cracking.

[1]Specimens 1, 2, and 3 of mixes A1.9 and A8.0 were sealed. Specimens 1 and 2 were sealed from mix A5.0.
[2]Comments on state of distress of sealed specimens was not possible because the translucent epoxy sealant covered any cracking that occurred.

AIR CONTENT AND EXTERNAL MOISTURE TEST

Specimen Designation[1]	Percent Axial Elongation	Specimen Condition/Description
Cycles Completed:156		Date: 8 November 1985
A1.9(1)	0.0572	------[2]
A1.9(2)	0.0139	------
A1.9(3)	0.0042	------
A1.9(4)	0.1399	Crack pattern propogating; becoming more pronounced.
A1.9(5)	0.1340	Crack pattern propogating; becoming more pronounced.
A1.9(6)	0.2291	Cracking increasing; rapid deterioration on "north" end.
A5.0(1)	0.0014	------
A5.0(2)	----	Failure due to aggregate expansion.
A5.0(3)	0.0093	------
A5.0(4)	0.0580	Cracking progressing; one additional small popout.
A5.0(5)	0.1224	Crack network and intensity of distress increasing rapidly.
Cycles Completed:151		Date: 21 November 1985
A8.5(1)	0.0073	------
A8.5(2)	0.0090	------
A8.5(3)	0.0099	------
A8.5(4)	0.0110	Some water under sealant; no tears in sealant,water expelled from specimen.
A8.5(5)	0.0079	No further deterioration.
A8.5(6)	0.0076	No further deterioration.

[1]Specimens 1, 2, and 3 of mixes A1.9 and A8.5 were sealed. Specimens 1 and 2 were sealed from mix A5.0.

[2]Comments on state of distress of sealed specimens was not possible because the translucent epoxy sealant covered any cracking that occurred.

AIR CONTENT AND EXTERNAL MOISTURE TEST

Specimen Designation[1]	Percent Axial Elongation	Specimen Condition/Description
Cycles Completed:184		Date: 15 November 1985
A1.9(1)	0.1013	------[2]
A1.9(2)	0.0167	------
A1.9(3)	0.0079	------
A1.9(4)	0.1938	Crack network propogating rapidly.
A1.9(5)	0.1862	Crack network propogating; deterioration at "north" end severe.
A1.9(6)	0.3038	Crack network propogating rapidly.
A5.0(1)	0.0051	------
A5.0(2)	----	Failed.
A5.0(3)	0.0121	------
A5.0(4)	0.0854	Crack network becoming larger.
A5.0(5)	0.1816	Cracking becoming severe.
Cycles Completed:177		Date: 27 November 1985
A8.5(1)	0.0133	------
A8.5(2)	0.0115	------
A8.5(3)	0.0127	------
A8.5(4)	0.0155	No further deterioration.
A8.5(5)	0.0133	No further deterioration.
A8.5(6)	0.0110	No further deterioration.

[1]Specimens 1, 2, and 3 of mixes A1.9 and A8.5 were sealed. Specimens 1 and 2 were sealed from mix A5.0.

[2]Comments on state of distress of sealed specimens was not possible because the translucent epoxy sealant covered any cracking that occurred.

AIR CONTENT AND EXTERNAL MOISTURE TEST

Specimen Designation[1]	Percent Axial Elongation	Specimen Condition/Description
Cycles Completed:214		Date: 21 November 1985
A1.9(1)	0.1547	------[2]
A1.9(2)	0.0174	------
A1.9(3)	0.0099	------
A1.9(4)	0.2690	Large scale deterioration; close to failure.
A1.9(5)	0.2612	Large aggregate failure; crack network growing.
A1.9(6)	0.3997	Severe distress, crack network growing.
A5.0(1)	0.0051	------
A5.0(2)	----	Failed.
A5.0(3)	0.0116	------
A5.0(4)	0.1171	Large popout, crack network growing.
A5.0(5)	0.2520	Severe deterioration, medium popout.
Cycles Completed:209		Date: 4 December 1985
A8.5(1)	0.0071	------
A8.5(2)	0.0087	------
A8.5(3)	0.0099	------
A8.5(4)	0.0110	Water under sealant.
A8.5(5)	0.0087	No further deterioration.
A8.5(6)	-0.0051	No further deterioration.

[1]Specimens 1, 2, and 3 of mixes A1.9 and A8.0 were sealed. Specimens 1 and 2 were sealed from mix A5.0.
[2]Comments on state of distress of sealed specimens was not possible because the translucent epoxy sealant covered any cracking that occurred.

AIR CONTENT AND EXTERNAL MOISTURE TEST

Specimen Designation[1]	Percent Axial Elongation	Specimen Condition/Description
Cycles Completed:240		Date: 27 November 1985
A1.9(1)	0.2426	Cracking due to aggregate failure visible under epoxy[2].
A1.9(2)	0.0203	------
A1.9(3)	0.0110	------
A1.9(4)	0.3603	Severe distress.
A1.9(5)	0.3661	Major aggregate distress at "north" end; major distress.
A1.9(6)	missed reading	Major aggregate distress at "north" end; major distress.
A5.0(1)	0.0084	------
A5.0(2)	----	Failed.
A5.0(3)	0.0144	------
A5.0(4)	0.1517	Large popouts; crack pattern continuing to develop.
A5.0(5)	0.3192	Two large popouts; severe cracking.
Cycles Completed:237		Date: 10 December 1985
A8.5(1)	0.0042	------
A8.5(2)	0.0059	------
A8.5(3)	0.0056	Water under sealant.
A8.5(4)	0.0082	No further deterioration.
A8.5(5)	0.0065	No further deterioration.
A8.5(6)	0.0051	No further deterioration.

[1]Specimens 1, 2, and 3 of mixes A1.9 and A8.0 were sealed. Specimens 1 and 2 were sealed from mix A5.0.

[2]Comments on state of distress of sealed specimens was not possible because the translucent epoxy sealant covered any cracking that occurred.

AIR CONTENT AND EXTERNAL MOISTURE TEST

Specimen Designation[1]	Percent Axial Elongation	Specimen Condition/Description
Cycles Completed:272		Date: 4 December 1985
A1.9(1)	0.4203	Crack visible under epoxy, efforts to seal tear were ineffective[2].
A1.9(2)	0.0188	------
A1.9(3)	0.0102	------
A1.9(4)	0.5349	Large popout imminent.
A1.9(5)	----	Loose stud, considered to be failure.
A1.9(6)	----	Failed.
A5.0(1)	0.0051	------
A5.0(2)	----	Failed.
A5.0(3)	0.0110	------
A5.0(4)	0.1944	Crack network progressing.
A5.0(5)	0.4283	Severe distress, failure immenent.
Cycles Completed:271		Date: 17 December 1985
A8.5(1)	0.0073	------
A8.5(2)	0.0110	------
A8.5(3)	0.0082	A small tear has developed in the sealant.
A8.5(4)	0.0099	Some cracking and staining.
A8.5(5)	0.0115	No further deterioration.
A8.5(6)	0.0082	Chip off of corner of specimen due to aggregate failure.

[1]Specimens 1, 2, and 3 of mixes A1.9 and A8.5 were sealed. Specimens 1 and 2 were sealed from mix A5.0.

[2]Comments on state of distress of sealed specimens was not possible because the translucent epoxy sealant covered any cracking that occurred.

AIR CONTENT AND EXTERNAL MOISTURE TEST

Specimen Designation[1]	Percent Axial Elongation	Specimen Condition/Description
Cycles Completed:300		Date: 10 December 1985
A1.9(1)	----	Failure due to one aggregate; failure perpendicular to bedding planes.
A1.9(2)	0.0236	------
A1.9(3)	0.0100	------
A1.9(4)	0.7433	Severe distress.
A1.9(5)	----	Failed.
A1.9(6)	----	Failed.
A5.0(1)	0.0020	------
A5.0(2)	----	------
A5.0(3)	0.0096	Major distress; extensive crack network.
A5.0(4)	0.5230	Major distress; extensive crack network.
A5.0(5)	0.5457	Major distress; extensive crack network.
Cycles Completed:302		Date: 24 December 1985
A8.5(1)	0.0170	------
A8.5(2)	0.0110	------
A8.5(3)	0.0135	Slight tear in sealant
A8.5(4)	0.0127	Some very fine cracking
A8.5(5)	0.0113	Very minor cracking and staining.
A8.5(6)	0.0079	Very minor cracking and staining.

[1]Specimens 1, 2, and 3 of mixes A1.9 and A8.5 were sealed. Specimens 1 and 2 were sealed from mix A5.0.
[2]Comments on state of distress of sealed specimens was not possible because the translucent epoxy sealant covered any cracking that occurred.